UNIVERSITÀ del SALENTO
Dipartimento di Fisica
Dottorato di Ricerca in Fisica – XX Ciclo

A numerical analysis of optical properties and of electron entanglement and a study of intermediate statistics in molecular systems

Ph.D. Student:
Tina Anna Cattolica Maiolo

Advisor:
Prof. **Giulio Soliani**
Coadvisor:
Prof. **Luigi Martina**

January 2008

Enfant
j'ai vécu drolement
le fou rire tous les jours
le fou rire vraiment
et puis une tristesse tellement triste
quelquefois les deux en même temps
Alors je me croyais désespéré
Tout simplement je n'avais pas d'espoir
je n'avais rien d'autre que d'être vivant
j'étais intact
j'étais content
et j'étais triste
mais jamais je ne faisais semblant
Je connaissais le geste pour rester vivant
Secouer la tête
pour dire non
secouer la tête
pour ne pas laisser entrer les idées des gens
Secouer la tête pour dire non
et sourire pour dire oui
oui aux choses et aux êtres
aux êtres et aux choses à regarder à caresser
à aimer
à prendre ou à laisser
J'étais comme j'étais
sans mentalité
Et quand j'avais besoin d'idées
pour me tenir compagnie
je les appelais
Et elle venaient
et je disais oui à celle qui me plaisent
les autres je les jetais
Maintenant j'ai grandi
les idées aussi
mais ce sont toujours de grandes idées
de belles idées
d'idéales idées
...

Jacques Prèvert

Contents

Introduction

Quantum entanglement is a concept commonly used with reference to the existence of certain correlations in a quantum system that have no classical interpretation. This concept was first introduced by Schrödinger in 1935 in a paper in which he underlined the typical quantum nature of entanglement. Indeed, he wrote: "*Maximal knowledge of a total (quantum) system does not nesessarily include total knowledge of all its parts, not even when these are fully separated from each other and at the moment are not influencing each other at all.*"

From a mathematical viewpoint, entanglement can be considered as a consequence of the linearity of standard quantum formalism based on Hilbert space, but it has an essential role in quantum mechanics and it is a very useful resource in Quantum Information .

As matter of fact, the physical notion of *information* is profoundly transformed by the transition from classical mechanics to quantum mechanics. In fact, some core concept of quantum mechanics relevant to quantum information are, first of all, quantum entanglement, and then the Schmidt decomposition, the density operator formalism for the rapresentation of pure and mixed states, the partial trace and consequently the reduced density matrix of a compound system and the von Neumann entropy.

The potential usefulness of this property has been demonstrated in a variety of applications, such as quantum teleportation, quantum key distribution, quantum cryptography, and it is a useful resource to accelerate some quantum processes as, for example, the factorization in Shor's algorithm or to enhance the mutual information of memory channels.

The quantum information community devoted a lot of efforts to analyze entanglement theoretically and experimentally in order to realize a quantum computer. For example, in 1998, Chuang, at the University of Berkeley, realized the first prototype of a quantum computer with two qubits, the fol-

lowing year he used three qubits for the construction of a quantum computer and subsequently, in 2000, the IBM group built a five qubits quantum computer. Recently, the researchers of Hahn–Meitner–Institut are working on the realization of molecular quantum computers whose quantum bits could be formed by fullerenes with a single nitrogen or phosphorus atom trapped inside.

For this reason, we have considered opportune to learn some notions and mathematical instruments of quantum computational chemistry in order to investigate the properties of some molecules and the interaction among them. Once we have learnt and implemented the most important computational instruments and theories to analyze many–body sisyems, we have applied the achieved goals to the study of entanglement in molecules.

A relatively new theory for many–body systems is the so–called *Density Functional Theory* (DFT). This give us an extremely useful approach for the description of the ground state properties in molecules and the success of this theory is due to its simplicity and its low computational cost.

The main idea of the DFT is to describe an interacting system of fermions via its density and not via its many–body wave function. For an N–electrons system this means to deal with the only three degrees of freedom of the electronic density rather than with the $3N$ degrees of freedom of the electronic wave function.

While DFT in principle gives an exact description of ground state properties, in the application we must employ some approximations for the so–called exchange–correlation (XC) potential. The XC potential describes the effects of the Pauli principle and of the Coulomb potential beyond a pure electrostatic interaction of the electrons.

DFT became an exact theory only in 1964, when the two fundamental theorems of *Hohenberg* and *Kohn* have been published.

The Hohenberg–Kohn theorems state that the total ground state energy of an electron system can be written as a functional of the electronic density, and this energy is at minimum if the density is an exact density for the ground state.

Since our aim has been the description of both ground state and excited state in molecules, we have extended our study to systems which evolve in time, refering to the so–called *Time Dependent Density Functional Theory* (TD–DFT). As DFT can be viewed as an alternative formulation to solve stationary Schrödinger equation, TD–DFT can be considered as an alter-

native formulation of time–dependent quantum mechanics. In the scheme of TD–DFT the Hohenberg–Kohn theorems are replaced by the *Runge–Gross* theorem that states that for a many–body system evolving from a fixed initial state there is a one–to–one correspondence between the external time–dependent potential and the electron density.

For all our studies about optical properties of substituted thiophene, investigation of polarizability of poliacethilene chain and investigation of exchange energy density in organic molecules, we have used the *Kohn–Sham* scheme. The idea of Kohn and Sham was to introduce an auxiliary non-interacting reference system such that its ground state electron density is exactly the same as that one of the interacting system.

In this scheme we have been able to approximate independently the exchange energy (E_x) and the correlation energy (E_c). The simplest approximation for the exchange is the *Local Density Approximation* (LDA) that assumes that the density of an inhomogeneus electron system can be locally described by the density of an homogeneus electron gas. Moreover, we have used the well–known *Generalized Gradient Approximation* (GGA) that introduces nonlocal functionals and in this approximation appear not only the dependence by the density ρ but also by $\nabla\rho$. For the correlation energy the current approximation is the one introduced by Lee Yang and Parr, known as LYP functional, that depends on $\rho, \nabla\rho$ and $\nabla^2\rho$. For our aims, we have implemented, with fortran code in the TURBOMOLE programm, the Colle–Salvetti (CS) functional that obtain the correlation energy starting from the exact Hartree–Fock density matrix; in this way, unlike the LYP functional, we have been able to obtain the kinetic energy directly by the Kohn–Sham orbitals. The results achieved in this way are satisfactory.

All this theoretical framework is described in the first Chapter of this PhD Thesis. Indeed, in the second Chapter we describe the application of these computational and theoretical tools for the ivestigation of the influence of methyl or phenil substitution in β–position of dioxygenated ter–thiophene and diphenyl–thiophene on the optical properties. TD–DFT well reproduces the shifts of excitation energies for different thiophene derivatives. We find that different substituents modify the inter–ring torsional angle which in turn strongly influences the excitation energies. The steric contribution to the excitation energies have been separated from the total substituent effects.

Once we have determined these succesfully results in the analysis of

molecular properties, we have focalized our attention on the study of the possibility to use some molecules in a quantum computing scheme. In particular, after we have described in the third Chapter, the difference between pure and mixed state, separable and entangled state, after we have shown the Einstein–Podolsky–Rosen paradox and the Bell inequality as consequences of entanglement and after we have discussed the relation among a compound physical system and its subsystems by means of the notion of partial trace, in the fourth Chapter, we have made a measurement of the degree of electron entanglement in some molecular systems.

Such a measurement is made using a density matrix in the spacial coordinates and computing the von Neumann entropy. Such an approach is based on an analogous of the Schmidt decompostion for state vectors of two fermionic particles: through an unitary transformation the antisymmetric wave function is expressed into a basis of Slater determinants with a minimum number of nonvanishing terms. This number, known as Slater rank, is a criterion to identify whether a system is entangled or not, which involves the evaluation of the von Neumann entropy of one particle reduced density matrix. After a first analysis of simple bipartite systems, we have investigated the relation between electron entanglement and correlation effects in some complex molecules.

The starting point has been the so–called Collin's conjecture, that is, the correlation energy in molecular systems is proportional to their entropy. This conjecture was confirmed by numerical evidence by Ramirez *et al.* and taken up by Huang and Kais who interpreted the degree of entanglement as an evaluation of correlation energy. Entanglement is in fact a physical observable directly measured by the von Neumann entropy of the system. This concept is used in order to give a physical meaning to the electron correlation energy, which is not directly observable since it is defined as the difference between the total energy of a given molecular system, with respect to the one obtained with the Hartree–Fock approximation method. The Hartree–Fock method, in fact, is typically used to solve Schrödinger equation for a multi–electron atom or molecule described in the fixed–nuclei approximation (Born–Oppenheimer approximation) by the electronic molecular Hamiltonian and the calculation of the error due to this approximation is a major problem in many–body theory and a vast amount of work has been done on this subject.

We have made a measurement of electron entanglement in two different

examples of bipartite systems, as Hydrogen molecule and the dimer of ethylene, where each hydrogen atom or each ethylene molecule, respectively, has been considered a qubit. Using the Klein's inequality for a bipartite system, we define the *interaction electron entanglement* in order to study the degree of entanglement between the two molecules of the dimer then, we compare it with the interaction electron correlation. In this scheme, we have choosen the von Neumann entropy of the density matrix to make an estimate of the degree of entanglement. Then, we have changed the relative orientation and the distance between the molecules, in order to get the configuration corresponding to maximum entanglement. In this way, the system can be considered bipartite and each molecule can be seen as a qubit for an application to quantum computing.

In the last Chapter of this PhD Thesis, we have described some important considerations dealt with *parastatistics*, or intermediate statistics interpolating between Bose–Einstein statistics and Fermi–Dirac one, interferometry and entanglement. By means of the Hong–Ou–Mandel interferometry it is possible to estimate whether the input states particles are entangled or factorizable.

According to the statistics of the input particles (fermions or bosons) it is possible to introduce a *coincidence parameter* defined as $C = \frac{1 \pm w}{2}$ where w is expressed in terms of the spectral amplitude of the two particles and of the delay due to the different path of the particles. The presence of the double sign is due to the different statistics of the particles: if the input particles are bosons the only possible output configuration is the so–called *bunching configuration* (it corresponds to the sign $-$ in the coincidence parameter); instead, if the input particles are fermions in output there is the *antibunching configuration* (that corresponds to the sign $+$ in the coincidence parameter). Since it has been demonstrated that for separable input states $w \equiv w_{sep} \geq 0$, by means of the study of the parameter C it is possible to obtain some information about the input state. In fact, in the bosonic case, if $C \geq 1/2$, then the input state is certainly entangled; instead, in the fermionic case the input state is certainly entangled if $C \leq 1/2$. We have analyzed other statistics, the intermediate ones (such as the quon statistics), in order to interpolate the bunching configuration with the antibunching one, from fermionic statistics to bosonic statistics with continuity.

Chapter 1

Theory and some implementations for molecular systems

1.1 Many–body problem

To describe completely the quantum mechanical behaviour of electrons in solids it is strictly necessary to calculate the many-electron wave function for the system. In principle this may be obtained from the time–independent Schrödinger equation, but in practice the potential experienced by each electron is dictated by the behaviour of all the other electrons in the solid. For an N–electron system, in the Born–Oppenheimer nonrelativistic approximation, the time-independent Schrödinger equation is

$$\widehat{H}\Psi = E\Psi \tag{1.1}$$

where E is the electronic energy, $\Psi = \Psi(\mathbf{x}_1, \mathbf{x}_2, \cdots, \mathbf{x}_n)$ is the wave function, and $\widehat{H}$ is the Hamiltonian operator:

$$\widehat{H} = \sum_{i=1}^{N} \Big(-\frac{1}{2}\nabla_i^2 \Big) + \sum_{i=1}^{N} v(\mathbf{r}_i) + \sum_{i<j}^{N} \frac{1}{\mathbf{r}_{ij}} \tag{1.2}$$

in which $v(\mathbf{r}_i) = -\sum_\alpha \frac{Z_\alpha}{r_{i\alpha}}$ is the "external " potential acting on electron i due to nuclei of charges Z_α.

Of course, the influence of nearby electrons will be much stronger than that of far-away electrons since the interaction is electrostatic in nature, but the fact remains that the motion of any one electron is strongly coupled to

the motion of the other electrons in the system. However, a rigorous solution is possible only for a very few special cases (e. g. simple potential wells, hydrogen atom, simple harmonic oscillator). One of the earliest attempts to solve the problem was made by Hartree [1]. He simplified the problem by making an assumption about the form of the many-electron wave function, namely that it was just the product of a set of single-electron wave functions. In a uniform system these wave functions would take the form of simple plane waves. Having made this assumption it was possible to proceed using the *variational principle.*

This principle is a very powerful concept in mathematics. In the form most commonly applied to theoretical physics it states that if a given system may be described by a set of unknown parameters then the set of parameter values which most correctly describes the ground state of the system (i.e. the state in which the system exists when not perturbed by outside influences) is just that set of values which minimises the total energy.

1.1.1 Variational principle for the ground state

By using the variational method Hartree found the Hamiltonian equation of the many-electron system. In fact, for an N-electron system there are N equations; one for each of the N single-electron wave functions which made up the many-electron product wave function. These equations turned out to look very much like the time-independent Schrödinger equation, except the potential (the Hartree potential) was no longer coupled to the individual motions of all the other electrons, but instead depended simply upon the time-averaged electron distribution of the system. This important fact meant that it was possible to treat each electron separately as a single-particle. Consequently the Hartree approximation allows us to calculate approximate single-particle wave functions for the electrons in crystals, and hence calculate other related properties. Unfortunately, the Hartree approximation does not provide us with particularly good results.

When a system is in the state Ψ, which may or may not satisfy Eq. (1.1), the average of many measurements of the energy is given by the formula

$$E[\Psi] = \frac{\langle \Psi | \widehat{H} | \Psi \rangle}{\langle \Psi | \Psi \rangle} \tag{1.3}$$

where

$$\langle\Psi|\widehat{H}|\Psi\rangle = \int \Psi^* \widehat{H}\Psi d\mathbf{x} \tag{1.4}$$

and the square brackets denote that Ψ determines E, *i. e.*, E is a *functional* of Ψ. Since, furthermore, each particular measurement of the energy gives one of the eigenvalues of $\widehat{H}$, we immediately have

$$E[\Psi] \geq E_0. \tag{1.5}$$

The energy computed from a guessed Ψ is an upper bound to the true ground–state energy E_0. Full minimization of the functional $E[\Psi]$ with respect to all allowed N–electron wave functions will give the true ground state Ψ_0 and energy $E[\Psi_0] = E_0$; that is,

$$E_0 = \min_{\Psi} E[\Psi]. \tag{1.6}$$

Formal proof of the minimum–energy principle of Eq. (1.5) goes as follows. Expand Ψ in terms of the normalized eigenstates of $\widehat{H}$, Ψ_k:

$$\Psi = \sum_k C_k \Psi_k \tag{1.7}$$

then the energy becomes

$$E[\Psi] = \frac{\sum_k |C_k|^2 E_k}{\sum_k |C_k|^2} \tag{1.8}$$

where E_k is the energy for the k–th eigenstate of $\widehat{H}$. Note that the orthogonality of the Ψ_k has been used. Because $E_0 \leq E_1 \leq E_2 \leq \ldots$, $E[\Psi]$ is always greater than or equal to E_0, and it reaches its minimum E_0 if and only if $\Psi = C_0\Psi_0$.

Every eigenstate Ψ is an extremum of the functional $E[\Psi]$. In other words, one may replace the Schrödinger equation Eq. (1.1) with the variational principle

$$\delta E[\Psi] = 0 \tag{1.9}$$

when Eq. (1.9) is satisfied, so is Eq. (1.1), and vice versa. In order to obtain normalized Ψ it is useful the method of *Lagrange multipliers*. Extremization of $\langle\Psi|\widehat{H}|\Psi\rangle$ subject to the constraint $\langle\Psi|\Psi\rangle = 1$ is equivalent to making stationary the quantity $[\langle\Psi|\widehat{H}|\Psi\rangle - E\langle\Psi|\Psi\rangle]$ without constraint, with E the Lagrange multiplier. This gives

$$\delta[\langle\Psi|\widehat{H}|\Psi\rangle - E\langle\Psi|\Psi\rangle] = 0. \tag{1.10}$$

Eq. (1.10) is essentially equivalent to Eq. (1.1), so one must solve this equation for Ψ as a function of E, then adjust E until normalization is achieved. Solutions of Eq. (1.10) with forms of Ψ restricted to approximate forms $\tilde{\Psi}$ of a given type will give well-defined best approximations $\tilde{\Psi}_0$ and $\tilde{E}_0$ to the correct Ψ_0 and E_0. By Eq. (1.5), $\tilde{E} \geq E_0$, and so convergence of the energy, from above, is assured as one uses more and more flexible $\tilde{\Psi}$. It is important to note that for a system of N electrons and given nuclear potential $v(\mathbf{r})$ defines a procedure for going from N and $v(\mathbf{r})$ to the ground–state wave function Ψ and hence through Eq. (1.3) to the ground–state energy $E[N, v]$ and other properties of interest, in other words E is a functional of N and $v(\mathbf{r})$.

1.1.2 The Hartree–Fock approximation

The most obvious reason for the failure of the Hartree approach lies in the initial assumption of a product wave function. The Pauli exclusion principle states that it is not possible for two fermions to exist at the same point in space with the same set of quantum numbers. This principle is manifest as an effective repulsion between any pair of identical fermions possessing the same set of quantum numbers. Mathematically, the Pauli exclusion principle can be accounted for by ensuring that the wave function of a set of identical fermions is antisymmetric under exchange of any pair of particles. That is to say that the process of swapping any one of the fermions for any other of the fermions should leave the wave function unaltered except for a change of sign. Any wave function possessing that property will tend to zero as any pair of fermions with the same quantum numbers approach each other. The Hartree product wave function is symmetric rather than antisymmetric, so the Hartree approach effectively ignores the Pauli exclusion principle.

The Hartree–Fock approach is an improvement over the Hartree theory in that the many-electron wave function is specially constructed out of single-electron wave functions in such a way as to be antisymmetric. The wave function has to be much more complicated than the Hartree product wave function, but it can be written in a compact way as a so-called *Slater determinant.*

Suppose that Ψ is approximated as an antisymmetrized product of N orthonormal spin orbitals $\psi_i(\mathbf{x})$, each a product of a spatial orbital $\phi_k(\mathbf{r})$ and a spin function $\sigma(s) = \alpha(s)$ or $\beta(s)$, that represent spin–up or spin–down,

respectively, the *Slater determinant* is

$$\Psi_{\rm HF} = \frac{1}{\sqrt{N!}} \begin{vmatrix} \psi_1(\mathbf{x_1}) & \psi_2(\mathbf{x_1}) & \cdots & \psi_N(\mathbf{x_1}) \\ \psi_1(\mathbf{x_2}) & \psi_2(\mathbf{x_2}) & \cdots & \psi_N(\mathbf{x_2}) \\ \vdots & \vdots & \vdots & \vdots \\ \psi_1(\mathbf{x_N}) & \psi_2(\mathbf{x_N}) & \cdots & \psi_N(\mathbf{x_N}) \end{vmatrix} \tag{1.11}$$

It was shown that a Slater determinant, a determinant of one-particle orbitals first used by Heisenberg and Dirac in 1926, satisfies the antisymmetric property of the exact solution and hence is a suitable *ansatz* for applying the variational principle. The original Hartree method can then be viewed as an approximation to the Hartree-Fock method by neglecting exchange.

The method

The Hartree–Fock approximation is the method whereby the orthonormal orbitals ψ_i are found that minimize Eq. (1.3) for the determinantal form of Ψ.

The normalization integral $\langle \Psi_{HF} | \Psi \rangle$ is equal to 1, and the energy expectation value is

$$E_{HF} = \langle \Psi_{HF} | \widehat{H} | \Psi_{HF} \rangle = \sum_{i=1}^{N} H_i + \frac{1}{2} \sum_{i,j}^{N} (J_{ij} - K_{ij}) \tag{1.12}$$

where

$$H_i = \int \psi_i^*(\mathbf{x}) \left[-\frac{1}{2}\nabla^2 + v(\mathbf{x}) \right] \psi_i(\mathbf{x}) d\mathbf{x} \tag{1.13}$$

$$J_{ij} = \int\int \psi_i(\mathbf{x}_1)\psi_i^*(\mathbf{x}_1) \frac{1}{\mathbf{r}_{12}} \psi_j^*(\mathbf{x}_2)\psi_j(\mathbf{x}_2) d\mathbf{x}_1 d\mathbf{x}_2 \quad \textit{Coulomb integrals}, \tag{1.14}$$

$$K_{ij} = \int\int \psi_i^*(\mathbf{x}_1)\psi_j(\mathbf{x}_1) \frac{1}{\mathbf{r}_{12}} \psi_i(\mathbf{x}_2)\psi_j^*(\mathbf{x}_2) d\mathbf{x}_1 d\mathbf{x}_2 \quad \textit{Exchange integrals}. \tag{1.15}$$

These integrals are all real, and $J_{ij} \geq K_{ij} \geq 0$. The J_{ij} are the so–called Coulomb integrals and the K_{ij} are called exchange integrals.

By minimization of Eq. (1.12), under the orthonormalization conditions

$$\int \psi_i^*(\mathbf{x})\psi_j(\mathbf{x}) d\mathbf{x} = \delta_{ij}, \tag{1.16}$$

one obtains the Hartree-Fock differential equations

$$\widehat{F}\psi_i(\mathbf{x}) = \sum_{j=1}^{N} \epsilon_{ij}\psi_j(\mathbf{x}) \tag{1.17}$$

where $\widehat{F}$ is the Fock operator defined as

$$\widehat{F} = -\frac{1}{2}\nabla^2 + v + \widehat{g} \tag{1.18}$$

in which the Coulomb–exchange operator $\widehat{g}$ is given by

$$\widehat{g} = \widehat{j} - \widehat{k}. \tag{1.19}$$

Here

$$\widehat{j}(\mathbf{x}_1)f(\mathbf{x}_1) \equiv \sum_{k=1}^{N} \int \psi_k^*(\mathbf{x}_2)\psi_k(\mathbf{x}_2)\frac{1}{\mathbf{r}_{12}}f(\mathbf{x}_1)d\mathbf{x}_2 \tag{1.20}$$

and

$$\widehat{k}(\mathbf{x}_1)f(\mathbf{x}_1) \equiv \sum_{k=1}^{N} \int \psi_k^*(\mathbf{x}_2)\psi_k(\mathbf{x}_2)\frac{1}{\mathbf{r}_{12}}f(\mathbf{x}_1)d\mathbf{x}_2 \tag{1.21}$$

with $f(\mathbf{x}_1)$ an arbitrary function.

The matrix ϵ in Eq. (1.17) is an Hermitian matrix whose entries are the Lagrangian multipliers; the *orbital energies* are given multiplying Eq. (1.17) by ψ^* and integrating:

$$\epsilon_i \equiv \epsilon_{ii} = \langle\psi_i|\widehat{F}|\psi_i\rangle = H_i + \sum_{j=1}^{N}(J_{ij} - K_{ij}), \tag{1.22}$$

summing over the index i and comparing with Eq. (1.12), one finds

$$E_{HF} = \sum_{i=1}^{N}\epsilon_i - \underbrace{\frac{1}{2}\sum_{i,j=1}^{N}(J_{ij} - K_{ij})}_{V_{ee}}, \tag{1.23}$$

where the symbol V_{ee} represents the total electron–electron repulsion energy. For the total molecular energy including nuclear–nuclear repulsion, one has

$$W_{HF} = \sum_{i=1}^{N}\epsilon_i - V_{ee} + V_{nn}, \tag{1.24}$$

where W_{HF} is the electronic energy E plus the nucleus–nucleus repulsion energy. Solution of Eq. (1.17) must proceed iteratively, since the orbitals ψ_i that solve the problem appear in the operator $\widehat{F}$. Consequently, the Hartree-Fock method is a nonlinear *"self–consistent–field"* method.

The Hartree–Fock approximation consists of two methods: one for describing system with an even number of electrons, the restricted Hartree-Fock method (RHF) and the other one for describing open shell system with a odd number of electrons (RHF).

1.1.3 Restricted Hartree–Fock (RHF) method

The RHF approximation is a useful method to describe an open shell system, indeed for a system with an even number of electrons, the N orbitals ψ_i are taken to comprise $N/2$ orbitals of form $\phi_k(\mathbf{r})\alpha(\mathbf{s})$ and $N/2$ orbitals of form $\phi_k(\mathbf{r})\beta(\mathbf{s})$. In this case, the energy formula is

$$E_{HF} = 2\sum_{k=1}^{N/2} H_k + \sum_{k,l}^{N/2} (2J_{kl} - K_{kl}), \tag{1.25}$$

where

$$H_k = \int \phi_k^*(\mathbf{r}) \left[-\frac{1}{2}\nabla^2 + v(\mathbf{r})\right] \phi_k(\mathbf{r}) d\mathbf{r} \tag{1.26}$$

$$J_{kl} = \int\int |\phi_k(\mathbf{r}_1)|^2 \frac{1}{\mathbf{r}_{12}} |\phi_l(\mathbf{r}_2)|^2 d\mathbf{x}_1 d\mathbf{x}_2 \quad \textit{Coulomb integrals} \tag{1.27}$$

$$K_{kl} = \int\int \phi_k^*(\mathbf{r}_1)\phi_l(\mathbf{x}_1)\frac{1}{\mathbf{r}_{12}}\phi_k(\mathbf{r}_2)\phi_l^*(\mathbf{r}_2) d\mathbf{r}_1 d\mathbf{r}_2 \quad \textit{Exchange integrals} \tag{1.28}$$

while Eq. (1.17), Eq. (1.20) and Eq. (1.21) are respectively replaced by

$$\widehat{F}\phi_k(\mathbf{r}) = \sum_{l=1}^{N/2} \epsilon_{kl}\phi_l(\mathbf{r}), \tag{1.29}$$

$$\widehat{j}(\mathbf{r}_1)f(\mathbf{r}_1) \equiv 2\sum_{m=1}^{N/2} \int |\phi_m(\mathbf{r}_2)|^2 \frac{1}{\mathbf{r}_{12}} d\mathbf{r}_2 f(\mathbf{r}_1) \tag{1.30}$$

and

$$\widehat{k}(\mathbf{r}_1)f(\mathbf{r}_1) \equiv \sum_{m=1}^{N/2} \int \phi_m^*(\mathbf{r}_2) f(\mathbf{r}_2) \frac{1}{\mathbf{r}_{12}} d\mathbf{r}_2 \phi_m(\mathbf{r}_1). \tag{1.31}$$

The determinantal wave function Eq. (1.11) for this "closed shell" case is

$$\Psi_{HF} = \frac{1}{\sqrt{N!}} \begin{vmatrix} \phi_1(\mathbf{r}_1)\alpha(s_1) & \phi_1(\mathbf{r}_1)\beta(s_1) & \cdots & \phi_{N/2}(\mathbf{r}_1)\beta(s_1) \\ \phi_1(\mathbf{r}_2)\alpha(s_2) & \phi_2(\mathbf{r}_2)\beta(s_2) & \cdots & \phi_{N/2}(\mathbf{r}_2)\beta(s_2) \\ \vdots & \vdots & \vdots & \vdots \\ \phi_1(\mathbf{r}_N)\alpha(s_N) & \phi_2(\mathbf{r}_N)\beta(s_N) & \cdots & \phi_N(\mathbf{r}_N)\beta(s_N) \end{vmatrix}. \tag{1.32}$$

A unitary transformation of the occupied orbitals ψ_k to another set of orbitals η_m leaves the wave function unchanged and the operators $\widehat{j}$, $\widehat{k}$ and $\widehat{F}$ of Eq. (1.29) through Eq. (1.31) are also invariant with respect to such a transformation.

That is, if one lets

$$\eta_m = \sum_k \mathbb{U}_{mk}\psi_k \tag{1.33}$$

where $\mathbb{U}$ is a unitary matrix,

$$\mathbb{U}^\dagger\mathbb{U} = 1 \tag{1.34}$$

then Eq. (1.29) becomes

$$\widehat{F}\eta_m = \sum_{n=1}^{N/2} \epsilon^\eta_{mn}\eta_n, \tag{1.35}$$

where

$$\epsilon^\eta = \mathbb{U}\epsilon\mathbb{U}^\dagger. \tag{1.36}$$

Since the matrix ϵ is hermitain, one may choose the matrix $\mathbb{U}$ to diagonalize it. The corresponding orbitals λ_m called the *canonical Hartree-Fock orbitals*, satisfy the *canonical Hartree-Fock equations*,

$$\widehat{F}\lambda_m(\mathbf{r}) = \epsilon^\lambda_m\lambda_m(\mathbf{r}). \tag{1.37}$$

Eq. (1.37) is considerably more convenient for calculation then Eq. (1.29). Furthermore, the orbitals that are solutions of Eq. (1.37) are uniquely appropriate for describing removal of electrons from the system in question. The *Koopmans theorem* [2] establishes that if one assumes no reorganization on ionization, the best (lowest–energy) single–determinant description for the ion is the determinant built from the canonical Hartree–Fock orbitals of Eq. (1.37). One then finds, approximately,

$$\epsilon^\lambda_m = -I_m, \tag{1.38}$$

where I_m is the *ionization energy* associated with the removal of an electron from the orbital λ_m. The main problem is that this equation ignores both reorganization and errors in the Hartree–Fock description (called *correlation energy*).

1.1.4 Unrestricted Hartree–Fock (UHF) method

When the number of electrons is not even, the standard Hartree-Fock scheme is what is called the *unrestricted open-shell Hartree-Fock* (UHF) *method* [5]. Spatial parts of spin orbitals with α spin are allowed to be different from spatial parts of spin orbitals with β spin, even within a single "pair" of electrons. Noting that orthogonality between all α-spin spin orbitals and all β-spin spin orbitals is still preserved, we see that the only problem in implementation is the complication associated with handling all N orbitals in the Hartree-Fock equations. The mathematical apparatus is Eq. (1.17) to Eq. (1.21). The UHF method then gives no energy lowering over the restricted HF method. But there are important cases in which energy lowering is found. For example, the UHF description of bond breaking in H_2 gives the proper dissociation products, while the RHF description of H_2 gives unrealistic ones.

Many physical properties of most molecules in their ground states are well accounted for by use of Hartree-Fock wave functions.

In actual implementations of Hartree-Fock theory (and also in calculations of wave functions to an accuracy higher than those of Hartree-Fock), one usually employs some set of fixed, one-electron basis functions, in terms of which orbitals are expanded and many-electrons wave functions are expressed. This transforms the mathematical problem into one (or more) matrix eigenvalue problem(s) of high dimension, in which the matrix elements are calculated from arrays of integrals evaluated for the basis functions. If we call the basis functions $\chi_p(\mathbf{r})$, one can see from Eq. (1.2) what the necessary integrals will be:

(i) *overlap integrals*,

$$S_{pq} \equiv \int \chi_p^*(\mathbf{r})\chi_q(\mathbf{r})d\mathbf{r}, \tag{1.39}$$

(ii) *kinetic energy integrals*,

$$T_{pq} \equiv \int \chi_p^*(\mathbf{r})(-\frac{1}{2}\nabla^2)\chi_q(\mathbf{r})d\mathbf{r}, \tag{1.40}$$

(iii) *electron-nucleus attraction integrals*,

$$(A|pq) \equiv \int \chi_p^*(\mathbf{r}_1)\frac{1}{r_{1A}}\chi_q(\mathbf{r}_1)d\mathbf{r}_1, \tag{1.41}$$

and

(iv) *electron-electron repulsion integrals*,

$$(pq|rs) \equiv \int\int \chi_p^*(\mathbf{r}_1)\chi_q(\mathbf{r}_1)\frac{1}{r_{12}}\chi_r(\mathbf{r}_2)\chi_s^*(\mathbf{r}_2)d\mathbf{r}_1 d\mathbf{r}_2. \tag{1.42}$$

In the HF approach the two-electron integrals $(pq|rs)$ dominate the computational effort. Moreover, the HF is an approximation, as it does not account for dynamic correlation due to the rigid form of single determinant wave function. To solve the HF equations, the assumption has to be made that electrons interact with the averaged potential coming from other electrons, while in fact, the interactions between electrons are pairwise. In reality, electrons correlate their movements trying to avoid each other, so there is least amount of electrostatic repulsion. To account for dynamic correlation, one has to go to correlated methods, which use multideterminant wave functions, while HF method is quite successful for geometries but it fails to describe bond breaking or forming.

1.2 Electron density

Since inception of quantum mechanics by Heisenberg, Born, and Jordan in 1925, and Schrödinger in 1926, there were basically two competing approaches to find the energy of a system of electrons. One was rooted in statisticial mechanics and the fundamental variable was the total electron density $\rho(\mathbf{r})$, i.e., the number of electrons per unit volume at a given point in space (e.g., in cartesian coordinates: $\mathbf{r} = (x, y, z)$). In this approach, electrons were treated as particles forming a special gas, called *electron gas*. The special case, the uniform electron gas, corresponds to $\rho(\mathbf{r}) = const$.

Another approach was to derive the many particle wave function $\Psi(\mathbf{r}_1, \mathbf{r}_2, \cdots \mathbf{r}_N, t)$ (where $\mathbf{r}_1$ denotes the coordinates of the 1st electron, $\mathbf{r}_2$ the 2nd electron, and so on, and t is time) and solve the stationary Schrödinger equation for the system:

$$\hat{H}\Psi_k(\mathbf{r}_1, \mathbf{r}_2, \cdots \mathbf{r}_N) = E_k\Psi_k(\mathbf{r}_1, \mathbf{r}_2, \cdots \mathbf{r}_N) \tag{1.43}$$

(where $\hat{H}$ is the hamiltonian, i.e., the operator of the total energy for the system), and calculate the set of possible eigenfunctions Ψ_k and corresponding eigenvalues E_k. The eigenfunctions have to be physically acceptable, and for finite systems:

1. they should be continuous functions,

2. they should be at least doubly differentiable,

3. its square should be integrable,

4. they should vanish at infinity (for finite systems).

Once we know the wave function Ψ for a given state of our system, we can calculate the expectation value for any quantity for which we can write down the operator. The wave function itself, does not correspond to any physical quantity, but its square represents the probability density. In other words:

$$|\Psi(\mathbf{r}_1, \mathbf{r}_2, \cdots \mathbf{r}_N)|^2 d\mathbf{r}_1 d\mathbf{r}_2 \cdots d\mathbf{r}_N \tag{1.44}$$

or

$$\Psi^*(\mathbf{r}_1, \mathbf{r}_2, \cdots \mathbf{r}_N)\Psi(\mathbf{r}_1, \mathbf{r}_2, \cdots \mathbf{r}_N) d\mathbf{r}_1 d\mathbf{r}_2 \cdots d\mathbf{r}_N \tag{1.45}$$

or

$$|\Psi\rangle \langle\Psi| \, dV \tag{1.46}$$

represents the probability that electron 1 is in the volume element $d\mathbf{r}_1$ around point $\mathbf{r}_1$, electron 2 is in the volume element of the size $d\mathbf{r}_2$ around point $\mathbf{r}_2$, and so on. If Ψ describes the system containing only a single electron, the $|\Psi(\mathbf{r})|^2 d\mathbf{r}$ simply represents the probability of finding an electron in the volume element of a size $d\mathbf{r}$ centered around point $\mathbf{r}$. If you use cartesian coordinates, then $d\mathbf{r} = dxdydz$ and the volume element would be a brick (rectangular parallelipiped) with dimensions $dx \times dy \times dx$ whose vertex closes to the origin of coordinate system is located at (x, y, z). Now, if we integrate the function Ψ over all the space for all the variables (i.e., sum up the probabilities in all the elements $d\mathbf{r}_i$), we should get a probability of finding our electrons anywhere in the Universe, i.e., 1. This is why it is a good idea to normalize function Ψ. If it is not normalized, it can easily be done by multiplying it by a normalization constant:

$$\Psi_{normalized} = \overbrace{\frac{1}{\sqrt{\langle \Psi_{unnormalized} | \Psi_{unnormalized} \rangle}}}^{Normalization\ constant} \Psi_{unnormalized}. \tag{1.47}$$

Since square of Ψ represents the probability density of finding electrons, one may suspect, that it should be easy to calculate the total electron density from it. And actually it is:

$$\rho(\mathbf{r}) = N \langle \Psi | \delta(\mathbf{r} - \mathbf{r}_i) | \Psi \rangle \tag{1.48}$$

where N is the total number of electrons, and $\delta(\mathbf{r}-\mathbf{r}')$ is the Dirac delta function. In cartesian coordinates, it simply amounts to integrating over all electron positions vectors $\mathbf{r}_i$ but one. Which one, is not important, since electrons are indistinguishable, and a proper wave function has to reflect this:

$$\rho(\mathbf{r}_1) = N \underbrace{\int\int\cdots\int}_{N-1} |\Psi(\mathbf{r}_1,\mathbf{r}_2,\cdots\mathbf{r}_N,)|^2 \underbrace{d\mathbf{r}_2 d\mathbf{r}_3\cdots d\mathbf{r}_N}_{N-1}. \tag{1.49}$$

It is interesting to note, that for the wave function which describes the system containing only a single electron:

$$\rho(\mathbf{r}) = \Psi^*(\mathbf{r})\Psi(\mathbf{r}) = |\Psi(\mathbf{r})|^2 = |\Psi\rangle\langle\Psi| \tag{1.50}$$

i.e., logically, the electron density and the probability density of finding the single electron are the same thing.

1.3 Density Functional Theory (DFT)

For many years, the use of electron density as a fundamental description of the system was based on intuition rather than hard proof that this can be done. The success of density functional theory (DFT) is due to its simplicity and low computational cost. Electron density is more attractive (depends only on x, y, z, and eventually, there may be two densities for spin polarized systems, one for spin up electrons $\rho_\uparrow(\mathbf{r})$ and one for spin down electrons $\rho_\downarrow(\mathbf{r})$, as opposed to many particle wave function which depends on all coordinates of all particles, i.e., for N electrons, it depends on $3N$ variables (or $4N$ if you count in spin). The fact that the ground state properties are functionals of the electron density $\rho(\mathbf{r})$ was proved by Hohenberg and Kohn (1964) and it provides the basic framework for modern Density Functional methods.

More specifically, according to the theorem proved by them, the total ground state energy of an electron system can be written as a functional of the electronic density, and this energy is at minimum if the density is an exact density for the ground state. The theorem of HK is an existence proof of such a functional, but there is no prescription how to construct it. If we knew the form of this functional accurately, and if it was not complicated, quantum chemistry would be a done deal. Unfortunately we do not know the exact form of energy functional. It is necessary to use approximations

regarding parts of the functional dealing with kinetic energy and exchange and correlation energies of the system of electrons.

In other words, while DFT in principle gives an exact description of ground state properties, practical applications of DFT are based on approximations for the so–called exchanged–correlation potential. The exchange–correlation (XC) potential beyond a pure electrostatic interaction of the electrons. In practice many approximations of the XC potential are employed.

1.3.1 Density operators

Let us define, with the Dirac notation, the *density operator*

$$\widehat{\gamma}_N \equiv |\Psi_N\rangle\langle\Psi_N|, \tag{1.51}$$

or equivalently in the coordinate representation we can define the *density matrix*

$$\gamma_N\left(\mathbf{x}_1^{'}\mathbf{x}_2^{'}\cdots\mathbf{x}_N^{'},\mathbf{x}_1\mathbf{x}_2\cdots\mathbf{x}_N\right) \equiv \Psi_N\left(\mathbf{x}_1^{'}\mathbf{x}_2^{'}\cdots\mathbf{x}_N^{'}\right)\Psi_N^*\left(\mathbf{x}_1\mathbf{x}_2\cdots\mathbf{x}_N\right). \tag{1.52}$$

The quantity

$$\Psi_N\left(\mathbf{x}_1\mathbf{x}_2\cdots\mathbf{x}_N\right)\Psi_N^*\left(\mathbf{x}_1\mathbf{x}_2\cdots\mathbf{x}_N\right) \tag{1.53}$$

is the probability distribution associated with a solution of the Schrödinger equation, indeed $\widehat{\gamma}_N$ in Eq. (1.51) is a more general quantity in that the variables in the first factor are primed. The two sets of independent quantities $\mathbf{x_1^{'}x_2^{'}}\cdots\mathbf{x_N^{'}}$ and $\mathbf{x_1x_2}\cdots\mathbf{x_N}$ can be thought of as two sets of indices that give Eq. (1.51) a numerical value, in contrast with the single set $\mathbf{x_1x_2}\cdots\mathbf{x_N}$ that sufficies for Eq. (1.53). If we set $\mathbf{x_i} = \mathbf{x_i^{'}}$, for all i we get the probability distribution for a system with coordinates $(\mathbf{x_1x_2}\cdots\mathbf{x_N})$.

It is easy to verify that $\widehat{\gamma}_N$ is a *projection operator* and is Hermitian. The following property is also verified:

$$\mathrm{Tr}\left(\widehat{\gamma}_N\right) = 1, \tag{1.54}$$

indeed, the *trace* operator is defined as the sum of diagonal element of the matrix representing $\widehat{A}$. Moreover, it is important to note that the expectation value of a general N–particle operator $\widehat{A}$ is obtained from

$$\langle\widehat{A}\rangle = \int d\mathbf{x}_1 \int d\mathbf{x}_2 \cdots \int d\mathbf{x}_N \Psi\left(\mathbf{x}_1\mathbf{x}_2\cdots\mathbf{x}_N\right)^* \widehat{A}\Psi\left(\mathbf{x}_1\mathbf{x}_2\cdots\mathbf{x}_N\right), \tag{1.55}$$

which for multiplicative operators becomes

$$\langle \widehat{A} \rangle = \int d\mathbf{x}_1 \int d\mathbf{x}_2 \cdots \int d\mathbf{x}_N \widehat{A} \gamma \left(\mathbf{x}_1 \mathbf{x}_2 \cdots \mathbf{x}_N, \mathbf{x}_1 \mathbf{x}_2 \cdots \mathbf{x}_N \right), \tag{1.56}$$

and involves only the function $\gamma \left(\mathbf{x}_1 \mathbf{x}_2 \cdots \mathbf{x}_N, \mathbf{x}_1 \mathbf{x}_2 \cdots \mathbf{x}_N \right)$, which is the diagonal element of the matrix γ; in fact the expectation value of the operator $\widehat{A}$ can be written as in the following:

$$\langle \widehat{A} \rangle = \mathrm{Tr} \left(\widehat{\gamma}_N \widehat{A} \right) = \mathrm{Tr} \left(\widehat{A} \widehat{\gamma}_N \right). \tag{1.57}$$

Once the density operator is known, via Eq. (1.57), all the properties of the system can be calculated. In this sense the density operator carries the same informations as the N–electron wave function. Indeed the density operator $\widehat{\gamma}$ is defined in the same space as the vector $|\Psi_N\rangle$. It is worth to note, however, that while the wave function is defined up to an arbitrary phase factor, the density operator is unique.

An operator description of a quantum state becomes necessary when the state cannot be represented by a linear superposition of eigenstates of a particular Hamiltonian $\widehat{H}_N$, or equivalently, by a vector in the Hilbert space $\mathscr{H}_N$. This occurs when one treats a subspace of a compound system, as for example an individual electron in a many–electron system. For such a system one does not have a complete Hamiltonian containing only its own degrees of freedom, thereby precluding the wave–function description. A state is said to be *pure* if it is described by a wave function, *mixed* if it cannot be described by a wave function.

A system in a mixed state can be characterized by a probability distribution over all the accessible pure states. Let us generalize the density operator of Eq. (1.51) to the *ensamble density operator*

$$\widehat{\Gamma} = \sum_i p_i |\Psi_i\rangle\langle\Psi_i|, \tag{1.58}$$

where p_i are the probabilities of the system being found in the state $|\Psi_i\rangle$, and the sum is over the complete set of all accessible pure states and they have the properties

$$\begin{cases} p_i \geq 0 \, ; \\ \sum_i p_i = 1. \end{cases} \tag{1.59}$$

For a system in a pure state, one p_i is 1 and the rest are zero; $\widehat{\Gamma}$ of Eq. (1.58) then reduces to $\widehat{\gamma}$ of Eq. (1.51).

The ensemble density operator has the following properties:

1. By construction $\widehat{\Gamma}$ is normalized: in an arbitrary complete basis $|f_k\rangle$

$$\begin{aligned} \mathrm{T}r\left(\widehat{\Gamma}\right) &= \sum_i \sum_k p_i \langle f_k|\Psi_i\rangle\langle\Psi_i|f_k\rangle \\ &= \sum_i p_i \langle\Psi_i| \sum_k |f_k\rangle\langle f_k|\Psi_i\rangle \\ &= \sum_i p_i \langle\Psi_i|\Psi_i\rangle = \sum_i p_i = 1. \end{aligned} \tag{1.60}$$

2. $\widehat{\Gamma}$ is Hermitian:

$$\begin{aligned} \langle f_k|\widehat{\Gamma}|f_l\rangle &= \sum_i p_i \langle f_k|\Psi_i\rangle\langle\Psi_i|f_l\rangle \\ &= \sum_i p_i \left\{\langle f_l|\Psi_i\rangle\langle\Psi_i|f_k\rangle\right\}^* \\ &= \langle f_l|\widehat{\Gamma}|f_k\rangle^* \end{aligned} \tag{1.61}$$

3. It is positive semidefinite

$$\langle f_k|\widehat{\Gamma}|f_k\rangle = \sum_i p_i |\langle f_k|\Psi_i\rangle|^2 \geq 0. \tag{1.62}$$

   The p_i are the eigenvalues of $\widehat{\Gamma}$.

4. For a system to be in a pure state, it is necessary and sufficient for the density operator to be *idempotent*:

$$\widehat{\gamma}\cdot\widehat{\gamma} = |\Psi\rangle\langle\Psi|\Psi\rangle\langle\Psi| = |\Psi\rangle\langle\Psi| = \widehat{\gamma} \tag{1.63}$$

   The ensemble density operator in general lacks this property:

$$\widehat{\Gamma}\cdot\widehat{\Gamma} = \sum_i p_i^2 |\Psi_i\rangle\langle\Psi_i| \neq \widehat{\Gamma} \tag{1.64}$$

5. For a mixed state, the expectation value for the observable $\widehat{A}$ is given by a generalization of Eq. (1.57)

$$\langle\widehat{A}\rangle = \mathrm{T}r\left(\widehat{\Gamma}\widehat{A}\right) = \sum_i p_i \langle\Psi_i|\widehat{A}|\Psi_i\rangle \tag{1.65}$$

6. The time-dependent Schrödinger equation can be written in terms of pure–state density operators $\widehat{\gamma}_N$ (or , more generally, in terms of the ensemble density operators $\widehat{\Gamma}$).

$$i\hbar\frac{\partial}{\partial t}|\Psi_N\rangle = \widehat{H}|\Psi_N\rangle \tag{1.66}$$

Moreover

$$\frac{\partial}{\partial t}\widehat{\gamma}_N = \left(\frac{\partial}{\partial t}|\Psi_N\rangle\right)\langle\Psi_N| + |\Psi_N\rangle\frac{\partial}{\partial t}\langle\Psi_N|$$

$$= \frac{\widehat{H}}{i\hbar}|\psi_N\rangle\langle\psi_N| - |\psi_N\rangle\langle\psi_N|\frac{\widehat{H}}{i\hbar}. \tag{1.67}$$

So that

$$i\hbar\frac{\partial}{\partial t}\widehat{\gamma}_N = \left[\widehat{H}, \widehat{\gamma}_N\right], \tag{1.68}$$

and by the linearity of Eq. (1.58)

$$i\hbar\frac{\partial}{\partial t}\widehat{\Gamma} = \left[\widehat{H}, \widehat{\Gamma}\right]. \tag{1.69}$$

For a stationary state, $\widehat{\Gamma}$ is independent of time and $\left[\widehat{H}, \widehat{\Gamma}\right] = 0$.

Most operators in quantum mechanics are one or two–particle operators and can be calculated from the so–called *reduced density matrices*, that depend on less than $2N$ variables.

Reduced Density Matrices

The basic operators describing an electronic system are either one–electron operators or two–electron operators. Expressions like "one–particle operator" and "two particle operator" refer to the number of particles involved in the definition of the operator (one for a potential energy, two in the case of an interaction, etc.), not to the total number of particles present in the system. It is important to remark that when one calculates expectation values only one or two variables are involved in the integration; thus we can integrate over the remaining $N-2$ variables and simplify the problem. This idea gives rise to the concept of reduced density matrix [6].

In general, the *density matrix of order p* is defined as

$$\gamma_p\left(\mathbf{x}_1\mathbf{x}_2\cdots\mathbf{x}_N, \mathbf{x}_1^{'}\mathbf{x}_2^{'}\cdots\mathbf{x}_N^{'}\right) \equiv$$

$$\equiv \binom{N}{p}\int \gamma_N\left(\mathbf{x}_1\mathbf{x}_2\cdots\mathbf{x}_p\mathbf{x}_{p+1}\cdots\mathbf{x}_N, \mathbf{x}_1^{'}\mathbf{x}_2^{'}\cdots\mathbf{x}_p^{'}\mathbf{x}_{p+1}\cdots\mathbf{x}_N\right)d\mathbf{x}_{p+1}\cdots\mathbf{x}_N. \tag{1.70}$$

In particular, the single–particle density matrix is defined as

$$\gamma_1(\mathbf{x}_1, \mathbf{x}_1^{'}) =$$

$$= N\int d\mathbf{x}_2\int d\mathbf{x}_3\int d\mathbf{x}_4\cdots\int d\mathbf{x}_N\gamma\left(\mathbf{x}_1\mathbf{x}_2\mathbf{x}_3\mathbf{x}_4\cdots\mathbf{x}_N, \mathbf{x}_1^{'}\mathbf{x}_2\mathbf{x}_3\mathbf{x}_4\cdots\mathbf{x}_N\right) =$$

$$= N \int d\mathbf{x}_2 \int d\mathbf{x}_3 \int d\mathbf{x}_4 \cdots \int d\mathbf{x}_N \Psi\left(\mathbf{x}_1\mathbf{x}_2\mathbf{x}_3\mathbf{x}_4\cdots\mathbf{x}_N\right)\Psi^*(\mathbf{x}_1^{'}\mathbf{x}_2\mathbf{x}_3\mathbf{x}_4\cdots\mathbf{x}_N). \tag{1.71}$$

The reduced two–particle density matrix is given by

$$\gamma_2(\mathbf{x}_1\mathbf{x}_2,\mathbf{x}_1^{'}\mathbf{x}_2^{'}) = \frac{N(N-1)}{2}\int d\mathbf{x}_3 \int d\mathbf{x}_4 \int d\mathbf{x}_N \gamma\left(\mathbf{x}_1\mathbf{x}_2\mathbf{x}_3\mathbf{x}_4\cdots\mathbf{x}_N,\mathbf{x}_1^{'}\mathbf{x}_2^{'}\mathbf{x}_3\mathbf{x}_4\cdots\mathbf{x}_N\right), \tag{1.72}$$

where $N(N-1)/2$ is a convenient normalization factor. This density matrix determines the expectation value of the particle–particle interaction, of static correlation and response functions and some related quantities.

The structure of reduced density matrices in quite simple: all coordinates that γ does not depend upon are set equal in Ψ and Ψ^*, and integrated over.

The reduced density matrices γ_1 and γ_2 have the following properties:

1. they are Hermitian

$$\gamma_1(\mathbf{x}_1,\mathbf{x}_1^{'}) = \gamma_1^*(\mathbf{x}_1,\mathbf{x}_1^{'}) \tag{1.73}$$

$$\gamma_2(\mathbf{x}_1\mathbf{x}_2,\mathbf{x}_1^{'}\mathbf{x}_2^{'}) = \gamma_1^*(\mathbf{x}_1\mathbf{x}_2,\mathbf{x}_1^{'}\mathbf{x}_2^{'}); \tag{1.74}$$

2. they are positive semidefinite

$$\gamma_1(\mathbf{x}_1,\mathbf{x}_1) \geq 0 \tag{1.75}$$

$$\gamma_2(\mathbf{x}_1\mathbf{x}_2,\mathbf{x}_1\mathbf{x}_2) \geq 0; \tag{1.76}$$

3. because of antisymmetry, they change sign on exchange of two primed or unprimed particles indices

$$\gamma_2(\mathbf{x}_1\mathbf{x}_2,\mathbf{x}_1^{'}\mathbf{x}_2^{'}) = -\gamma_2(\mathbf{x}_2\mathbf{x}_1,\mathbf{x}_1^{'}\mathbf{x}_2^{'}) = -\gamma_2(\mathbf{x}_1\mathbf{x}_2,\mathbf{x}_2^{'}\mathbf{x}_1^{'}) = \gamma_2(\mathbf{x}_2\mathbf{x}_1,\mathbf{x}_2^{'}\mathbf{x}_1^{'}); \tag{1.77}$$

4. γ_1 normalizes to the total number of electrons (N):

$$\mathrm{Tr}\gamma_1(\mathbf{x}_1,\mathbf{x}_1^{'}) = \int \gamma_1(\mathbf{x}_1,\mathbf{x}_1)d\mathbf{x}_1 = N \tag{1.78}$$

and γ_2 normalizes to the number of electrons pair:

$$\mathrm{Tr}\gamma_2(\mathbf{x}_1\mathbf{x}_2,\mathbf{x}_1^{'}\mathbf{x}_2^{'}) = \int\int \gamma_2(\mathbf{x}_1\mathbf{x}_2,\mathbf{x}_1\mathbf{x}_2)d\mathbf{x}_1 d\mathbf{x}_2 = \frac{N(N-1)}{2} \tag{1.79}$$

the reduces density matrices γ_1 and γ_2, admit eigenfunctions and eigenvalues. The eigenfunctions of γ_1 are called *natural spin orbitals* and the relative eigenvalues are called *occupation numbers*. The eigenfunction of γ_2 are called *natural germinals*.

Spinless Density Matrices

Many operators of interest in the electronic problem do not depend on the spin variables. This makes useful to sum over the spin variables and work with spinless density matrices [7].

The first and the second–order spinless density matrices are

$$\rho_1(\mathbf{r}_1, \mathbf{r}_1^{'}) \equiv \sum_{s_1} \gamma_1(\mathbf{r}_1 s_1, \mathbf{r}_1^{'} s_1), \tag{1.80}$$

$$\rho_1(\mathbf{r}_1 \mathbf{r}_2, \mathbf{r}_1^{'} \mathbf{r}_2^{'}) \equiv \sum_{s_1, s_2} \gamma_2(\mathbf{r}_1 s_1 \mathbf{r}_2 s_2, \mathbf{r}_1^{'} s_1 \mathbf{r}_2^{'} s_2). \tag{1.81}$$

The diagonal element of the first–order spinless density matrix is just the electron density.

1.4 The Hohenberg–Kohn (HK)Theorems

In 1964, Hohenberg and Kohn showed that the many–electron wave function was a too complicated entity to deal with as the fundamental variable in a variational approach. They chose instead to use the electron density as their fundamental variable. That is, they considered the ground state of the system to be defined by that electron density distribution which minimises the total energy. Furthermore, they showed that all other ground state properties of the system (e.g. lattice constant, cohesive energy, etc) are functionals of the ground state electron density. That is, that once the ground state electron density is known all other ground state properties follow (in principle, at least). The field of rigorous density functional theory was born in 1964 with the publication of the Hohenberg and Kohn paper (1964). They proved the following:

I. *Every observable of a stationary quantum mechanical system (including energy), can be calculated, in principle exactly, from the ground-state density alone, i.e., every observable can be written as a functional of the ground-state density.*

II. *The ground state density can be calculated, in principle exactly, using the variational method involving only density,*

The original theorems refer to the time independent (stationary) ground state, but are being extended to excited states and time-dependent potentials (see section 1.7).

These theorems were derived in the following way. Within a Born-Oppenheimer approximation, the ground state of the system of electrons is a result of positions of nuclei. If we rewrite the Hamiltonian in Eq. (1.2) in the following explicit form:

$$\hat{H}_{el} = \hat{T}_e + \hat{U}_{ee} + \hat{V}_{ext} \tag{1.82}$$

In this hamiltonian, the kinetic energy of electrons ($\hat{T}_e$) and the electron-electron interaction ($\hat{U}_{ee}$) "adjust" themselves to the external (i.e., coming from nuclei) potential $\hat{V}_{ext}$. Once the $\hat{V}_{ext}$ is in place, everything else is, including electron density, which simply adjusts itself to give the lowest possible total energy of the system. The external potential $\hat{V}_{ext}$ is the only variable term in this equation, and everything else depends indirectly on it.

Hohenberg and Kohn established and underlined an important point: $\hat{V}_{ext}$ is uniquely determined from the knowledge of electron density $\rho(\mathbf{r})$. In other words, there is a precise mapping from $\rho(\mathbf{r})$ to $\hat{V}_{ext}$ and, actually, the mapping is accurate within a constant, which would not change anything, since Schrödinger equations with $\hat{H}_{el}$ and $\hat{H}_{el}+const$ yields exactly the same eigenfunctions, i.e., states (it is easy to prove based on the linear property of the hamiltonian), and the energies will be simply elevated by the value of this *const*. Note that all energies are known only within some constant, which establishes the frame of reference.

This mapping is so important because the knowledge of density provides total information about the system, and formally if we know the density, we know everything there is to known. Since $\rho(\mathbf{r})$ determines number of electrons, N:

$$N = \int \rho(\mathbf{r}) d\mathbf{r} \tag{1.83}$$

and ρ determines the $\hat{V}_{ext}$, the knowledge of total density is as good, as knowledge of Ψ, i.e., the wave function describing the state of the system. They proved it through a contradiction:

1. Assume that we have an exact ground state density $\rho(\mathbf{r})$.

2. Assume that the ground state is nondegenerate (i.e., there is only one wave function Ψ for this ground state.

3. Assume that for the density $\rho(\mathbf{r})$ there are two possible external potentials: $\hat{V}_{ext}$ and $\hat{V}'_{ext}$, which obviously produce two different hamiltonians: $\hat{H}_{el}$ and $\hat{H}'_{el}$, respectively. They obviously produce two different

wave functions for the ground state: Ψ and Ψ', respectively. In correspondence the energies are: $E_0 = \langle\Psi|H|\Psi\rangle$ and $E_0' = \langle\Psi'|H'|\Psi'\rangle$.

4. Now, let us calculate the expectation value of energy for the Ψ' with the hamiltonian $\hat{H}$ and use the variational theorem:

$$E_0 < \langle\Psi'|H|\Psi'\rangle = \overbrace{\langle\Psi'|H'|\Psi'\rangle}^{E_0'} + \langle\Psi'|H - H'|\Psi'\rangle =$$

$$= E_0' + \int \rho(\mathbf{r})[\hat{V}_{ext} - \hat{V}'_{ext}]d\mathbf{r}. \tag{1.84}$$

5. Now let us calculate the expectation value of energy for the Ψ with the hamiltonian $\hat{H}'$ and use the varational theorem:

$$E_0' < \langle\Psi|H'|\Psi\rangle = \underbrace{\langle\Psi|H|\Psi\rangle}_{E_0} + \langle\Psi|H' - H|\Psi\rangle =$$

$$E_0 - \int \rho(\mathbf{r})[\hat{V}_{ext} - \hat{V}'_{ext}]d\mathbf{r}. \tag{1.85}$$

6. By adding equations (1.84) and (1.85) by sides we obtain:

$$E_0 + E_0' < E_0' + E_0 \tag{1.86}$$

and it leads to a contradiction.

Since now, we know that $\rho(\mathbf{r})$ determines N and $\hat{V}_{ext}$, it also determines all properties of the ground state, including the kinetic energy of electrons T_e and energy of interaction among electrons U_{ee}, i.e., the total ground state energy is a functional of density with the following components

$$E[\rho] = T_e[\rho] + V_{ext}[\rho] + U_{ee}[\rho] \tag{1.87}$$

Additionally, HK grouped together all functionals which are secondary (i.e., which are responses) to the $V_{ext}[\rho]$:

$$E[\rho] = V_{ext}[\rho] + F_{HK}[\rho] = \int \rho(\mathbf{r})\hat{V}_{ext}(\mathbf{r})d\mathbf{r} + F_{HK}[\rho] \tag{1.88}$$

The F_{HK} functional operates only on density and is universal, i.e., its form does not depend on the particular system under consideration (note that N-representable densities integrate to N, and the information about the number of electrons can be easily obtained from the density itself).

$$F[\rho] \equiv T[\rho] + U_{ee}[\rho] \tag{1.89}$$

The second HK theorem provides variational principle in electron density representation $\rho(\mathbf{r})$ For a trial density $\tilde{\rho}(\mathbf{r})$ such that $\tilde{\rho}(\mathbf{r}) \geq \mathbf{0}$ and for which $\int \tilde{\rho}(\mathbf{r}) d\mathbf{r} = N$,

$$E_0 \leq E[\tilde{\rho}] \tag{1.90}$$

where $E[\tilde{\rho}]$ is the energy functional. In other words, if some density represents the correct number of electrons N, the total energy calculated from this density cannot be lower than the true energy of the ground state.

As to the necessary conditions for this theorem, there is still some controversy concerning the socalled representability of density. The N-representability, i.e., the fact that the trial $\tilde{\rho}$ has to sum up to N electrons is easy to achieve by simple rescaling. It is automatically insured if $\rho(\mathbf{r})$ can be mapped to some wave function. Assuring that the trial density has also V_{ext}-representability (usually denoted in the literature as v-representability) is not so easy. Levy (1982) and Lieb (1983) have shown, that there are some "reasonable" trial densities, which are not the ground state densities for any possible V_{ext} potential, i.e., they do not map to any external potential. Such densities do not correspond therefore to any ground state, and their optimization will not lead to a ground state. Moreover, during energy minimization, we may take a wrong turn, and get stuck into some non v-representable density and never be able to be converged to a physically relevant ground state density. For an interesting discussion, see Hohenberg *et al.* (1990). Assuming that we restrict ourselves only to trial densities which are both N and v representable, the variational principle for density is easly proven, since each trial density $\tilde{\rho}$ defines a hamiltonian $\hat{\tilde{H}}_{el}$. From the hamiltonian we can derive the corresponding wave function $\tilde{\Psi}$ for the ground state represented by this hamiltonian. And according to the traditional variational principle, this wave function $\tilde{\Psi}$ will not be a ground state for the hamiltonian of the real system $\hat{H}_{el}$:

$$\tilde{\rho} \rightarrow \hat{\tilde{H}}_{el} \rightarrow \tilde{\Psi}; \quad \langle\, \tilde{\Psi} | H | \tilde{\Psi} \,\rangle = E[\tilde{\rho}] \geq E[\rho_0] \equiv E_0 \tag{1.91}$$

where $\rho_0(\mathbf{r})$ is the true ground state density of the real system.

The condition of minimum for the energy functional: $\delta E[\rho(\mathbf{r})] = 0$ needs to be constrained by the N-representability of density which is optimized[1]. The Lagrange's method of undetermined multipliers is a very convenient

[1]It also needs to be constrained by v-representability, but we still do not know how to express v-representability in a closed mathematical form. There exist, however, methods, e.g., *constrained search* (Levy, 1982) and *local-scaling transformation* (Petkov *et al*, 1986)

approach for the constrained minimization problems. In this method we represent constraints in such a way that their value is exactly zero when they are satisfied. In our case, the N representability constraint can be represented as:

$$constraint = \int \rho(\mathbf{r})d\mathbf{r} - N = 0 \tag{1.92}$$

These constraints are then multiplied by an undetermined constants and added to a minimized function or functional.

$$E[\rho(\mathbf{r})] - \mu \left[\int \rho(\mathbf{r})d\mathbf{r} - N \right] \tag{1.93}$$

where μ is yet undetermined Lagrange multiplier. Now, we look for the minimum of this expression by requiring that its differential is equal to zero (a necessary condition of minimum).

$$\delta \left\{ E[\rho(\mathbf{r})] - \mu \left[\int \rho(\mathbf{r})d\mathbf{r} - N \right] \right\} = 0 \tag{1.94}$$

Solving this differential equation will provide us with a prescription of finding a minimum which satisfies the constraint. In our case it leads to:

$$\delta E[\rho(\mathbf{r})] - \mu\delta \left\{ \int \rho(\mathbf{r})d\mathbf{r} \right\} = 0 \tag{1.95}$$

since μ and N are constants. Using the definition of the differential of the functional (see [8]):

$$F[f + \delta f] - F[f] = \delta F = \int \frac{\delta F}{\delta f(x)} \delta f(x)dx \tag{1.96}$$

and the fact that differential and integral signs may be interchanged, we obtain

$$\int \frac{\delta E[\rho(\mathbf{r})]}{\delta \rho(\mathbf{r})} \delta\rho(\mathbf{r})d\mathbf{r} - \mu \int \delta\rho(\mathbf{r})d\mathbf{r} = 0. \tag{1.97}$$

Since integration runs over the same variable and has the same limits, we can write both expressions under the same integral:

$$\int \left\{ \frac{\delta E[\rho(\mathbf{r})]}{\delta \rho(\mathbf{r})} - \mu \right\} \delta\rho(\mathbf{r})d\mathbf{r} = 0 \tag{1.98}$$

which provides the condition for constrained minimisation and defines the value of the Lagrange multiplier at minimum. It is also expressed here via external potential from equation (1.88):

$$\mu = \frac{\delta E[\rho(\mathbf{r})]}{\delta \rho(\mathbf{r})} = \hat{V}_{ext}(\mathbf{r}) + \frac{\delta F_{HK}(\rho(\mathbf{r})}{\delta \rho(\mathbf{r})}. \tag{1.99}$$

which assure v-representability during density optimization, though their algorithmic implementation needs to be done.

Density functional theory gives a firm definition of the chemical potential μ, and leads to several important general conclusions (Chapters 4 and 5 of [8]).

1.5 Kohn–Sham Method

Eq. (1.99) gives the expression to calculate the ground state electron density of a many–electron system. Unfortunately this equation is difficult to handle, consequently one commonly employs a scheme suggested by Kohn and Sham. They proposed the use of an auxiliary noninteracting system, the *Khon–Sham system*, whose ground state electron density is exactly the same as that of the interacting system and they introduced an *exchange term* (E_{xc}) in order to take care of electron correlation. The Hamiltonian of the noninteracting reference system is

$$H_s = \sum_i^N \Big(-\frac{1}{2}\nabla_i^2 \Big) + \sum_i^N v_i(\mathbf{r}). \tag{1.100}$$

It is described by the determinantal wave function

$$\Psi_s = \frac{1}{\sqrt{N!}} det[\psi_1 \psi_2 \cdots \psi_N] \tag{1.101}$$

where the ψ_i are the lowest eigenstate of the eigenvalue equation

$$\Big[-\frac{1}{2}\nabla^2 + v_s(\mathbf{r}) \Big] \psi_i = \varepsilon_i \psi_i. \tag{1.102}$$

The kinetic energy and the correlation density in the Kohn–Sham method are

$$T_s = \sum_i^N \langle \psi_i | -\frac{1}{2}\nabla^2 | \psi_i \rangle \tag{1.103}$$

$$\rho = \sum_i^N |\psi_i|^2; \tag{1.104}$$

while, in general, the same quantities for an interacting system are respectively,

$$T = \sum_i n_i \langle \psi_i | -\frac{1}{2}\nabla^2 | \psi_i \rangle \tag{1.105}$$

$$\rho(\mathbf{r}) = \sum_s \sum_i n_i |\psi_i(\mathbf{r}, s)|^2; \tag{1.106}$$

where ψ_i and n_i are natural spin orbitals and occupation numbers, respectively. In Kohn–Sham method the universal functional (1.89) is usually rewritten

$$F[\rho] = T_s[\rho] + J[\rho] + E_{xc}[\rho] \tag{1.107}$$

where $J[\rho]$ is the self repulsion energy of an electron distribution $\rho(\mathbf{r})$, and

$$E_{xc} \equiv T[\rho] - T_s[\rho] + U_{ee} - J[\rho] \tag{1.108}$$

is the exchange–correlaton energy. Using equations (1.107) and (1.108) the energy functional (1.88) becomes

$$E[\rho] = T_s[\rho] + J[\rho] + E_{xc}[\rho] + \int \rho(\mathbf{r}) v(\mathbf{r}) d\mathbf{r}. \tag{1.109}$$

The energy expressed in terms of N Kohn–Sham orbital is

$$E[\rho] = \sum_i^N \int \psi_i^*(\mathbf{r}) \Big(-\frac{1}{2}\nabla_i^2 \Big) \psi_i(\mathbf{r}) d\mathbf{r} + J[\rho] + E_{xc}[\rho] + \int \rho(\mathbf{r}) v(\mathbf{r}) d\mathbf{r}. \tag{1.110}$$

Applying the variational principle under the constraint

$$\int \psi_i^*(\mathbf{r}) \psi_j(\mathbf{r}) d\mathbf{r} = \delta_{ij} \tag{1.111}$$

we found

$$\Big[-\frac{1}{2}\nabla^2 + v_{eff}(\mathbf{r}) \Big] \psi_i = \sum_j \varepsilon_{ij} \psi_j \tag{1.112}$$

where v_{eff} is the effective potential defined as

$$v_{eff} \equiv v(\mathbf{r}) + \frac{\delta J[\rho]}{\delta[\rho]} + v_{xc}(\mathbf{r}) \tag{1.113}$$

and $v_{xc}(\mathbf{r})$ is the *exchange–correlation potential*

$$v_{xc}(\mathbf{r}) \equiv \frac{\delta E_{xc}[\rho]}{\delta \rho(\mathbf{r})}. \tag{1.114}$$

Following the standard procedure used to solve the Hartree–Fock equations, a diagonalization of the ε_{ij} matrix gives us the *Kohn–Sham equation* in canonical form

$$\Big[-\frac{1}{2}\nabla + v_{eff}(\mathbf{r}) \Big] \psi_i = \varepsilon_i \psi_i. \tag{1.115}$$

In other words, within the Kohn–Sham system, the electrons obey a simple, one–particle, Schrödinger equation with an effective external potential, v_{eff}. As v_{eff} is a functional of the electronic density, the solution of this equation

has to be performed self–consistently as well as for the Hartree-Fock equations, with the only difference that v_{eff} is local. It is usually decomposed in the form represented in Eq. (1.113) where the first term is the external potential (generally the Coulomb interaction between the electrons and nuclei), whereas the second includes the classical part of electron–electron interaction and the third one (unknown) takes into account all the many body effects.

1.6 Approximations

Kohn–Sham theory is, in principle, exact but, in order to make DFT practical it needs some approximations for the unknown exchange-correlation potential that includes all the non-Coulomb electron–electron interactions. This approximation involves constructing an expression for the unknown $E_{xc}[\rho]$ functional, which contains all many–body aspects of the problem. It is with this type of approximations that the present section is concerned, therefore I deal with local functional (as *Local Density Approximation* (LDA)), semilocal (or *Gradient Dependent functionals* (GGA)) and nonlocal or hybrid functional (as *Colle–Salvetti*).

1.6.1 Local Density Approximation (LDA)

Historically (and in many applications also practically) the most important type of approximation is the local-density approximation (LDA). To understand the concept of an LDA recall first how the noninteracting kinetic energy $T_s[\rho]$ is treated in the Thomas-Fermi approximation [3], [4]. In a homogeneous system one knows that, per volume (the change from chapital T to a lower–case t is commonly used to indicated quantities per volume)

$$t_s^{hom}(\rho) = \frac{3\hbar^2}{10m}(3\pi^2)^{2/3}\rho^{5/3} \tag{1.116}$$

where $\rho = const.$ In an inhomogeneous system, with $\rho = \rho(r)$, one approximates locally

$$t_s(\mathbf{r}) \approx t_s^{hom}(\rho(\mathbf{r})) = \frac{3\hbar^2}{10m}(3\pi^2)^{2/3}\rho^{5/3}(\mathbf{r}) \tag{1.117}$$

and obtains the full kinetic energy by integration over all space

$$T_s^{LDA}[\rho] = \int d^3r t_s^{hom}(\rho(\mathbf{r})) = \frac{3\hbar^2}{10m}(3\pi^2)^{2/3}\int d^3r\rho^{5/3}(\mathbf{r}). \tag{1.118}$$

For the kinetic energy the approximation $T_s[\rho] \approx T_s^{LDA}[\rho]$ is much inferior to the exact treatment of T_s in terms of orbitals, offered by the Kohn-Sham equations, but the LDA concept turned out to be highly useful for another component of the total energy (1.110), the exchange-correlation energy E_{xc}. At this point it is useful to separate the exchange and correlation potential part ε_{xc} in

$$\varepsilon_{xc} = \varepsilon_x + \varepsilon_c. \tag{1.119}$$

The exchange part has been calculated within the Thomas Fermi model [3], [9], [10] and [11] to be

$$\varepsilon_x = -\frac{3}{4}\Big(\frac{3}{\pi}\Big)^{\frac{1}{3}}\rho^{\frac{1}{3}}. \tag{1.120}$$

For the correlation part ε_c the situation is more complicated since ε_c^{hom} is not known exactly: the determination of the correlation energy of a homogeneous interacting electron system (an electron liquid) is already a difficult many-body problem on its own! Early approximate expressions for ε_c^{hom} were based on applying perturbation theory (e.g. the random phase approximation) to this problem [12], [13]. These approximations became outdated with the advent of highly precise Quantum Monte Carlo (QMC) calculations for the electron liquid, by Ceperley and Alder [14].

1.6.2 Semilocal functionals: Generalized–Gradient Approximations (GGA)

In the LDA one exploits knowledge of the density at point $\mathbf{r}$. Any real system is spatially inhomogeneous, *i. e.*, it has a spatially varying density$\rho(\mathbf{r})$, and it would clearly be useful to also include information on the rate of this variation in the functional. The simplest improvement that can be done to *LDA* is to correct for the inhomogeneities of the atomic and molecular electron density. This can be done by adding to the *LDA* potential corrections depending on the local density gradient of electron density. Such a functional, of the general form

$$E_{xc}^{GGA}[\rho] = E_{xc}^{LDA} + \int d^3r\; f\Big(\rho(\mathbf{r}), \nabla\rho(\mathbf{r})\Big), \tag{1.121}$$

is known as *Generalized–Gradient Approximation* (GGA). Different GGAs differ in the choice of the function $f(\rho, \nabla\rho)$. Note that this makes different GGA much more different from each other than the different parametrizations of the LDA: essentially there is only one correct expression for $\varepsilon_{xc}(\rho)$,

and the various parametrizations of the LDA [12], [13], [15], [16], [17] are merely different ways of writing it. On the other hand, depending on the method of construction employed for obtaining $f(\rho, \nabla\rho)$ one can get very different GGA. In particular, GGA used in quantum chemistry typically proceed by fitting parameters to test sets of selected molecules. On the other hand, GGA used in physics tend to emphasize exact constraints. In fact, an espansion of Eq. (1.121) retains both even and odd terms, while the exchange energy must be even in the electron density. Thus, the lowest order gradient correction to the LDA exchange–correlation energy is determined by symmetry considerations and dimensional analysis

$$E_{xc}^{GGA} = E_{xc}^{LDA} - \beta \int \frac{\nabla\rho(\mathbf{r})^2}{\rho(\mathbf{r})^{4/3}} d\mathbf{r}, \tag{1.122}$$

where β is a constant. This equation presents a divergence asymptotically. Anyway it is possible to find many other corrections of the form $f\Big(\rho(\mathbf{r}), (\nabla\rho(\mathbf{r}))^2\Big)$ that have the right asympotic behaviour. Among these, one of the most used is the *Becke-exchange* functional [18]:

$$E_{xc}^{B} = E_{xc}^{LDA} - \beta \int \rho^{4/3} \frac{x^2}{1 + 6\beta x \sinh^{-1} x} d\mathbf{r}, \tag{1.123}$$

where β is a constant and $x = \frac{|\nabla\rho|}{\rho^{4/3}}$.

Nowadays the most popular (and most reliable) GGA are PBE (denoting the functional proposed in 1996 by Perdew, Burke and Ernzerhof [19]) in physics, and BLYP (denoting the combination of Becke's 1988 exchange functional [18] with the 1988 correlation functional of Lee, Yang and Parr [20]) in chemistry.

1.6.3 Hybrid functionals. Colle–Salvetti functional

The idea of using hybrid functionals was introduced by Alex Becke in 1993 [22] who suggested that the simple *ab initio* functionals [23] are inadequate to reproduce many molecular properties, such as atomization energies, bond lengths, *etc.* and he proposed the hybridization of exchange–correlation functionals with Hartree–Fock exact exchange.

A hybrid functional, in fact, is an exchange–correlation functional used in density functional theory that incorporates a portion of exact exchange from Hartree–Fock theory with exchange and correlation from other sources (*ab initio*, such as LDA, or empirical).

The exchange correlation functional for a hybrid is usually a linear combination of the Hartree–Fock exchange ($E_x^{\rm HF}$) and some other ones combinations of exchange and correlation functionals. The parameters relating the amount of each functional can be arbitrarily assigned and is usually fitted to reproduce well some set of observables (bond lengths, band gaps, etc.). For example, the popular B3LYP (Becke, three-parameter, Lee-Yang-Parr) exchange-correlation functional is:

$$E_{xc}^{\rm B3LYP} = E_{xc}^{\rm LDA} + a_0(E_x^{\rm HF} - E_x^{LDA}) + a_x(E_x^{\rm GGA} - E_x^{LDA}) + a_c(E_c^{\rm GGA} - E_c^{LDA}) \tag{1.124}$$

where $a_0 = 0.20$, $a_x = 0.72$, $a_c = 0.81$ and are the three empirical parameters; $E_x^{\rm GGA}$ and $E_c^{\rm GGA}$ are the generalized gradient approximation formulated with the Becke 88 exchange functional [18] and the correlation functional of Lee, Yang and Parr (LYP) [20].

Another important example of hybrid functional is the so–called *Colle–Salvetti* (CS) functional. In 1975, R. Colle and O. Salvetti [21] proposed a correlation energy formula in which the correlation energy density is expressed in terms of the electron density and Laplacian of the second–order Hartree–Fock density matrix:

$$E_c = -4a \int \frac{\rho_2^{\rm HF}(\mathbf{r},\mathbf{r})}{\rho(\mathbf{r})} \Big(\frac{1 + b\rho^{-8/3}(\mathbf{r})[\nabla_s^2 \rho_2^{\rm HF}(\mathbf{r},\mathbf{s})]_{s=0} exp[-c\rho^{-1/3}(\mathbf{r})]}{1 + d\rho(\mathbf{r})^{-1/3}} \Big) d\mathbf{r} \tag{1.125}$$

where $\rho_2^{\rm HF}(\mathbf{r},\mathbf{s})$ is the second–order Hartree-Fock reduced density matrix expressed in terms of interparticles coordinates

$$\mathbf{r} = \frac{\mathbf{r}_1 + \mathbf{r}_2}{2}, \quad \mathbf{s} = \mathbf{r}_1 - \mathbf{r}_2, \tag{1.126}$$

and $a = 0.04918$, $b = 0.132$, $c = 0.2533$ and $d = 0.349$.

This formula was arrived at by Colle and Salvetti by a theoretical analysis accompained by a series of approximations, beginning from the reasonable proposition that the second–order density matrix including correlation may be approximated by the Hartree–Fock second order density matrix times a correlation factor. The constants a, b, c and d in the final formula were obtained by a fitting procedure using only the Hartree–Fock orbital for the helium atom. In this formulation, the correlation kinetic energy is assumed to be zero. The only contribution to the correlation energy comes from the electron–electron potential energy, computed from the model of two–electron reduced density matrix. Lee, Yang and Parr, in [20], restated the Colle–Salvetti formula in Eq. (1.125) including the density, a local "Weizsacker"

kinetic–energy density $t_{\rm W}$ and the local Hartree–Fock kinetic–energy density $t_{\rm HF}$ defined as following, respectivley:

$$t_{\rm W}(\mathbf{r}) = \frac{1}{8}\frac{|\nabla\rho(\mathbf{r})|^2}{\rho(\mathbf{r})} - \frac{1}{8}\nabla^2\rho, \tag{1.127}$$

$$t_{\rm HF}(\mathbf{r}) = \frac{1}{2}\sum|\psi_i|^2 - \frac{1}{8}\nabla^2\rho \tag{1.128}$$

The CS correlation energy formula in terms of density, $t_{\rm W}$ and $t_{\rm HF}$ is

$$E_c = -a\int\frac{\rho(\mathbf{r}) + b\rho^{-2/3}(\mathbf{r})[t_{\rm HF}(\mathbf{r}) - 2t_{\rm W}(\mathbf{r})]e^{-c\rho^{-1/3}(\mathbf{r})}}{1 + d\rho^{-1/3}(\mathbf{r})}d\mathbf{r}. \tag{1.129}$$

and in terms of density and its gradient can be written as in the following:

$$E_c = \int\Big[\frac{-a\rho}{1+d\rho^{-1/3}} + \frac{ab\rho^{-5/3}|\nabla\rho|^2e^{-c\rho^{-1/3}}}{4\rho(1+d\rho^{-1/3})} - \frac{ab\rho^{-2/3}e^{-c\rho^{-1/3}}T_{\rm HF}}{(1+d\rho^{-1/3})} + \frac{abe^{-c\rho^{-1/3}}\rho^{-2/3}\nabla^2\rho}{8(1+d\rho^{-1/3})}\Big]d\mathbf{r}, \tag{1.130}$$

where in $T_{\rm HF}$ we have included a local kinetic part and a term with $\nabla^2\rho$: $T_{\rm HF} = \tilde{t}_{\rm hf} + \eta\nabla^2\rho$. Equation (1.130) lacks of being pure density functionals because of the appearance in it of the Hartree–Fock kinetic–energy density $T_{\rm HF}$ which depends on individual orbital densities. It is possible to turn Eq. (1.130) into explicit density–functional formulas by using expansions, whereby $T_{\rm HF}$ is expanded, by Lee, Yang and Parr, about the Thomas–Fermi local kinetic–energy density to second order:

$$T_{\rm HF}^{\rm LYP} = \underbrace{C_{\rm F}\rho^{5/3} + \frac{1}{72}\frac{|\nabla\rho|^2}{\rho}}_{\tilde{t}_{hf}} + \underbrace{\frac{1}{24}}_{\eta}\nabla^2\rho. \tag{1.131}$$

For the Colle and Salvetti expansion

$$T_{\rm HF}^{\rm CS} = \underbrace{\frac{1}{2}\sum|\nabla\psi|^2}_{\tilde{t}_{hf}}\underbrace{-\frac{1}{8}}_{\eta}\nabla^2\rho. \tag{1.132}$$

We have implemented a fortran code in the TURBOMOLE programm [78] in which the correlation functional has been obtained starting from the LYP functional but inserting the kinetic energy in therms of Kohn–Sham orbitals:

$$E_c = \int\Big[-\frac{a\rho}{1+d\rho^{-1/3}} - \frac{abe^{-c\rho^{-1/3}}\rho^{-2/3}\tilde{t}_{hf}}{1+d\rho^{-1/3}} + \frac{abce^{-c\rho^{-1/3}}\rho^{-2}|\nabla\rho|^2}{12(1+d\rho^{-1/3})} +$$

$$+\frac{abde^{-c\rho^{-1/3}}\rho^{-2}|\nabla\rho|^2}{12(1+d\rho^{-1/3})^2}-\frac{abe^{-c\rho^{-1/3}}\rho^{-5/3}|\nabla\rho|^2}{12(1+d\rho^{-1/3})}\Big]d\mathbf{r}. \qquad (1.133)$$

In our implementation $\tilde{t}_{hf}$ is the one described in Eq. (1.132) and the term of the second order expansion ($\nabla^2\rho$) has been treated with the gradent theorem in order to obtain only terms in ρ and $\nabla\rho$.

In Table 1.1 we report the results of our implementation with some atoms and ions, and in Table 1.2 the implementation with some molecules.

Atom	Energy [20]	Energy (implementation CS)
He	0.0416	0.04158
Li^+	0.0438	0.04390
He^{2+}	0.0442	0.04421
Be	0.0926	0.09265

Table 1.1: *Implementation of Colle–Salvetti correlation functional for some atoms and ions with comparing to the results obtained by Lee Yang and Parr [20].*

Molecule	R	E_{HF} [24]	E_{HF} implemented	E_{XC} [24]	E_{XC} implemented
C_2	2.00	75.32869	75.32873	0.3872	0.38747
	2.10	75.36906	75.36909	0.3845	0.38480
	2.35	75.40182	75.40184	0.3785	0.37879
	4.00	75.15516	75.15516	0.3561	0.35633
F_2	2.30	198.75462	198.75448	0.6732	0.67353
	2.50	198.77194	198.77182	0.6690	0.66934
	2.725	198.76284	198.76271	0.6650	0.66533
	4.00	198.60303	198.60286	0.6527	0.65242
CH_4	—	—	40.21540	0.290	0.29023
H_2O	—	—	76.06436	0.336	0.33643

Table 1.2: *Implementation of Colle–Salvetti correlation functional for some molecules with comparing to the results obtained by Lee Yang and Parr [24].*

1.7 Time-Dependent Density Functional Theory

Time–dependent density functional theory (TD–DFT) extends the basic ideas of groundstate density functional theory (DFT) to the treatment of time-dependent phenomena and in particular of excitations. As DFT can

be viewd as an alternative formulation to solve the stationary Schrödinger equation, TD–DFT can be viewed as an alternative formulation of time–dependent quantum mechanics. Also, TD–DFT retains all the advantages of DFT: the $3N$–dimensional wave function is replaced by the 3–dimensional electron density.

The scheme for the construction of TD–DFT is similar to the one used to derive DFT. Firts the Runge–Gross theorem, which is the time–dependent analog of the Hohenberg–Kohn theorem, is proved, then the time–dependent Kohn–Sham equations are derived. This scheme can be applied for the solution of almost any time–dependent situatio. However two regimes are usually observed: if the time–dependent perturbation is weak, it is sufficient to study the system by linear–response theory; if the perturbation is strong a full solution of the Kohn–Sham equation is needed.

Let us introduce a system of N electrons, the Hamiltonian that described this system is:

$$H(\mathbf{r},t) = -\frac{1}{2}\sum_{i=1}^{N}\nabla_i^2 - \sum_{A=1}^{Nnuc}\sum_{i=1}^{N}\frac{Z_A}{|\mathbf{r}_i - \mathbf{R}_A(t)|} + \frac{1}{2}\sum_{i,j=1}\frac{1}{|\mathbf{r}_i - \mathbf{r}_j|} + V(\mathbf{r},t), \tag{1.134}$$

where $V(\mathbf{r},t)$ is a generical external time–dependent field. The time–dependent wave function of the system is a solution of the time–dependent Schrödinger equation

$$i\frac{\partial}{\partial t}\Psi(\mathbf{r},t) = H(\mathbf{r},t)\Psi(\mathbf{r},t). \tag{1.135}$$

From the wave function the electron density can be evaluated by quadrature. The electron density is the main variable in TD-DFT.

1.7.1 Runge–Gross Theorem

The Runge–Gross theorem is the time–dependent counterpart of the Hoenberg–Kohn theorem. It states that:

for a many–body system envolving from a fixed initial state there is a one–to–one correspondence between the external time–dependent potential and the electron density.

The proof of this theorem is by reduction ad absurdum. We have to demonstrate that if two potentials $v(\mathbf{r},t)$ and $v'(\mathbf{r},t)$ differ by more than a purely time–dependent function $c(t)$ they can not produce the same time-dependent density $\rho(\mathbf{r},t)$. The demonstration is splitted in two parts. First we will proove that if $v(\mathbf{r},t) \neq v'(\mathbf{r},t) + c(t)$ than the current densities $\mathbf{j}$ and

$\mathbf{j}'$, generated by v and v' respectively, are different. Then we will show that this implies, via the continuity equation, that also the densities are different.

Let us consider the Taylor expansion of the external potential with respect to the time coordinate around the initial time t_0.

$$v(\mathbf{r},t) = \sum_{k=0}^{\infty} a_k(\mathbf{r})(t-t_0)^k \tag{1.136}$$

with the expansion coefficients

$$a_k(\mathbf{r}) = \frac{1}{k!}\frac{\partial^k}{\partial t^k} v(\mathbf{r},t)\Big|_{t=t_0}, \tag{1.137}$$

and let us define the function

$$u_k(\mathbf{r}) \equiv \frac{\partial^k}{\partial t^k}\Big[v(\mathbf{r},t) - v'(\mathbf{r},t)\Big]\Big|_{t=t_0}. \tag{1.138}$$

Of course if the two potentials differ by more than a purely time–dependent function, there will be at least one k in their Taylor expansion for which $a_k(\mathbf{r}) - a'_k(\mathbf{r}) \neq$constant; that is there will be at least on k for which $u_k(\mathbf{r}) \neq$ constant.

Now let us demonstrate that if $v \neq v' + c(t)$ then the current densities $\mathbf{j}$ and $\mathbf{j}'$, generated by v and v' respectively, are different. The current density is defined as

$$\mathbf{j}(\mathbf{r},t) \equiv \langle\Psi(t)|\widehat{\mathbf{j}}(\mathbf{r})|\Psi(t)\rangle, \tag{1.139}$$

where the current density operator is

$$\widehat{\mathbf{j}}(\mathbf{r}) \equiv \frac{i}{2}\Big[\Big(\nabla\psi^\dagger(\mathbf{r})\Big)\psi(\mathbf{r}) - \psi^\dagger(\mathbf{r})\Big(\nabla\psi(\mathbf{r})\Big)\Big]. \tag{1.140}$$

The equation of motion for $\mathbf{j}$ and $\mathbf{j}'$ are

$$i\frac{d}{dt}\mathbf{j}(\mathbf{r},t) = \langle\Psi(t)|\Big[\widehat{\mathbf{j}}(\mathbf{r}), \widehat{H}(t)\Big]|\Psi(t)\rangle \tag{1.141}$$

$$i\frac{d}{dt}\mathbf{j}'(\mathbf{r},t) = \langle\Psi'(t)|\Big[\widehat{\mathbf{j}'}(\mathbf{r}), \widehat{H'}(t)\Big]|\Psi'(t)\rangle. \tag{1.142}$$

At the fixed initial state, the wave functions, the densities and the current densities must be equal in the primed and unprimed systems. Thus, at $t = t_0$ the only difference is the Hamiltonian. If we take the difference between Eq. (1.141) and Eq. (1.142) at $t = t_0$ we have

$$i\frac{d}{dt}\Big[\mathbf{j}(\mathbf{r},t) - \mathbf{j}'(\mathbf{r},t)\Big]\Big|_{t=t_0} = \langle\Psi_0|\Big[\widehat{\mathbf{j}}(\mathbf{r}), \widehat{H}(t_0) - \widehat{H'}(t_0)\Big]|\Psi_0\rangle =$$

$$= \langle\Psi_0|\left[\widehat{\mathbf{j}}(\mathbf{r}), v(\mathbf{r},t_0)-v'(\mathbf{r},t_0\right]|\Psi_0\rangle = i\rho_0(\mathbf{r})\nabla\left[v(\mathbf{r},t_0)-v'(\mathbf{r},t_0\right] = i\rho_0(\mathbf{r})\nabla u_0(\mathbf{r}). \tag{1.143}$$

If we apply the equation of motion $k+1$ times we finally have

$$\frac{d^{k+1}}{dt^{k+1}}\left[\mathbf{j}(\mathbf{r},t)-\mathbf{j}'(\mathbf{r},t)\right]\Big|_{t=t_0} = \rho_0(\mathbf{r})\nabla u_k(\mathbf{r}). \tag{1.144}$$

We have seen that, if the two time–dependent external potential differ by more than a purely time–dependent function, there will be at least one k for which $u_k(\mathbf{r}) \neq$ constant, that is there will be at least one k for which

$$\frac{d^{k+1}}{dt^{k+1}}\left[\mathbf{j}(\mathbf{r},t)-\mathbf{j}'(\mathbf{r},t)\right]\Big|_{t=t_0} \neq 0. \tag{1.145}$$

This implies that $\mathbf{j}(\mathbf{r},t) \neq \mathbf{j}'(\mathbf{r},t)$ for $t > t_0$.

Now, let us consider the continuity equation

$$\frac{\partial}{\partial t}\rho(\mathbf{r},t) = -\nabla\cdot\mathbf{j}(\mathbf{r},t). \tag{1.146}$$

If we write the continuity equation for the primed and unprimed system and take the difference, we have

$$\frac{\partial}{\partial t}\left[\rho(\mathbf{r},t)-\rho'(\mathbf{r},t)\right] = -\nabla\cdot\left[\mathbf{j}(\mathbf{r},t)-\mathbf{j}'(\mathbf{r},t)\right]. \tag{1.147}$$

We take the $(k+1)$th time derivative, at $t=t_0$ of Eq. (1.147)

$$\frac{\partial^{k+2}}{\partial t^{k+2}}\left[\rho(\mathbf{r},t)-\rho'(\mathbf{r},t)\right]\Big|_{t=t_0} = -\nabla\cdot\frac{\partial^{k+1}}{\partial t^{k+1}}\left[\mathbf{j}(\mathbf{r},t)-\mathbf{j}'(\mathbf{r},t)\right]\Big|_{t=t_0}. \tag{1.148}$$

By Eq. (1.144) we have

$$\frac{\partial^{k+2}}{\partial t^{k+2}}\left[\rho(\mathbf{r},t)-\rho'(\mathbf{r},t)\right]\Big|_{t=t_0} = -\nabla\cdot\left[\rho_0(\mathbf{r})\nabla u_k(\mathbf{r})\right]. \tag{1.149}$$

If $u_k(\mathbf{r}) \neq$ constant, as it is the case, then

$$\nabla\cdot\left[\rho_0(\mathbf{r})\nabla u_k(\mathbf{r})\right] \neq 0 \tag{1.150}$$

and from Eq. (1.149) it is clear that $\rho \neq \rho'$, from which the Runge–Gross theorem follows.

1.7.2 Time–dependent Kohn–Sham Equations

In possession of Runge–Gross theorem, it is fairly strightfoward to construct a scheme to find the electron density. Similary to what is done in

DFT, where a Kohn–Sham scheme is adopted, we can introduce an auxiliary noninteracting system subject to an external potential $v_s(\mathbf{r},t)$ such that its electron density is the same as that of the interacting system. Again we can introduce into the problem, which are solutions of the time–dependent Schrödinger equation

$$i\frac{\partial}{\partial t}\psi_i(\mathbf{r},t) = \Big[-\frac{1}{2}\nabla^2 + v_s(\mathbf{r},t)\Big]\psi_i(\mathbf{r},t). \tag{1.151}$$

The electron density can be evaluated from the time–dependent Kohn–Sham orbitals

$$\rho(\mathbf{r},t) = \sum_{i=1}^{N} |\psi_i(\mathbf{r},t)|^2. \tag{1.152}$$

Eq. (1.151) is a one–particle equation and can be. in principle, easily solved once v_s is known.

The potential v_s is usually separated into three contributions:

$$v_s(\mathbf{r},t) = v_{ext}(\mathbf{r},t) + J[\rho(\mathbf{r},t)] + v_{xc}(\mathbf{r},t), \tag{1.153}$$

where v_{ext} is the time–dependent external potential, $J[\rho]$ is the classical Coulomb potential and v_{xc} is the exchange–correlation potential that comprise all the many body effects. Unlike ordinary DFT, in TD-DFT the formal definition of the exchange–correlation potential is not easy to write because of a problem related to causality. The solution of the problem was given by van Leeuwen [25]. Usually approximate expressions for v_{xc} are used.

1.7.3 Functionals

In Eq. (1.153) the time–dependent Kohn–Sham potential is divided in two known terms v_{ext} and J, and one unknown term v_{xc} that we try to approximate using physical and mathematical arguments.

It is important to stress that v_{xc}, because of the Runge–Gross theorem is not only a functional of the electron density, but also of the initial Kohn–Sham determinant and of initial many–body wavefunctio. For pratical reasons the latter dependence is always negletted.

The *adiabatic approximation* is the simplest procedure to obtain a time–dependent exchange–correlation potential. The adiabatic time–dependent exchange–correlation potential is

$$v_{xc}^{A}(\mathbf{r},t) = v_{xc}\Big[\rho(\mathbf{r})\Big]\Big|_{\rho=\rho(t)}, \tag{1.154}$$

where $v_{xc}[\rho(\mathbf{r})]$ is any approximation to the ground state exchange–correlation potential. In practice in the adiabatic approximation we employ at each time t the ground state functional v_{xc} evaluated at the density $\rho(\mathbf{r},t)$. This approximation is quite strong, but it may be expected to work well when the system is locally close to equilibrium. This may be the case, for example, of low laying excited states, but is not the case of matter interacting with strong laser fields.

The adiabatic approximation allows to naturally extend the use of all the existing functionals for ground state DFT to TD-DFT. For example, by taking $v_{xc} = v_{xc}^{LDA}$ we obtain the so–called adiabatic local density approximation (ALDA).

1.7.4 Linear Response Theory

When the external time–dependent perturbation is small, it may not be necessary to solve time–dependent Kohn–Sham equations. The behaviour of the system can be determined, instead, via perturbation theory. In particular linear perturbation theory has prooved to be a valuable tool for the calculation of excited states energies and properties.

Consider as interacting many–particle system with a time–independent Hamiltonian H. The time–dependent Schrödinger equation for the system is

$$i\hbar\frac{\partial}{\partial t}|\Phi(t)\rangle = H|\Phi(t)\rangle \tag{1.155}$$

with the formal solution

$$|\Phi(t)\rangle = e^{-i\frac{Ht}{\hbar}}|\Psi_0\rangle, \tag{1.156}$$

where $|\Psi_0\rangle$ is the stationary solution of Schrödinger equation. If at time t_0 we turn on a time–dependent perturbation $V(t)$ the new wave function $|\Phi(t)\rangle$ must satisfy

$$i\hbar\frac{\partial}{\partial t}|\Phi(t)\rangle = \Big[H + V(t)\Big]|\Phi(t)\rangle. \tag{1.157}$$

We can solve Eq. (1.157) searching for a solution of the type

$$|\Phi(t)\rangle = e^{-i\frac{Ht}{\hbar}}A(t)|\Phi_0\rangle. \tag{1.158}$$

by substitution of Eq. (1.158) into Eq. (1.157) we find

$$i\hbar\frac{\partial}{\partial t}A(t) = e^{i\frac{Ht}{\hbar}}V(t)e^{-i\frac{Ht}{\hbar}}A(t). \tag{1.159}$$

Let us define $V_H(t) = e^{i\frac{Ht}{\hbar}} V(t) e^{-i\frac{Ht}{\hbar}}$, then, to the first order in V_H we have

$$A(t) = 1 - \frac{i}{\hbar}\int_{t_0}^{t} V_H(t')dt'. \tag{1.160}$$

Substituting in Eq. (1.158) we obtain the solution to first order

$$|\Phi(t)\rangle = e^{i\frac{Ht}{\hbar}}\Big[1 - \frac{i}{\hbar}\int_{t_0}^{t} V_H(t')dt'\Big]|\Phi_0\rangle. \tag{1.161}$$

Let us, now, compute the expectation value of a generic operator $\mathcal{O}(t)$

$$\langle\mathcal{O}(t)\rangle = \langle\Phi(t)|\mathcal{O}(t)|\Phi(t)\rangle =$$

$$= \langle\Psi_0|\Big[1 + \frac{i}{\hbar}\int_{t_0}^{t} V_H(t')dt'\Big] e^{i\frac{Ht}{\hbar}}\mathcal{O}(t)e^{-i\frac{Ht}{\hbar}}\Big[1 - \frac{i}{\hbar}\int_{t_0}^{t} V_H(t')dt'\Big]|\Psi_0\rangle. \tag{1.162}$$

This is at the first order

$$\langle\mathcal{O}(t)\rangle = \langle\Phi(t)|\mathcal{O}(t)|\Phi(t)\rangle + \frac{i}{\hbar}\int_{t_0}^{t}\langle\Psi_0|[V_H(t'), \mathcal{O}_H(t)]|\Psi_0\rangle dt', \tag{1.163}$$

where we have defined $\mathcal{O}_H(t) = e^{i\frac{Ht}{\hbar}}\mathcal{O}(t)e^{-i\frac{Ht}{\hbar}}$. A more interesting quantity is the variation of the expectation value of any operator due to the external perturbation V. This is

$$\delta\langle\mathcal{O}(t)\rangle = \langle\Psi(t)|\mathcal{O}(t)|\Psi(t)\rangle - \langle\Phi(t)|\mathcal{O}(t)|\Phi(t)\rangle =$$

$$= \frac{i}{\hbar}\int_{t_0}^{t}\langle\Psi_0|[V_H(t'), \mathcal{O}_H(t)]|\Psi_0\rangle dt'. \tag{1.164}$$

If V and $\mathcal{O}$, as it often happens, are one–body operators we can write

$$\mathcal{O}_H(t) = \int d\mathbf{r}_1 \Psi_H^\dagger(\mathbf{r}_1, t) o(\mathbf{r}_1, t)\Psi_H(\mathbf{r}_1, t) = \int d\mathbf{r}_1 o(\mathbf{r}_1, t)\rho_H(\mathbf{r}_1, t) \tag{1.165}$$

$$V_H(t') = \int d\mathbf{r}_2 \Psi_H^\dagger(\mathbf{r}_2, t') v(\mathbf{r}_2, t')\Psi_H(\mathbf{r}_2, t') = \int d\mathbf{r}_2 v(\mathbf{r}_2, t')\rho_H(\mathbf{r}_2, t') \tag{1.166}$$

where $\rho_H(\mathbf{r}, t) = e^{i\frac{Ht}{\hbar}}\rho(\mathbf{r})e^{-i\frac{Ht}{\hbar}}$ is the electron density in the Heisenberg picture. By substitution of Eq. (1.165) and Eq. (1.166) into Eq. (1.164) we find

$$\delta\langle\mathcal{O}(t)\rangle = \frac{i}{\hbar}\int_{t_0}^{t} dt' \int d\mathbf{r}_1 d\mathbf{r}_2 o(\mathbf{r}_1, t)v(\mathbf{r}_2, t')\langle\Psi_0|\Big[\rho_H(\mathbf{r}_2, t'), \rho_H(\mathbf{r}_1, t)\Big]|\Psi_0\rangle. \tag{1.167}$$

Because the integral on t' implies $t' < t$ we write

$$\delta\langle\mathcal{O}(t)\rangle =$$

$$\frac{i}{\hbar}\int_{-\infty}^{\infty} dt' \int d\mathbf{r}_1 d\mathbf{r}_2 o(\mathbf{r}_1,t)v(\mathbf{r}_2,t')\theta(t-t')\langle\Psi_0|\Big[\rho_H(\mathbf{r}_2,t'),\rho_H(\mathbf{r}_1,t)\Big]|\Psi_0\rangle, \tag{1.168}$$

where we have allowed $t_0 \to -\infty$. We can call the quantity

$$\chi(\mathbf{r}_1 t,\mathbf{r}_2 t') \equiv i\theta(t-t')\langle\Psi_0|\Big[\rho_H(\mathbf{r}_2,t'),\rho_H(\mathbf{r}_1,t)\Big]|\Psi_0\rangle \tag{1.169}$$

linear density–density response function.

Poles of the response function

We can write Eq. (1.169):

$$-i\chi(\mathbf{r}_1 t,\mathbf{r}_2 t') =$$

$$\theta(t-t')\langle\Psi_0|\rho_H(\mathbf{r}_2,t')\rho_H(\mathbf{r}_1,t)|\Psi_0\rangle - \theta(t-t')\langle\Psi_0|\rho_H(\mathbf{r}_1,t')\rho_H(\mathbf{r}_2,t)|\Psi_0\rangle. \tag{1.170}$$

By inserting a complete set of states $\{\psi_n\}$ we have

$$-i\chi(\mathbf{r}_1 t,\mathbf{r}_2 t') = \theta(t-t')\sum_n \Big[\langle\Psi_0|\rho_H(\mathbf{r}_2,t')|\Psi_n\rangle\langle\Psi_n|\rho_H(\mathbf{r}_1,t)|\Psi_0\rangle$$

$$-\langle\Psi_0|\rho_H(\mathbf{r}_1,t)|\Psi_n\rangle\langle\Psi_n|\rho_H(\mathbf{r}_2,t')|\Psi_0\rangle\Big] =$$

$$\theta(t-t')\sum_n \Big[e^{i\frac{E_n-E_0}{\hbar}(t-t')}\langle\Psi_0|\rho(\mathbf{r}_2)|\Psi_n\rangle\langle\Psi_n|\rho(\mathbf{r}_1)|\Psi_0\rangle -$$

$$-e^{-i\frac{E_n-E_0}{\hbar}(t-t')}\langle\Psi_0|\rho(\mathbf{r}_2)|\Psi_n\rangle\langle\Psi_n|\rho(\mathbf{r}_1)|\Psi_0\rangle\Big]. \tag{1.171}$$

It is evident that $\chi(\mathbf{r}_1 t,\mathbf{r}_2 t')$ depends on the difference $t-t'$, thus we can perform a Fourier transform and shift to frequency representation. We can also use the integral formula for the θ function:

$$\theta(t-t') = -\frac{1}{2\pi i}\int d\omega' \frac{e^{-i\omega'(t-t')}}{\omega'+i\eta}, \tag{1.172}$$

with η an infinitasimal complex factor. We find for the first term

$$-2\pi\int d(t-t')e^{i\omega(t-t')}\sum_n \frac{1}{2\pi i}\int d\omega' \frac{e^{-i\omega'(t-t')}}{\omega'+i\eta}e^{-i\frac{E_n-E_0}{\hbar}(t-t')}\times$$

$$\times\langle\Psi_0|\rho(\mathbf{r}_2)|\Psi_n\rangle\langle\Psi_n|\rho(\mathbf{r}_1)|\Psi_0\rangle =$$

$$= i\sum_n \langle\Psi_0|\rho(\mathbf{r}_2)|\Psi_n\rangle\langle\Psi_n|\rho(\mathbf{r}_1)|\Psi_0\rangle \int d(t-t')\int d\omega' \frac{e^{-i\omega'(t-t')}}{\omega'+i\eta}e^{-i\frac{E_n-E_0}{\hbar}(t-t')} =$$

$$i\sum_n \langle\Psi_0|\rho(\mathbf{r}_2)|\Psi_n\rangle\langle\Psi_n|\rho(\mathbf{r}_1)|\Psi_0\rangle \int \frac{d\omega'}{\omega'+i\eta}\delta\Big(\omega'-\Big(\omega+\frac{E_n-E_0}{\hbar}\Big)\Big) =$$

$$i\sum_n \frac{\langle\Psi_0|\rho(\mathbf{r}_2)|\Psi_n\rangle\langle\Psi_n|\rho(\mathbf{r}_1)|\Psi_0\rangle}{\omega+\delta\omega_n+i\eta}, \tag{1.173}$$

where we havw defined $\delta\omega_n = (E_n - E_0)/\hbar$. The second term on the right hand side of Eq. (1.171) similarly yields

$$-i\sum_n \frac{\langle\Psi_0|\rho(\mathbf{r}_1)|\Psi_n\rangle\langle\Psi_n|\rho(\mathbf{r}_2)|\Psi_0\rangle}{\omega-\delta\omega_n+i\eta} \tag{1.174}$$

From Eqs. (1.173) and (1.174) we finally obtain the *Lehmann representation* of the response function

$$\chi(\mathbf{r}_1,\mathbf{r}_2,\omega) = \sum_n \Big[\frac{\langle\Psi_0|\rho(\mathbf{r}_1)|\Psi_n\rangle\langle\Psi_n|\rho(\mathbf{r}_2)|\Psi_0\rangle}{\omega-\delta\omega_n+i\eta} - \frac{\langle\Psi_0|\rho(\mathbf{r}_2)|\Psi_n\rangle\langle\Psi_n|\rho(\mathbf{r}_1)|\Psi_0\rangle}{\omega+\delta\omega_n+i\eta}\Big]. \tag{1.175}$$

From the Lehmann rapresentation it is evident that the poles of the linear response function are frequencies of the excited states of the system.

Linear Response Function of a Noninteracting Fermion System

Consider Eq. (1.175) in the case of a noninteracting fermion system. in this case the states of the system are described by Slater determinants. The density operator can be written

$$\rho(\mathbf{r}) = \psi^\dagger(\mathbf{r})\psi(\mathbf{r}) = \sum_{i,j}\phi_i^\star(\mathbf{r})\phi_j(\mathbf{r})a_i^\dagger a_j \tag{1.176}$$

where $\phi(\mathbf{r})$ are single particle orbitals and $a_i^\dagger$ is the creation operator of an electron in orbital i and a_j is the destruction operator of an electron in orbital j. In Eq. (1.175), let us consider elements of the type

$$\langle\Psi_0|\rho(\mathbf{r}_1)|\Psi_n\rangle\langle\Psi_n|\rho(\mathbf{r}_2)|\Psi_0\rangle \tag{1.177}$$

where, by virtue of the sum over n, Ψ_n is any excited Slater determinant.

We can write

$$\sum_{i\in occ}\sum_j \phi_i^\star(\mathbf{r}_1)\phi_j(\mathbf{r}_1)\langle\Psi_0|a_i^\dagger a_j|\Psi_n\rangle \sum_{l\in occ}\sum_k \phi_k^\star(\mathbf{r}_2)\phi_l(\mathbf{r}_2)\langle\Psi_n|a_k^\dagger a_l|\Psi_0\rangle. \tag{1.178}$$

The matrix element are both non zero only if $|\Psi_n\rangle$ differs from $|\Psi_0\rangle$ by at most one orbital and if $i = l$ and $j = k$. In this case we have

$$\sum_{i\in occ}\sum_j \phi_i^\star(\mathbf{r}_1)\phi_j(\mathbf{r}_1)\phi_j^\star(\mathbf{r}_2)\phi_i(\mathbf{r}_2). \tag{1.179}$$

Introducing f_i, the occupation number of the i–th orbital, we can remove limitations on the sum over i. We can write

$$\sum_i \sum_j f_i \phi_i^\star(\mathbf{r}_1)\phi_j(\mathbf{r}_1)\phi_j^\star(\mathbf{r}_2)\phi_i(\mathbf{r}_2). \tag{1.180}$$

Hence, the first term in Eq. (1.175) is

$$\sum_i \sum_j f_i \frac{\phi_i^\star(\mathbf{r}_1)\phi_j(\mathbf{r}_1)\phi_j^\star(\mathbf{r}_2)\phi_i(\mathbf{r}_2)}{\omega - \frac{\varepsilon_j - \varepsilon_i}{\hbar} + i\eta}, \tag{1.181}$$

where the sum over n has been replaced by the sum over j and $\delta\omega_n = (\varepsilon_j - \varepsilon_i)/\hbar$ because $|\Psi_n\rangle$ differs from $|\Psi_0\rangle$ by at most one orbital. Similarly the second term of Eq. (1.175) is

$$\sum_i \sum_j \frac{\phi_i^\star(\mathbf{r}_2)\phi_j(\mathbf{r}_2)\phi_j^\star(\mathbf{r}_1)\phi_i(\mathbf{r}_1)}{\omega + \frac{\varepsilon_j - \varepsilon_i}{\hbar} + i\eta}. \tag{1.182}$$

We can interchange the dummy index and finally write for Eq. (1.175)

$$\chi(\mathbf{r}_1, \mathbf{r}_2, \omega) = \sum_i \sum_j (f_i - f_j) \frac{\phi_i^\star(\mathbf{r}_1)\phi_j(\mathbf{r}_1)\phi_j^\star(\mathbf{r}_2)\phi_i(\mathbf{r}_2)}{\omega - \frac{\varepsilon_j - \varepsilon_i}{\hbar} + i\eta}. \tag{1.183}$$

1.7.5 Kohn–Sham Linear Response Theory

Consider the variation of the electron density of a system due to an external time–dependent potential $v(\mathbf{r}_2, \omega)$. From Eq. (1.168) and Eq. (1.169) we can write, after a Fourier transformation

$$\delta\rho(\mathbf{r}, \omega) = \int d\mathbf{r}_2 \chi(\mathbf{r}, \mathbf{r}_2, \omega)\delta v(\mathbf{r}_2, \omega), \tag{1.184}$$

where we have used $o(\mathbf{r}_1, t) = \delta(\mathbf{r} - \mathbf{r}_1)$. In time–dependent Kohn–Sham framework, the density of the interacting system under the time–dependent perturbation v is identical to the density of a noninteracting system under the external potential v_s as described in Eq. (1.153). So we can calculate the variation of the density in the noninteracting system as well

$$\delta\rho(\mathbf{r}, \omega) = \int d\mathbf{r} \chi_s(\mathbf{r}, \mathbf{r}_2, \omega)\delta v_s(\mathbf{r}_2, \omega). \tag{1.185}$$

The main difference is that now $\chi_s(\mathbf{r}, \mathbf{r}_2, \omega)$ is the linear density–density response function of a non interacting system and is given by Eq. (1.183), where ϕ are the Khon–Sham orbitals and ε are the orbital energies. Following Eq. (1.153) we can divide v_s in three contributions:

$$\delta v_s(\mathbf{r}, \omega) = \delta v_{ext}(\mathbf{r}, \omega) + \delta J[\rho] + \delta v_{xc}(\mathbf{r}, \omega). \tag{1.186}$$

The variational of the external potential is simply $\delta v(\mathbf{r}_2, \omega)$, while the change in the Coulomb potential is

$$\delta J[\rho] = \int d\mathbf{r}' \frac{\delta\rho(\mathbf{r}', \omega)}{|\mathbf{r} - \mathbf{r}'|}. \tag{1.187}$$

The linear variation of the exchange–correlation potential is the linear part in $\delta\rho$ of v_{xc}

$$\delta v_{xc}(\mathbf{r}, \omega) = \int d\mathbf{r}' \frac{\delta \mathbf{v_{xc}}(\mathbf{r}, \omega)}{\delta\rho(\mathbf{r}, \omega)} \delta\rho(\mathbf{r}', \omega). \tag{1.188}$$

It is useful to introduce the *exchange–correlation* kernel

$$f_{xc}(\mathbf{r}, \mathbf{r}', \omega) \equiv \frac{\delta v_{xc}(\mathbf{r}, \omega)}{\delta\rho(\mathbf{r}, \omega)}. \tag{1.189}$$

Hence, Eq. (1.185) becomes

$$\delta\rho(\mathbf{r}, \omega) = \int d\mathbf{r}_2 \chi_s(\mathbf{r}, \mathbf{r}_2, \omega) +$$

$$+ \int d\mathbf{r}_1 d\mathbf{r}_2 \chi_s(\mathbf{r}, \mathbf{r}_2, \omega) \Big[\frac{1}{|\mathbf{r}_2 - \mathbf{r}_1|} + f_{xc}(\mathbf{r}_2, \mathbf{r}_1, \omega) \Big] \delta\rho(\mathbf{r}_1, \omega). \tag{1.190}$$

Using Eq. (1.184) for the density in Eq. (1.190) we find an equation for the linear response function, that is the following one:

$$\chi(\mathbf{r}, \mathbf{r}', \omega) = \chi_s(\mathbf{r}, \mathbf{r}'\omega) +$$

$$+ \int d\mathbf{r}_1 d\mathbf{r}_2 \chi_s(\mathbf{r}, \mathbf{r}_1, \omega) \Big[\frac{1}{|\mathbf{r}_1 - \mathbf{r}_2|} + f_{xc}(\mathbf{r}_1, \mathbf{r}_2, \omega) \Big] \chi(\mathbf{r}_2, \mathbf{r}', \omega). \tag{1.191}$$

A self–consisten solution of Eq. (1.191) would yield the response function of the interacting system and consequently the excitation energies. Unfortunately, this equation is hard to solve and so, often, some other methods are used to compute the excitation energies of the system.

1.7.6 Pseudo–Eigenvalue Solution

To avoid the difficulties due to Eq. (1.191) it is possible to rewrite Eq. (1.190) as a pseudo–eigeinvalue equation, which eigenvalues are the excitation energies of the system. Consider Eq. (1.190). We can rearrange the terms in the following way:

$$\int d\mathbf{r}_2 \delta(\mathbf{r} - \mathbf{r}_2) \delta\rho(\mathbf{r}_2, \omega) = \int d\mathbf{r}_2 \chi_s(\mathbf{r}, \mathbf{r}_2, \omega) \delta v(\mathbf{r}_2, \omega) +$$

$$+ \int d\mathbf{r}_1 d\mathbf{r}_2 \chi_s(\mathbf{r}, \mathbf{r}_2, \omega) \Big[\frac{1}{|\mathbf{r}_1 - \mathbf{r}_2|} + f_{xc}(\mathbf{r}_1, \mathbf{r}_2, \omega) \Big] \delta\rho(\mathbf{r}_2, \omega) \tag{1.192}$$

$$\int d\mathbf{r}_2 \Big\{ \delta(\mathbf{r}-\mathbf{r}_2) - \int d\mathbf{r}_1 \chi_s(\mathbf{r},\mathbf{r}_1,\omega) \Big[\frac{1}{|\mathbf{r}_1-\mathbf{r}_2|} + f_{xc}(\mathbf{r}_1,\mathbf{r}_2,\omega) \Big] \Big\} \delta\rho(\mathbf{r}_2,\omega) = \int d\mathbf{r}_2 \chi_s(\mathbf{r},\mathbf{r}_2,\omega)\delta v(\mathbf{r}_2,\omega). \tag{1.193}$$

Let us define

$$\Xi(\mathbf{r},\mathbf{r}_2,\omega) \equiv \int d\mathbf{r}_1 \chi_s(\mathbf{r},\mathbf{r}_1,\omega) \Big[\frac{1}{|\mathbf{r}_1-\mathbf{r}_2|} + f_{xc}(\mathbf{r}_1,\mathbf{r}_2,\omega) \Big]. \tag{1.194}$$

Eq. (1.193) can be written

$$\int d\mathbf{r}_2 \{ \delta(\mathbf{r}-\mathbf{r}_2) - \Xi(\mathbf{r},\mathbf{r}_2,\omega) \} \delta\rho(\mathbf{r}_2,\omega) = \int d\mathbf{r}_2 \chi_s(\mathbf{r},\mathbf{r}_2,\omega)\delta v(\mathbf{r}_2,\omega). \tag{1.195}$$

As we have seen, the linear response function has poles at the excitation energies of the system. Because of the external potential does not have any special pole structure, this implies, via Eq. (1.184), that also the linear variation of the density $\delta\rho$ has poles at the excitation energies. Thus in Eq. (1.195) the left hand side has poles at the excitation energies of the system, while the right hand side remains finite. For the equality to hold we must therefore require that the operator multipling $\delta\rho$ on the left hand side of Eq. (1.195) has zero eigenvalues at the excitation energies. This is equivalent to the requirement

$$\lim_{\omega\to\Omega_n} \lambda(\omega) = 1 \tag{1.196}$$

where Ω_n are the excitation energies and λ is the solution of the eigenvalue equation

$$\int d\mathbf{r}' \Xi(\mathbf{r},\mathbf{r}',\omega)\xi(\mathbf{r}',\omega) = \lambda(\omega)\xi(\mathbf{r}',\omega). \tag{1.197}$$

It is possible to transform this equation into another eigenvalue equation which has the true excitation energies of the system Ω, as eigenvalues. Let us define

$$\zeta_{ij} = \int d\mathbf{r}_1 d\mathbf{r}_2 \phi_i^\star(\mathbf{r}_1)\phi_j(\mathbf{r}_1) \Big[\frac{1}{|\mathbf{r}_1-\mathbf{r}_2|} + f_{xc}(\mathbf{r}_1,\mathbf{r}_2,\omega) \Big] \xi(\mathbf{r}_2,\omega). \tag{1.198}$$

Equation (1.197) can be written

$$\sum_{ij} (f_i - f_j) \frac{\phi_i(\mathbf{r})\phi_j^\star(\mathbf{r})}{\omega - (\varepsilon_i - \varepsilon_j) + i\eta} \zeta_{ij}(\omega) = \lambda(\omega)\xi(\mathbf{r}',\omega). \tag{1.199}$$

By solving this equation for ξ and substituting in Eq. (1.198) we find

$$\sum_{ml} \frac{M_{ijml}}{\omega - \varepsilon_m - \varepsilon_l + i\eta} \zeta_{lm}(\omega) = \lambda(\omega)\zeta_{ij}(\omega), \tag{1.200}$$

where we have defined

$$M_{ijml} \equiv (f_l - f_m) \int d\mathbf{r}_1 d\mathbf{r}_2 \phi_i^\star(\mathbf{r}_1)\phi_j(\mathbf{r}_1)\Big[\frac{1}{|\mathbf{r}_1 - \mathbf{r}_2|} + f_{xc}(\mathbf{r}_1, \mathbf{r}_2, \omega)\Big]\phi_l(\mathbf{r}_2)\phi_m^\star(\mathbf{r}_2). \tag{1.201}$$

Introducing the new eigenvector

$$\beta_{ij} \equiv \frac{\zeta_{ij}(\Omega)}{\Omega - (\varepsilon_i - \varepsilon_j)}, \tag{1.202}$$

taking the limit $\eta \to 0$ and using the condition $\lambda(\Omega) = 1$ we finally find

$$\sum_{ml}[\delta_{im}\delta_{jl}(\varepsilon_m - \varepsilon_l) + M_{ijml}]\beta_{ml} = \Omega\beta_{ij} \tag{1.203}$$

RPA–Like Solution

It is also possible to rewrite Eq. (1.190) as an RPA–like equation [26].

In this section we will adopt the convention of calling i, j the occupied orbitals and a, b the unoccupied ones. The indices k, l, m, n will denote general orbitals.

From equations (1.185) and (1.183) it is clear that only elements of the first order variation of the density $\delta\rho$ that are nonzero are those coming from particle–hole ($f_i > f_j$) and hole–particle ($f_i < f_j$) contributions. Then, it is convenient to divide $\delta\rho$ in particle–hole and hole–particle contributions. We can use for the linear variation of the density the expansion

$$\delta\rho(\mathbf{r}, \omega) = \sum_{ia}\Big[P_{ia}(\omega)\phi_a^\star(\mathbf{r})\phi_i(\mathbf{r}) + P_{ai}(\omega)\phi_a(\mathbf{r})\phi_i^\star(\mathbf{r})\Big]. \tag{1.204}$$

Substituting in Eq. (1.190), and using Eq. (1.183) for the Kohn–Sham response function, we find two coupled–equations for P_{ia} and P_{ai}

$$[\delta_{ij}\delta_{ab}(\varepsilon_a - \varepsilon_i + \omega) + K_{iajb}]P_{jb} + K_{iabj}P_{bj} = -v_{ia} \tag{1.205}$$

$$[\delta_{ij}\delta_{ab}(\varepsilon_a - \varepsilon_i - \omega) + K_{aibj}]P_{bj} + K_{aijb}P_{jb} = -v_{ai} \tag{1.206}$$

where we have defined

$$v_{kl} = \int d\mathbf{r}\phi_k^\star(\mathbf{r})\delta v\phi_l(\mathbf{r}), \tag{1.207}$$

and

$$K_{klmn} = \int d\mathbf{r}d\mathbf{r}'\phi_k^\star(\mathbf{r})\phi_l(\mathbf{r})\Big[\frac{1}{|\mathbf{r} - \mathbf{r}'|} + f_{xc}(\mathbf{r}, \mathbf{r}', \omega)\Big]\phi_n^\star(\mathbf{r}')\phi_m(\mathbf{r}'). \tag{1.208}$$

Using the notation $X_{ia} = P_{ia}$, $Y_{ia} = P_{ai}$ and $V_{ia} = v_{ia}$ we can write the coupled–equation in a compact form:

$$\left[\begin{pmatrix} L & M \\ M^\star & L^\star \end{pmatrix} - \omega \begin{pmatrix} -1 & 0 \\ 0 & -1 \end{pmatrix}\right] \begin{pmatrix} X \\ Y \end{pmatrix} = - \begin{pmatrix} V \\ V^\star \end{pmatrix} \tag{1.209}$$

with

$$L_{iajb} = \delta_{ij}\delta_{ab}(\varepsilon_a - \varepsilon_i) + K_{iajb} \tag{1.210}$$

$$M_{iajb} = K_{iabj}. \tag{1.211}$$

As we have seen, the linear response function has poles at the excitation energies of the system. Because the external potential does not have any special pole structure, this implies, via Eq. (1.184) that also the linear variation of the density $\delta\rho$ has poles at the excitation energies. The same must be obviously true for X and Y. So at excitation energies the left hand side of Eq. (1.209) diverges, while the right hand side remains finite. This implies that at excitation energies the matrix on the left hand side of Eq. (1.209) must have zero eigenvalue, that is,

$$\begin{pmatrix} L & M \\ M^\star & L^\star \end{pmatrix} \begin{pmatrix} X \\ Y \end{pmatrix} = \Omega \begin{pmatrix} -1 & 0 \\ 0 & -1 \end{pmatrix} \begin{pmatrix} X \\ Y \end{pmatrix} \tag{1.212}$$

where Ω are the excitation energies of the system. Equation (1.212) has the same structure as the RPA problem in HF theory .

If the orbitals ϕ_i are real, as it is usual in quantum chemistry, also the matrices M and L are real. The eigenvalue problem Eq. (1.212) can be further simplified by a unitary transformation

$$u = \frac{1}{\sqrt{2}} \begin{pmatrix} 1 & 1 \\ 1 & -1 \end{pmatrix}. \tag{1.213}$$

Equation (1.212) becomes

$$U \begin{pmatrix} L & M \\ M & L \end{pmatrix} U^\dagger U \begin{pmatrix} X \\ Y \end{pmatrix} = \Omega U \begin{pmatrix} -1 & 0 \\ 0 & -1 \end{pmatrix} \begin{pmatrix} X \\ Y \end{pmatrix} \tag{1.214}$$

$$\begin{pmatrix} L+M & 0 \\ 0 & L-M \end{pmatrix} \begin{pmatrix} X+Y \\ X-Y \end{pmatrix} = \Omega \begin{pmatrix} -1 & 1 \\ -1 & -1 \end{pmatrix} \begin{pmatrix} X \\ Y \end{pmatrix} \tag{1.215}$$

$$\begin{pmatrix} L+M & 0 \\ 0 & L-M \end{pmatrix} \begin{pmatrix} X+Y \\ X-Y \end{pmatrix} = \Omega \begin{pmatrix} -(X-Y) \\ -(X+Y) \end{pmatrix}. \tag{1.216}$$

From Eq. (1.216) we get coupled equations

$$(L+M)(X+Y) = -\Omega(X-Y) \tag{1.217}$$

$$(L-M)(X-Y) = -\Omega(X+Y) \tag{1.218}$$

Solveing for $(X-Y)$ in Eq. (1.218) and substituting in Eq. (1.217) we find

$$(L-M)(L+M)(X+Y) = \Omega^2(X+Y). \tag{1.219}$$

Equation (1.219) reduces the dimension of the problem of a factor of two. Nevertheless the matrix product on the left hand side is non-Hermitian. If $(L-M)$ is positive defined, Eq. (1.219) can be transformed into an Hermitian eigenvalue equation

$$(L-M)^{1/2}(L-M)^{1/2}(L+M)(L-M)^{1/2}(L-M)^{1/2}(X+Y) =$$

$$= \Omega^2(L-M)^{1/2}(L-M)^{1/2}(X+Y). \tag{1.220}$$

We call $(X+Y)' \equiv (L-M)^{1/2}(X+Y)$ and we write

$$(L-M)^{1/2}(L+M)(L-M)^{1/2}(X+Y)' = \Omega^2(X+Y)'. \tag{1.221}$$

Since in TD–DFT the matrix $(L-M)$ is diagonal with diagonal elements $\varepsilon_a - \varepsilon_i$, Eq. (1.221) is particulary simple to solve in this case.

1.7.7 Spin formalism

To properly describe an electron system it is necessary to include in the description the spin degrees of freedom. In this section we will review the result presented in sec. 1.7.4 when spin is presented.

The spin variables will be denoted by greek indices $\sigma, \tau, \ldots$, and considered discrete variables.

Linear response Theory

The variation of the expectation value operator due to the external perturbation V, is

$$\delta\langle\mathcal{O}(t)\rangle = \langle\Psi(t)|\mathcal{O}(t)|\Psi(t)\rangle - \langle\Phi(t)|\mathcal{O}|\Phi(t)\rangle =$$

$$= \frac{i}{\hbar}\int_{t_0}^{t}\langle\Psi_0|[V_H(t'),\mathcal{O}_H(t)]|\Psi_0\rangle dt'. \tag{1.222}$$

If V and $\mathcal{O}$ are one–body operators we can write

$$\mathcal{O}_H(t) = \sum_\sigma \int d\mathbf{r}_1 \Psi^\dagger_{\sigma H}(\mathbf{r}_1,t) o_\sigma(\mathbf{r}_1,t) \Psi_{\sigma H}(\mathbf{r}_1,t) = \sum_\sigma \int d\mathbf{r}_1 o_\sigma(\mathbf{r}_1,t) \rho_{\sigma H}(\mathbf{r}_1,t) \tag{1.223}$$

$$V_H(t') = \sum_\tau \int d\mathbf{r}_2 \Psi^\dagger_{\tau H}(\mathbf{r}_2,t') v_\tau(\mathbf{r}_2,t') \Psi_{\tau H}(\mathbf{r}_2,t') = \sum_\tau \int d\mathbf{r}_2 v_\tau(\mathbf{r}_2,t') \rho_{\tau H}(\mathbf{r}_2,t'). \tag{1.224}$$

We find

$$\delta\langle\mathcal{O}(t)\rangle =$$

$$\frac{i}{\hbar}\sum_{\sigma\tau}\int_{-\infty}^{+\infty} dt' \int d\mathbf{r}_1 d\mathbf{r}_2 o_\sigma(\mathbf{r}_1,t) v_\tau(\mathbf{r}_2,t') \theta(t-t') \langle\Psi_0|[\rho_{\tau H}(\mathbf{r}_2,t'), \rho_{\tau H}(\mathbf{r}_2,t')]|\Psi_0\rangle. \tag{1.225}$$

We can call the quantity

$$\chi_{\sigma,\tau}(\mathbf{r}_1 t, \mathbf{r}_2 t') \equiv i\theta(t-t')\langle\Psi_0|[\rho_{\tau H}(\mathbf{r}_2,t'), \rho_{\sigma H}(\mathbf{r}_1,t)]|\Psi_0\rangle \tag{1.226}$$

linear density–density response function. In the Lehmann rappresentation this is written

$$\chi_{\sigma,\tau}(\mathbf{r}_1,\mathbf{r}_2,\omega) =$$

$$\sum_n \Big[\frac{\langle\Psi_0|\rho_\sigma(\mathbf{r}_1)\Psi_n\rangle\langle\Psi_n|\rho_\tau(\mathbf{r}_2)\Psi_0\rangle}{\omega - \delta\omega_n + i\eta} - \frac{\langle\Psi_0|\rho_\tau(\mathbf{r}_2)\Psi_n\rangle\langle\Psi_n|\rho_\sigma(\mathbf{r}_1)\Psi_0\rangle}{\omega + \delta\omega_n + i\eta}\Big]. \tag{1.227}$$

In the special case of a noninteracting fermion system the linear density–density response function can be written

$$\chi_{\sigma,\tau}(\mathbf{r}_1,\mathbf{r}_2,\omega) = \delta_{\sigma\tau}\sum_i\sum_j (f_{i\sigma} - f_{j\tau}) \frac{\phi^\star_{i\sigma}(\mathbf{r}_1)\phi_{j\sigma}(\mathbf{r}_1)\phi^\star_{j\tau}(\mathbf{r}_2)\phi_{i\tau}(\mathbf{r}_2)}{\omega - \frac{\varepsilon_j - \varepsilon_i}{\hbar} + i\eta}. \tag{1.228}$$

Kohn–Sham Linear Response Theory

From Eq. (1.225) and Eq. (1.226) we can write the linear variation of the spin density ρ_σ due to external perturbation δv_τ, as

$$\delta\rho_\sigma(\mathbf{r},\omega) = \int d\mathbf{r}_2 \chi_{\sigma,\tau}(\mathbf{r},\mathbf{r}_2,\omega)\delta v^s_\tau(\mathbf{r}_2,\omega), \tag{1.229}$$

where we have used $o_{\sigma'} = \delta_{\sigma\sigma'}\delta(\mathbf{r}-\mathbf{r}_1)$. In the time–dependent Kohn–Sham framework we can calculate the variation of the spin density in the Khon–Sham noninteractiong system

$$\delta\rho_\sigma(\mathbf{r},\omega) = \int d\mathbf{r}_2 \chi_{\sigma,\tau}(\mathbf{r},\mathbf{r}_2,\omega)\delta v^s_\tau(\mathbf{r}_2,\omega), \tag{1.230}$$

where $\chi^s_{\sigma,\tau}$ is given by Eq. (1.228). As usual we can divide δv^s into three contributions:

$$\delta v^s_\tau(\mathbf{r},\omega) = \delta v^{ext}_\tau(\mathbf{r},\omega) + \delta J[\rho_\tau] + \delta v^{xc}_\tau(\mathbf{r},\omega) \tag{1.231}$$

where v^{ext}_τ is the variation of the external potential, $\delta J[\rho_\tau]$ is the variation of the Coulomb potential and

$$\delta v^{xc}_\tau(\mathbf{r},\omega) = \int d\mathbf{r}' \frac{\delta v^{xc}_\tau(\mathbf{r},\omega)}{\delta\rho_\alpha(\mathbf{r}',\omega)}\delta\rho_\alpha(\mathbf{r}',\omega). \tag{1.232}$$

We define the *exchange–correlation* kernel

$$f^{xc}_{\tau\alpha} \equiv \frac{\delta v^{xc}_\tau(\mathbf{r},\omega)}{\delta\rho_\alpha(\mathbf{r}',\omega)}. \tag{1.233}$$

Thus, we can write Eq. (1.230) as

$$\delta\rho_\alpha(\mathbf{r},\omega) = \int d\mathbf{r}_2 \chi^s_{\sigma,\tau}(\mathbf{r},\mathbf{r}_2,\omega)\delta v_\tau(\mathbf{r}_2,\omega) +$$

$$+ \int d\mathbf{r}_1 d\mathbf{r}_2 \chi^s_{\sigma,\lambda}\Big[\frac{\delta_{\lambda\alpha}}{|\mathbf{r}_2-\mathbf{r}_1|} + f^{xc}_{\lambda\alpha}\Big]\delta\rho_\alpha(\mathbf{r}_1,\omega). \tag{1.234}$$

RPA–Like Solution

Equation (1.233) can be written as an RPA–like equation. We will call i,j the occupied orbitals and a,b the unoccupied ones. The indices k,l,m,n will denote general orbitals. In analogy with the section 1.7.6 we can use for the spin density the expansion

$$\delta\rho_\alpha(\mathbf{r},\omega) = \sum_{ia}[P_{ia\sigma}(\omega)\phi^\star_{a\sigma}(\mathbf{r})\phi_{i\sigma}(\mathbf{r}) + [P_{ai\sigma}(\omega)\phi_{a\sigma}(\mathbf{r})\phi^\star_{i\sigma}(\mathbf{r})]. \tag{1.235}$$

Substituting in Eq. (1.233), and using Eq. (1.228) for the Kohn–Sham response function, we find two coupled–equations for $P_{ia\sigma}$ and $P_{ai\sigma}$

$$[\delta_{\sigma,\tau}\delta_{ij}\delta_{ab}(\varepsilon_a - \varepsilon_i + \omega) + K_{ia\sigma,bj\tau}]P_{jb\tau} + K_{ia\sigma,bj\tau}P_{bj\tau} = -v_{ia\sigma} \tag{1.236}$$

$$[\delta_{\sigma,\tau}\delta_{ij}\delta_{ab}(\varepsilon_a - \varepsilon_i - \omega) + K_{ai\sigma,bj\tau}]P_{jb\tau} + K_{ai\sigma,jb\tau}P_{jb\tau} = -v_{ai\sigma} \tag{1.237}$$

where we have defined

$$v_{kl\sigma}\delta_{\sigma\tau}\int d\mathbf{r}\phi^\star_{k\tau}(\mathbf{r})\delta v_\tau\phi_{l\tau}(\mathbf{r}), \tag{1.238}$$

and

$$K_{kl\sigma,mn\tau} = \delta_{\sigma\lambda}\int d\mathbf{r}d\mathbf{r}'\phi^\star_{k\lambda}(\mathbf{r})\phi_{l\lambda}(\mathbf{r})\Big[\frac{\delta_{\lambda\tau}}{|\mathbf{r}-\mathbf{r}'|} + f^{xc}_{\lambda\tau}(\mathbf{r},\mathbf{r}',\omega)\Big]\phi^\star_{n\tau}(\mathbf{r}')\phi_{m\tau}(\mathbf{r}'). \tag{1.239}$$

Using the notation $X_{ia\sigma} = P_{ia\sigma}$, $Y_{ia\sigma} = P_{ai\sigma}$ and $V_{ia\sigma} = v_{ia\sigma}$, Eqs. (1.236) and (1.237) can be wirtten in compact form:

$$\left[\begin{pmatrix} L & M \\ M^\star & L^\star \end{pmatrix} - \omega \begin{pmatrix} -1 & 0 \\ 0 & -1 \end{pmatrix}\right] \begin{pmatrix} X \\ Y \end{pmatrix} = - \begin{pmatrix} V \\ V^\star \end{pmatrix}, \tag{1.240}$$

with

$$L_{ia\sigma,jb\tau} = \delta_{\sigma\tau}\delta_{ij}\delta_{ab}(\varepsilon_a - \varepsilon_i) + K_{ia\sigma,jb\tau} \tag{1.241}$$

$$M_{ia\sigma,jb\tau} = K_{ia\sigma,bj\tau}. \tag{1.242}$$

In analogy with section 1.7.6 we must require that at excitation energies the matrix on the left hand side has zero eigenvalue, *i.e.*

$$\begin{pmatrix} L & M \\ M^\star & L^\star \end{pmatrix} \begin{pmatrix} X \\ Y \end{pmatrix} = \Omega \begin{pmatrix} -1 & 0 \\ 0 & -1 \end{pmatrix} \begin{pmatrix} X \\ Y \end{pmatrix} \tag{1.243}$$

with Ω excitation energies of the system.

If the orbitals ϕ_i are real, we can perform a unitary transformation and obtain

$$(L - M)^{1/2}(L + M)(L - M)^{1/2}(X + Y)' = \Omega^2(X + Y)', \tag{1.244}$$

where $(X + Y)' \equiv (L - M)^{1/2}(X + Y)$.

Chapter 2

Torsional Effects on Excitation Energies of Thiophene Derivatives Induced by β–Substituent: Comparison between Time-Dependent Density Functional Theory and Approximated Coupled Cluster Approaches

In this chapter, the influence of methyl or phenil substitution in β–position of dioxygenated ter–thiophene and diphenyl–thiophene on the optical properties is investigated by first–principles calculations. We compare the approximated singles and doubles coupled cluster (CC2) approach with time–dependent functional theory methods. CC2 reproduces experimental excitation energies with accuracy of 0.1 eV. We find that different substituents modify the inter–ring torsional angle which in turn strongly influences the excitation energies. The steric contribution to the excitation energies have been separated from the total substituent effects [27].

2.1 Introduction

Oligothiophenes [28] and their S, S-dioxygenated derivatives [29], [30] have attracted great research interest because of the wide applicability of these materials, ranging from medicine and biology [31], [32] over electronic devices, such as field-effect transistors,[33]–[35] to opto-electronic devices, as

light emitting diodes [36]–[43] or solar cells[44]. For all these applications is very important to achieve a fine tuning of the absorption and/or emission energies. In oligothiophene derivatives this tuning can be efficiently obtained by different functionalization schemes. From a theoretical point of view, several first principles studies on oligothiophenes [45]–[52] and S, S-dioxygenated oligothiophenes [53]–[57] have investigated the structural, electronic, and optical properties, such as molecular geometry, substituent effects, absorption, and emission energies. In particular, theoretical investigations [53], [54], [56] on terthiophene, S, S-dioxo-terthiophene, and S, S-dioxo-diphenylthiophene have shown how the oxygen func-tionalization of the sulfur atom modifies the optical properties, and which is the correlation between changes in the inter-ring torsional potential and shifts of the excitation energies. Additional substituents in β-position can further influence the geometric and electronic structures of the compounds, allowing a fine tuning of the optical properties, where the chemical and sterical nature of different groups determine the inter-ring torsional angles and thereby the absorption wavelengths [47], [57], [58]. Because of the reduced symmetry in nonplanar oligothiophenes theoretical investigations are computationally more expensive and therefore often restricted to semi-empirical approaches [58]–[63]. In this work we will employ ab initio approaches to inves-tigate ground-state geometries and absorption energies of S, S di-oxygenated terthiophene and diphenylthiophene carrying hydrogen-, methyl, or phenyl-substituents on both β–position on the central thiophene ring as shown in Figure 2.1.

We will compare theoretical approaches with different degrees of accuracy in the description of molecular geometry (in particular the inter-ring torsional angle) and excitation energies. Most present day excited state calculations of small organic compounds are done using Time-dependent density-functional theory (TD-DFT) [64]–[67] employing gradient-corrected or hybrid density functional methods. It is well established, that these approaches have severe shortcomings in the description of charge-transfer bands or Rydberg states [68], but they are considered as reliable tools for single-reference valence excitations. However, there are reports on unexpected substantial failures even for valence transitions [69]. In a previous hybrid density functional theory study on β–unsubstituted S, S-dioxothiophenes [56] the experimental excitation energies were underestimated by 0.20.4 eV and it was unclear if these deviations have to be attributed to a poor description of the molecular geometry, i.e. the inter-ring torsional

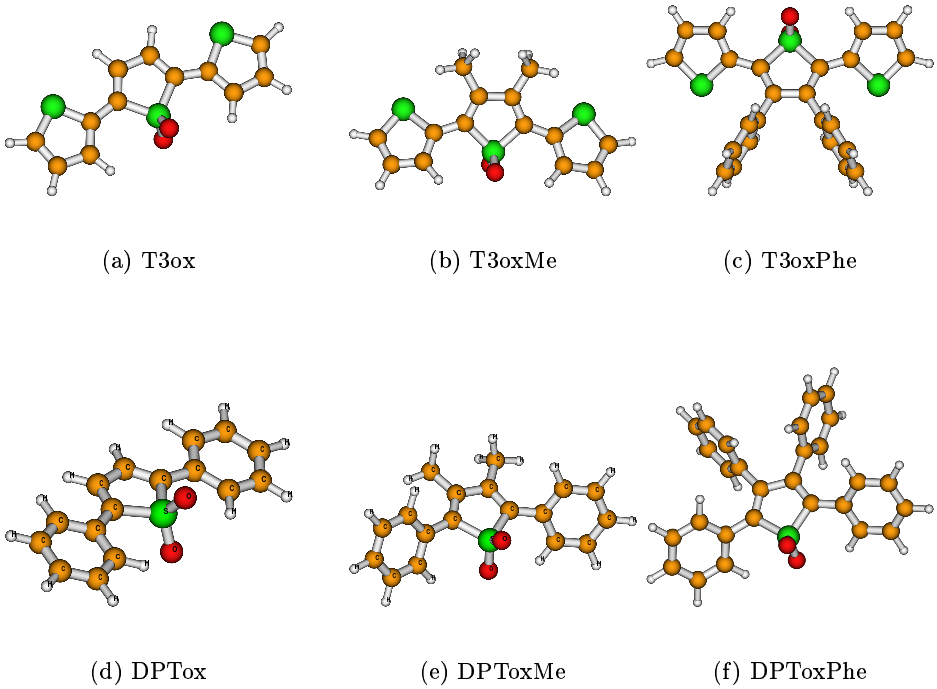

(a) T3ox (b) T3oxMe (c) T3oxPhe

(d) DPTox (e) DPToxMe (f) DPToxPhe

Figure 2.1: *Investigated terthiophene and diphenylthiophene structures*

angles, or to inaccurate electronic structure description. For this reason it is highly desirable to compare the DFT results with higher level ab initio calculations. The approximate coupled-cluster singles and doubles model (CC2) [70] has recently attracted strong interest [49], [69], [71] thanks to the implementation of the resolution-of-identity approximation, i.e. the RICC2 [72], [73] approach, which allows an efficient computation of excitation energies of medium-size organic molecules, such as the ones considered in this work. RICC2 is well suited for single-reference systems that are indicated by sufficiently small D1 diagnostic values [74]. Multi-reference effects can be investigated with the DFT-based multi reference configuration interaction (DFTMRCI) [75] method, which is significantly cheaper in terms of the computational cost than e.g. Complete active space (CAS) based methods [46], [50], [76], [77]. In this work we compare molecular geometries obtained from DFT and RICC2 calculations as well as excitation energies obtained for the optimized structures. Vertical excitation energies are calculated at the RICC2, DFTMRCI, and TD-DFT level of theory, employing hybrid density functionals, containing different amounts of exact exchange. The effects of the basis set size on the description of molecular geometries and excited

states are also investigated. We describe how the different substituents modify the molecular conformations and excitation energies.

2.2 Computational Details

All calculations were performed using the TURBOMOLE 5.7 [78] package. In particular the modules DSCF [79], ESCF [66], and RICC2 [72], [73] have been used. In the DFT ground and excited state calculations we employed the B3-LYP [80], [20] and BH-LYP [81] hybrid functionals. The default *m3* numerical quadrature grid was used in all DFT calculations. The basis sets were taken from the TURBOMOLE basis set library (TURBOMOLE homepage via the FTP Server Button (in the subdirectories basen, jbasen, and cbasen)) [82]. For RICC2 calculations, basis sets of valence-triple-ξ quality with double polarization functions (TZVPP) [83] have been employed. The corresponding auxiliary basis sets [83], [84] were used in all RICC2 calculations. For a further save of computation time, core orbitals have been kept frozen in the framework of this approach. RICC2 calculations were well converged and the ground state wavefunctions did not show significant multi-reference character (D1 diagnostic values in the range 0.07–0.08). The neglect of triple or higher excitations was also unproblematic, because the single excitation contribution were always greater than 90%. For DFT calculations we use basis sets of valence-triple–ξ quality with polarization functions (TZVP) [85] and augmented (ATZVP) with one additional diffuse functions for each angular momentum (the exponents have been determined by a geometric series from the last two exponents). For DFT geometry optimization we also use the TZVPP basis set. DFT-MRCI calculations were carried out with the DFT/MRCI code of Grimme and Waletzke [75] using the BH-LYP density functional and a configuration selection cutoff of 0.8 E_h. Core orbitals with energies below $-0.2E_h$ and virtual orbitals above $2.0E_h$ were excluded from the correlation treatments.

2.3 Results

2.3.1 Ground State Geometries

As stated in the Introduction the S_1 excitation energy strongly depends on the inter-ring torsional angle of the system, hence the discussion of the

molecular geometries mainly focuses on this parameter. The results of the RICC2 calculations are taken as reference values for the density functional calculations, because no experimental data for these structures are available. Inter-ring torsional angles can be found in Table 2.1. The unsubstituted ter-

	RICC2 TZVP	B3–LYP TZVP	B3–LYP ATZVP	B3–LYP TZVP	BH–LYP TZVPP
T30x	1.0	3.4	3.3	3.6	3.7
T3oxMe	17.5	22.3	22.1	27.8	31.6
T3oxPhe	0.2	0.4	0.4	0.4	0.6
DPTox	16.7	16.6	16.6	21.2	17.2
DPToxMe	45.8	49.0	48.5	50.7	50.4
DPToxPhe	19.9	38.2	37.5	41.3	39.5

Table 2.1: *Inter–ring Torsional Angles in Ground Geometries, Optimized with RICC2, B3–LYP, and BH–LYP Methods, Applying Triple–ξ Valence Basis Sets.*

thiophene species T3ox is almost planar with a dihedral angle of 1.0°. This represents a major difference to the unoxidized ter-thiophene, which is not planar, but shows an inter-ring torsion of 25° [53]. The methyl substituted structure T3oxMe has a torsional angle of 17.5°, and thus it is strongly twisted, whereas the phenyl-derivative T3oxPhe is almost planar. A similar trend is observed for the Diphenyl (DPT) systems, albeit all values are considerably larger and no planar structure can be found. DPTox, which carries hydrogen substituents on the central thiophene unit, is twisted by 16.7° and the methyl-groups in DPToxMe enforce a torsional angle of 45.8°. For DPToxPhe it is 19.9°. For the T3ox system the deviations of the DFT/TZVPP results from the RICC2 reference values are small.With the B3-LYP functional, the dihedral angle is found to be 2.4° above the RICC2 result and with BH-LYP (last column of Table 2.1) the difference slightly increases to 2.7°. The B3-LYP result for T3oxMe is 22.3°, which is somewhat larger than in the RICC2 geometry and the BH-LYP optimization yields a significantly larger value of 31.6°. For the phenyl substituted compound T3oxPhe, the agreement of all methods is within the range of 0.4° almost perfect. This also holds for the DPTox molecule, where the B3-LYP result is 0.1° below and the BH-LYP result 0.5° above the reference value. At this point it should be mentioned, that the torsional potential for DPTox obtained from DFT

calculations is rather flat. A scan of the potential surface with constrained geometry optimizations, keeping the values of the dihedral angles fixed between 0.0 and 30.0°, revealed that over the whole range, energetic differences were not larger than 0.1 kcal/mol, indicating a large flexibility along this torsion coordinate. The DFT results for DPToxMe are again quite similar to the reference value, the B3-LYP angle is only 3.2° and the BH-LYP value only 4.6° above the dihedral angle obtained by the RICC2 optimization. The situation is quite different for the phenyl-substituted structure DPToxPhe. Here the DFT calculations predict torsional angles, that are nearly 20° larger than the ones obtained with the RICC2 method. The basis set effects can bee seen in Table 2.1. When comparing the B3-LYP results for the additionally polarized (TZVPP) and augmented (ATZVP) triple–ξ basis sets, almost no difference is found for the individual structures. The largest deviation is 0.7° for DPToxPhe. In case of the smaller TZVP basis set, some structures show slightly increased dihedral angles compared to the larger basis sets. But only in the case of T3oxMe the difference between the TZVP and TZVPP calculation exceeds 5°. The effect of diffuse functions is thus similar to the additional polarization functions. In the following section we will present results for excitation energies computed employing the RICC2/TZVPP and the B3-LYP/ATZVP geometries.

2.3.2 Excitation Energies of the Electric Dipole Allowed S_1 Transition

In Table 2.2 the excitation energies and oscillator strengths of the S_1 transition of the six molecular species obtained by RI-CC2 and TD-DFT (B3-LYP) calculations using RI-CC2/TZVPP optimized geometries (A) and by TD-DFT (B3-LYP and BH-LYP) as well as DFT-MRCI (BH-LYP) using B3-LYP/ATZVP optimized geometries (B) are shown. Experimental results, from absorption spectra in THF solution [86], are reported in the last column of Table 2.2. No solvent-dependence of the absorption peak has been found in experiments [56], [86]. The DFT-MRCI (RICC2) calculations for all systems have shown that the single excitation from the highest occupied molecular orbital (HOMO) to the lowest unoccupied molecular orbital (LUMO) contributes by more than 94% (91%) to the S_1 excited-state. In the TD-DFT treatment the HOMO-LUMO transition contributes by more than 98% to the S_1 excited-state. A first inspection of the RI-CC2/TZVPP

(A) RICC2/TZVPP optimized structure

	RICC2/TZVP		B3–LYP/TZVP		Exp[a]
	Energy(eV)	f_L	Energy(eV)	f_L	Energy(eV)
T3ox	2.99	0.692	2.60	0.598	2.92
T3oxMe	3.11	0.592	2.72	0.508	3.12
T3oxPhe	2.92	0.628	2.60	0.526	2.87
DPTox	3.332	0.606	2.86	0.536	3.25
DPToxMe	3.67	0.370	3.20	0.342	3.62
DPToxPhe	3.22	0.485	2.83	0.400	3.31

(B) B3–LYP/ATZVPP optimized structure

	B3–LYP/TZVP		B3–LYP/ATZVP	
	Energy(eV)	f_L	Energy(eV)	f_L
T3ox	2.72	0.612	2.69	0.590
T3oxMe	2.88	0.494	2.87	0.489
T3oxPhe	2.78	0.531	2.76	0.525
DPTox	3.00	0.563	2.96	0.545
DPToxMe	3.41	0.330	3.40	0.328
DPToxPhe	3.21	0.328	3.11	0.329
	BH–LYP/TZVP		DFT–MRCI/TZVP	
	Energy(eV)	f_L	Energy(eV)	f_L
T3ox	2.96	0.622	3.00	0.785
T3oxMe	3.19	0.513	3.20	0.655
T3oxPhe	3.03	0.542	2.98	0.744
DPTox	3.28	0.565	3.24	0.717
DPToxMe	3.81	0.349	3.76	0.420
DPToxPhe	3.50	0.354	3.42	0.472

[a] From [86]

Table 2.2: *Calculated Excitation Energies [eV] and Oscillator Strenghts of the Electric Dipole Allowed S_1 Transition from RICC2/TZVPP and B3–LYP/TZVP, B3–LYP/TZVP Calculations, and Experimental Values. The Molecular Geometries have been Optimized Either on the RICC2/TZVPP (A) or B3–LYP–ATZVP (B) Level of Theory. The DFT–MRCI Calculations have benn Performed with the BH–LYP Density Functional and a SV(P) Basis set.*

values shows, that the resulting excitation energies lie between 2.92 and 3.67 eV. The almost planar species (T3ox and T3oxPhe) show the lowest excitation energies, whereas the energy of the more distorted T3oxMe structures is blue-shifted by about 0.2 eV and it has a smaller oscillator strength with respect to T3ox and T3oxPhe. Replacing the two lateral thiophene substituents by phenyl groups in general leads to higher excitation energies. As described in [56], this increase in energy is due to larger torsional angles and decreased polarization of the phenyl groups with respect to thiophene. The oscillator strength for DPTox is with 0.606 of the same magnitude as for the ter-thiophene species, whereas for DPToxMe and DPToxPhe this value drops below 0.5. The corresponding B3-LYP excitation energies for these geometries are all at lower values. For the ter-thiophene structures this red-shift is between 0.3 and 0.4 eV, while it is even larger (0.4.0.5 eV) for the diphenyl substituted systems. The oscillator strengths of the TD-DFT calculations are somewhat lower than those of the RI-CC2 calculations but show more or less the same trend. Employing DFT (B3-LYP/ATZVP) optimized structures rather than RI-CC2 geometries leads to somewhat higher values for the TD-DFT excitation energies. The differences are in the range of 0.1.0.2 eV for most molecules and the largest deviation (0.29 eV) is observed for DPToxPhe. This can be easily understood, since the two optimized geometries also show the largest deviation in the inter-ring torsional angle of 20°. To check the basis set effect on the excitation energies, we repeated the TD-DFT (B3-LYP) calculations with the larger ATZVP basis set. The difference in absorption energy is at most 0.05 eV (for DPTox), which is close to the limits of computational accuracy. The oscillator strengths are more or less unchanged. Thus the use of the smaller basis set is clearly justified for TD-DFT calculations of oligothiophenes of this type. Increasing the amount of Hartree.Fock exchange from 20% (B3-LYP) to 50% (BH-LYP) yields higher (0.3.0.4 eV) excitation energies while the oscillator strengths are not affected. Finally, DFT-MRCI excitation energies are very close to BHLYP because neither the ground state, nor the lowest lying excited state feature any significant multi-reference character.

2.4 Discussion

2.4.1 Ground State Geometries

The geometry optimizations of the molecular structures revealed that the oxygenated diphenylthiophenes generally show larger torsional angles between the lateral substituents and the central thiophene unit than the oxygenated terthiophenes. Despite this effect on the dihedral angles between the central thiophene unit and the lateral substituents, there are only minor changes in the structures caused by the different substitution patterns. One additional difference is found, when comparing the T3oxPhe with the DPToxPhe structure. In T3oxPhe, the central phenyl-substituents are found in a perfect perpendicular orientation to the thiophene ring, but they are tilted by about 20° in DPToxPhe. This probably can be attributed to the steric interaction with the lateral phenyl substituents in DPTox- Phe, where a too close contact of the lateral and central substituents has to be avoided. Generally speaking, the terthiophene species are more planar and thus better conjugated than their diphenyl analogues and methyl substitution significantly increases the relevant dihedral angles. So both changes in the substitution pattern offer a strategy to manipulate the inter-ring torsion of the π-conjugated system and such to take influence upon the absorption wavelength. From a theoretical point of view it could be shown that increasing the amount of Hartree–Fock exchange in density functional theory calculation leads to larger, sometimes even too large, inter-ring torsional angles. The application of an augmented triple-ξ (ATZVP) instead of an additionally polarized (TZVPP) basis set does not lead to significant changes in the molecular structures, whereas calculations with the TZVP basis set result in small deviations of the geometries. Nevertheless, the ATZVP basis set seems to represent a good compromise between accuracy and computational cost of the geometry optimizations. The largest differences in the molecular structures, depending on the computational method, are found for the DPToxPhe system. The inter-ring torsional angle as obtained from RICC2 calculations is $\sim 20°$ smaller than the ones received form density functional theory calculations.

2.5 Excitation Energies

2.5.1 Molecular Orbitals

Before discussing the calculated excitation energies and comparing them to experimental results, we have to regard the HOMO and LUMO orbitals, which characterize the electric dipole allowed S_1 transition. Figure 2.2 shows Kohn–Sham (KS) HOMO and LUMO wavefunctions for the methyl and phenyl substituted structures. For the plots of T3ox and DPTox see [56].

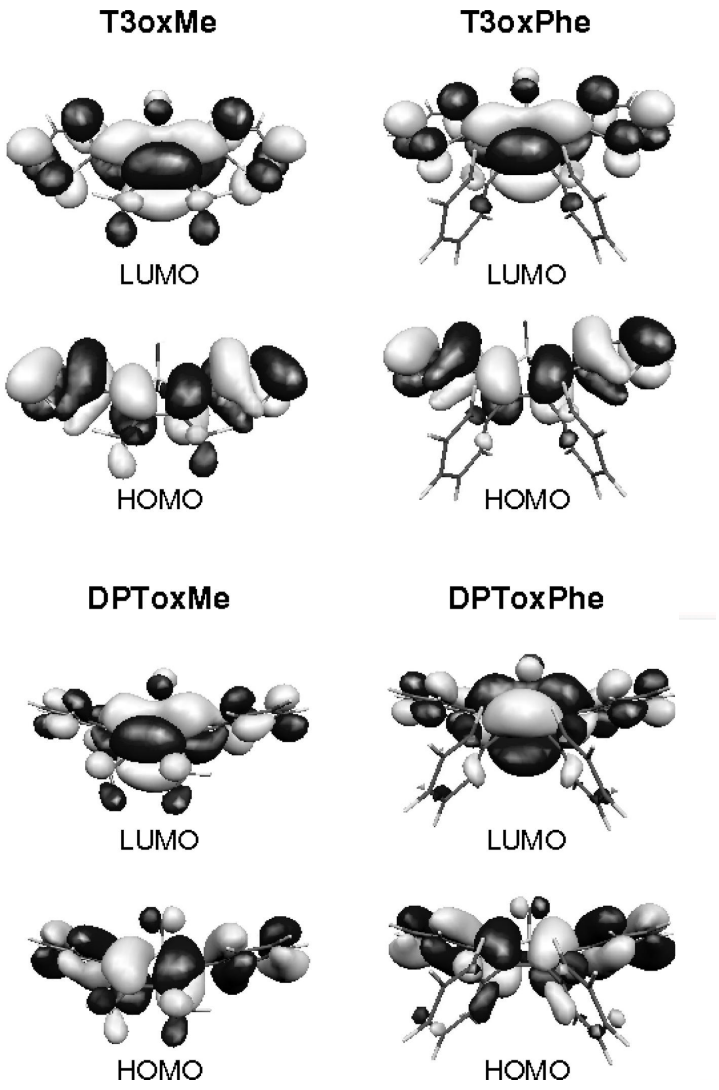

Figure 2.2: *HOMO and LUMO orbitals at an iso density value of 0.02 au of the investigated structures, obtained from B3–LYP/TZVP//RICC2/TZVPP calculations.*

Apparently there are no big differences in the atomic-orbital (AO) coefficients on the central thiophene unit, with respect to the various substitution patterns. A certain contribution for HOMO and LUMO is located on the central methyl and phenyl substituents, but a significant influence on the main π–system is not recognizable. The interaction of these small AO coefficients located on the β-substituents with the π coefficients on the central ring is in all cases of antibonding character. The largest difference in the molecular orbitals is of course caused by the most important change in structure, namely the torsion of the lateral substituents. In case of the HOMO, a nodal plane is located on the carbon-carbon bonds, which connect the central with the lateral rings. In the LUMO a bonding π contribution is found at this position. The corresponding orbital energies are given in Table 2.3.

System	HOMO	LUMO	GAP
T3ox	-5.71	-2.90	2.81
T3oxMe	-5.58(-5.57)	-2.60(-2/289)	2.98(2.88)
T3oxPhe	-5.47(-5.68)	-2.65(-2.90)	2.82(2.78)
DPTox	-6.05	2.83	3.22
DPToxMe	-6.07(-6.30)	-2.35(-2.68)	3.72(3.62)
DPToxPhe	-5.78(-6.08)	-2.65(-2.83)	3.22(3.25)

Table 2.3: *Energies in eV of Frontier Orbitals and Resulting Kohn–Sham Energy Gap from B3–LYP/TZVP//RICC2/TZVPP Calculations.*

In terthiophenes (diphenylthiophenes), methyl substitution strongly destabilizes the LUMO energy by +0.30 eV (0.48 eV), while HOMO eigenvalues are much less affected. As a consequence the HOMO-LUMO Kohn–Sham gap of T3oxMe (DPToxMe) is increased by 0.17 eV (0.50 eV) with respect to the unsubstituted system. In contrast, the phenyl substituents destabilize both, the HOMO and the LUMO by approximately the same amount (0.24-0.25 eV for terthiophenes and 0.18 eV for diphenylthiophene) so the resulting energy gap remains unchanged when compared to the unsubstituted molecules. Because of the fact, that the phenyl groups are orientated almost perpendicular to the central thiophene ring, no conjugative stabilization as usually expected for $+M$ substituents can occur. The Kohn–Sham

energy-gaps reported in Table 2.3 are very close to the corresponding B3-LYP/TZVP excitation energies reported in Table 2.2 and they show the same trend among the different systems. In fact the KS energy-gap represents a zero-order approximation to the lowest TD-DFT excitation energy [87].

2.5.2 Comparison with Experiments

For the excitation energies of the S_1 transition, excellent agreement is found between the results of the RICC2 calculations and the experimental data, as shown in Figure 2.3. The calculated excitation energies deviate by less

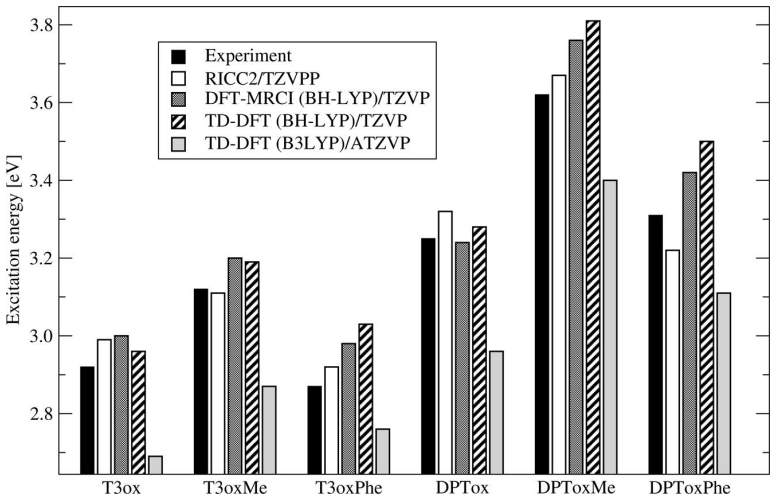

Figure 2.3: *Experimental and theoretical excitation energies for the electric dipole allowed S_1 transition. Experimental values are taken from [86].*

than 0.1 eV from the experimentally observed ones and for most of the structures errors are even below 0.05 eV. The largest difference (0.09 eV) is found for the DPToxPhe system. The corresponding TD-DFT energies are systematically redshifted, when calculated with the B3-LYP density functional. Using the BH-LYP density functional better agreement with the experimental values are obtained. The deviations of the BH-LYP results from experimental values are in a range between +0.03 and +0.19 eV and in three cases (T3oxPhe, DPToxMe, DPToxPhe) larger than 0.1 eV. The smallest error of the B3-LYP calculations with respect to experiment is −0.11 eV for T3oxPhe, all other results deviate by −0.20 to −0.29 eV. The values obtained from DFT-MRCI calculations are rather close to the RICC2 and

experimental results and slightly better than the TDDFT BH-LYP results. For the ter-thiophenes the deviations from experiment are found between +0.04 and +0.11 eV and for the diphenyl-thiophene between −0.01 and 0.14 eV. The use of diffuse or additional polarization functions in the basis set are not strictly mandatory for the TD-DFT calculations. No significant multi-reference character was found, neither for the ground, nor for the excited states of the investigated structures, so single-reference methods are safely applicable for analyses of the systems investigated here. In general the results from both, experimental and theoretical data can be summarized as follows. First, the excitation energies of the diphenylthiophene species are higher than for the terthiophene structures and second the energies for the methyl substituted structures are always higher than for the hydrogen or phenyl substituted species. Both observations can be clearly related to the influence of the different torsional angles discussed in the previous section, which are larger for the diphenyl compared to the terthiophene systems and also for the methyl substituted compared to the other structures.

2.6 Substituent Effects

The effect of changes in the substitution pattern on the inter-ring torsional angle and thus on their excitation energies could be characterized as a steric effect. The question is, if besides another more direct effect exists. To separate both influences, we decided to repeat the excited state calculations on the RICC2/TZVPP level of theory, substituting the phenyl and methyl ligands by hydrogen atoms, but keeping the remaining atoms in fixed positions, as obtained from the RICC2/TZVPP optimization of the fully substituted structures. The difference between the excitation energies of the fully substituted structures (solid lines in Figure 2.4) and the excitation energies of the hydrogen substituted ones (dashed lines in Figure 2.4) reflect the individual shifts caused by the methyl and phenyl substituents. From Figure 2.4, it can be seen that the methyl groups cause a blue shift of 0.08 eV and 0.06 eV for T3oxMe and DPToxMe, respectively, whereas phenyl substitution induces a small red shift of the excitation energies. For DPToxPhe this shift is 0.11 eV and thus slightly larger than for the T3oxPhe system where the energy only changes by 0.05 eV. The remaining difference between the values of the hydrogen substituted systems to the T3ox and DPTox excitation energies (horizontal lines in Figure 2.4) reflects the purely steric influence, caused

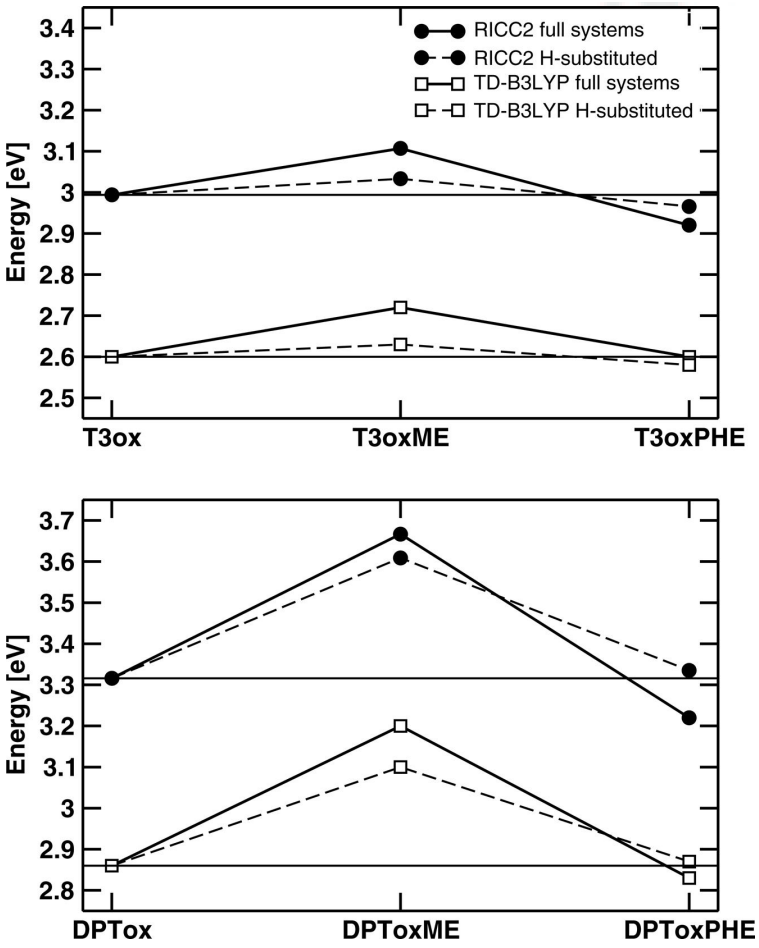

Figure 2.4: *Effects of methyl– and phenyl–substituents on the excitation energies from RICC2/TZVPP//RICC2/TZVPP calculations (filled circles) and B3–LYP/TZVP//RICC2/TZVPP calculations (hollow squares). Solid lines represent the fully substituted structures (H, Me, Phe) and dashed lines the hydrogen substituted structures (H in all cases) using geometries of fully substituted structures.*

by the different torsional angles. The steric effect is for T3oxMe 0.04eV and for T3oxPhe -0.02 eV and thus of similar magnitude as the pure substituent effect. For DPToxMe the difference in the torsional angle compared to DPTox contributes 0.29 eV to the total shift and thus clearly dominates for this species. In case of the DPToxPhe structure the dihedral angle is slightly larger than for the DPTox system, resulting in a small blue-shift of

0.01 eV, which is one order of magnitude smaller than the redshift caused by the phenyl substituents. Nevertheless it should be mentioned, that the relative geometrical orientation of the different substituents with respect to the central thiophene unit, like the tilting of the phenyl groups in DPToxPhe might have an influence on the results. The corresponding TD-DFT calculations qualitatively yield the same results, with the exception of T3oxPhe, where the absorption energy of the fully substituted system is slightly above the one of the hydrogen substituted structure. The individual shifts can be traced back to Kohn–Sham (KS) orbital eigenvalues. In Table 2.3 we report in brackets the HOMO, LUMO, and the KS gap energies if the substituent are replaced by hydrogen atoms. In the hydrogen substituted structures, the KS gap increases with inter-ring torsion angle. As already found in [53], the HOMO energy is much more sensitive to the interring torsion angle than the LUMO energy. This is more evident for terthiophenes in which the LUMO energy is fixed to 2.9 eV. The methyl substituents induce an increase of the HOMO-LUMO gap, due to a larger destabilization of the LUMO than the HOMO, whereas phenyl substituents almost do not affect the gap size.

2.7 Relevant aspects

In this theoretical study we have investigated the effect of β–substituents on the torsional angle of S, S-dioxygenated thiophene derivatives. We have compared several quantum chemical methods and different basis sets with respect to their applicability for molecular structure and electronically excited states calculations for thiophenes with different substitution patterns. The RI-CC2 results represent state of the art benchmark values for these kind of systems, as they are close to the limit of computational feasibility with present day hard- and software. Nevertheless it was found, that more approximated computational schemes, such as DFT with valence triple-ξ basis set can yield a qualitatively correct description of the investigated systems. However, the BH-LYP hybrid-functional is much better suited to reproduce experimental excitation energies than B3-LYP. We have shown that methyl substitution leads to a strong blueshift of the excitation energies compared to the unsubstituted species. The reasons for this are (i) a relatively large change in the inter-ring torsional angle and (ii) a pure substituent effect. The former is the predominant effect for DPToxMe and the latter is for T3oxMe. Phenyl substitution yields a negligible change in the

torsional angle and destabilizes HOMO and LUMO to a similar extend, so the overall effect on excitation energies remains small.

Chapter 3

Entanglement

3.1 What is entanglement

Quantum entanglement is a concept commonly used with reference to the existence of certain correlations in a quantum system that have no classical interpretation. This concept was first introduced by Schrödinger in 1935 in a paper in which he underlined the typical quantum nature of entanglement. Indeed, he wrote: "*Maximal knowledge of a total (quantum) system does not nesessarily include total knowledge of all its parts, not even when these are fully separated from each other and at the moment are not influencing each other at all.*" [88]

From a mathematical viewpoint, entanglement can be considered as a consequence of the linearity of standard quantum formalism based on Hilbert space, but it has an essential role in quantum mechanics (QM) and it is a very useful resource in Quantum Information (QI) [89]. Let us now describe how.

One of the most important principles of QM is the superposition principle which is a direct consequence of the linearity of the Hilbert space: if a system can be in two different states rapresented by the kets $|a\rangle$, $|b\rangle \in \mathscr{H}$, then it can also be in the state represented by the linear superposition $\alpha|a\rangle + \beta|b\rangle$ with $\alpha, \beta \in \mathbb{C}$ and $|\alpha|^2 + |\beta|^2 = 1$.

In general, we can distinguish between *pure state* and *mixed states*, depending on the information we have on the state.

The pure states are those states that we use when we want to describe a particle that is in a well defined state, i.e., it is in a given state with certainty and are represented by unit vectors of the Hilbert space associated

with the system. Let ρ be a pure state represented by the vector $|\psi\rangle$. Then, the corresponding density operator is $\rho = |\psi\rangle\langle\psi|$ and it has the following properties:

$$\mathcal{T}r\rho = \mathcal{T}r\rho^2 = 1. \tag{3.1}$$

When we don't know exactly in which state the system is, but there is only a probability p_i for the system to be in the pure state represented by $|\psi_i\rangle$, then we say that the system is in a mixed state that we represent with the density operator

$$\rho = \sum_i p_i |\psi_i\rangle\langle\psi_i| = \sum_i p_i \rho_i, \tag{3.2}$$

where $p_i \geqslant 0$, $\sum_i p_i = 1$ and ρ_i is the density operator associated with the pure state $|\psi_i\rangle$. On the contrary, mixed states are such that

$$\mathcal{T}r\rho = 1 \neq \mathcal{T}r\rho^2. \tag{3.3}$$

The most important consequence of the mathematical structure of the state space is in the study of compound systems. For example, let us consider a system T made up by the two subsystems A and B whose states are represented by the elements of the Hilbert space $\mathscr{H}_A$ and $\mathscr{H}_B$, respectively. Then, the system T is described by $\mathscr{H}_T = \mathscr{H}_A \otimes \mathscr{H}_B$ and a pure state of T can be represented by $|\psi\rangle \in \mathscr{H}_T$. Let us denote by $\{|\phi_i\rangle\}_{i\in\mathbb{N}}$, the elements of $\mathscr{H}_A$ and by $\{|\chi_j\rangle\}_{j\in\mathbb{N}}$ the ones in $\mathscr{H}_B$. Thus, if the state $|\psi\rangle \in \mathscr{H}_T$ can be written as a tensor product of an element of $\mathscr{H}_A$ and an element of $\mathscr{H}_B$, as in the following,

$$|\psi\rangle = |\psi\rangle \otimes |\chi\rangle \equiv |\phi, \chi\rangle, \tag{3.4}$$

we say that $|\psi\rangle$ is a *product* or *separable* pure state.

For example, the system can be in a pure state $|a, a\rangle$ or $|b, b\rangle$. But, the linearity of the Hilbert space $\mathscr{H}_T$ implies that any superposition of this states is represented by $|\psi\rangle = \alpha|a, a\rangle + \beta|b, b\rangle \in \mathscr{H}_T$. Such a state is a pure state of $\mathscr{H}_T$, but there is no element $|\phi\rangle \in \mathscr{H}_A$ and $|\chi\rangle \in \mathscr{H}_B$ such that $|\psi\rangle = |\phi, \chi\rangle$. In this case, we say that the system is in an entangled state.

In order to recognize whether a pure state is entangled or not we can consider the *biorthogonal decomposition* (also called *Schmidt decomposition* [90]) on the correlated elements of the two subspaces as in the following:

$$|\psi\rangle = \sum_{i=1}^{n} \sqrt{p_i} |\phi_i(A)\rangle |\chi_i(B)\rangle, \tag{3.5}$$

where $1 \leq n \leq \infty$, $0 < p_i \leq 1$ and $\sum_i p_i = 1$. The origin of the name "biorthogonal" is due to the fact that

$$\langle \phi_i(A)|\phi_j(A)\rangle = \delta_{ij}, \qquad \langle \chi_i(B)|\chi_j(B)\rangle = \delta_{ij}.$$

The number n of the term that appears in the decomposition described in Eq. (3.5) characterized uniquely the state $\psi\rangle$. In fact, if the Schmidt decomposition (3.5) contains only one coefficient, $p_1 = 1$, the state $|\psi\rangle$ is a product pure state (in other words, if $p_1 = 1$, the pure state $|\psi\rangle$ described in Eq. (3.5) assumes the form of the separable state in Eq. (3.4)); if there are more than one nonzero Schmidt coefficients the pure state in entangled.

3.2 Consequences of entanglement: from EPR to Bell

In 1935 Einstein, Podolsky and Rosen (EPR) wrote a paper [91], later become famous, in which they aimed to prove that QM is incomplete. Let us briefly resume their argument. Firstly, EPR stated the following two conditions.

Condition of completeness: Every element of the physical reality must have a counterpart in the physical theory;

Condition of reality: If, without in any waty disturbing a system, we can predict with certainty (i.e. with probability equal to unity) the value of a physical quantity, then there exists an element of physical reality corresponding to this physical quantity.

By using a modern argument, we can say that the EPR paradox is based on the fact that the result of a measurement is in presence of local correlation, a property associated with the quantum system right before the measurement was performed. To explain it we use the Bohm model whose results are equivalent to those of the EPR paradox. In this model we consider a system T in the singlet state with total spin 0 made up by the two qubits $\mathcal{A}$ and $\mathcal{B}$ with spin 1/2

$$|\psi_T\rangle = \frac{1}{\sqrt{2}}\Big[|0_{\mathcal{A}}1_{\mathcal{B}}\rangle - |1_{\mathcal{A}}0_{\mathcal{B}}\rangle\Big]. \tag{3.6}$$

We assume that the two qubits, which are in the quantum state (3.6), are spatially separated, and that a measurement of their polarization is done on each qubit: let $|1_{\mathcal{A}}\rangle$ denote vertical polarization of qubit $\mathcal{A}$, and $|0_{\mathcal{A}}\rangle$ horizontal polarization. Analogously for qubit $\mathcal{B}$. According to the laws of QM the

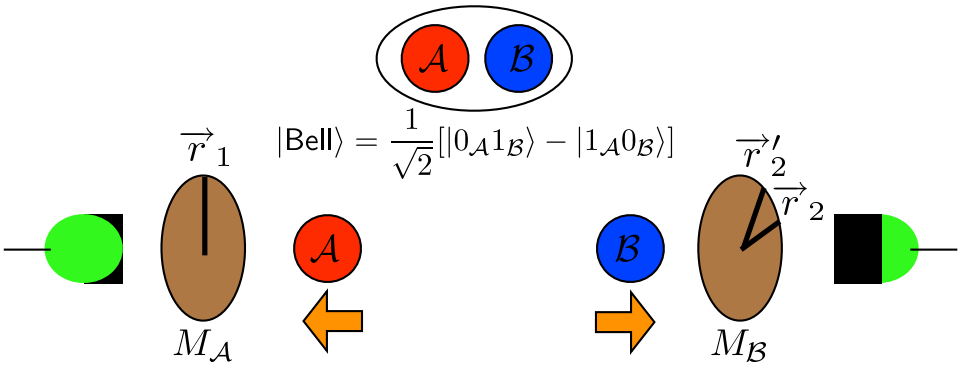

Figure 3.1: *Bohm's representation of Bell's experiment.*

outcome of the measurement on qubit $\mathcal{A}$ projects the state $|\psi\rangle$ onto the state $|0_\mathcal{A}\rangle|1_\mathcal{B}\rangle$ (or $|1_\mathcal{A}\rangle|0_\mathcal{B}\rangle$) with probability 1/2. But if we find + as outcome for the measurement on $\mathcal{A}$, the state of the system after the measurement is $|1_\mathcal{A}\rangle|0_\mathcal{B}\rangle$ with certainty. Thus, horizontal polarization is an element of reality for qubit $\mathcal{B}$ after this measurement. Hence, even if we don't make any measurement on $\mathcal{B}$ we can have some information on it. Thus, if we accept the hypothesis of locality we say that before measurement, $\mathcal{B}$ had an element of reality that QM was not able to predict. Thus EPR concluded that QM was incomplete. EPR proof of incompleteness was immediately criticized by the majority of scientific comunity, but raised a fundamental problem: if QM is incomplete, how it could be completed? If the vector $|\psi\rangle$ representing the state of the system does not describe completely the system itself, is it possible to introduce new "hidden" variables such that their specification allows to describe now completely the system? In 1964 J. Bell proved that any hidden variables theory that satisfied conditions of reality and locally is experimentally distinguishable from QM since it gives rise for some experiments to results that contrast with quantum predictions [92]. Let us briefly follow Bell reasoning. The ket $|\psi\rangle$ cannot describe all the properties of a system, but there exist some hidden variables λ that complete the information. Basically, he envisaged an experiment such that the measurements could be performed in any direction, that is, in a possible basis different to the logical one. For example, when working with photons, such measurements could be performed by using polarized rotated by different angles. Bell introduced a *correlation function* $\mathcal{P}(\vec{r}_1, \vec{r}_2)$ which denotes the average product of the outcomes of the corresponding measurements for

different directions $\vec{r}_j$ and that is defined as the following:

$$\mathcal{P}(\vec{r}_1,\vec{r}_2) := \langle\psi_T|\widetilde{\sigma}_{\vec{r}_1}(\mathcal{A})\widetilde{\sigma}_{\vec{r}_2}(\mathcal{B})|\psi_T\rangle = -\vec{r}_1\cdot\vec{r}_2, \tag{3.7}$$

where

$$\widetilde{\sigma}_{\vec{r}_1}(\mathcal{A}) = \sigma_{\vec{r}_1}(\mathcal{A})\otimes\mathbb{1}_{\mathcal{B}} = \Big[\sigma(\mathcal{A})\cdot\widehat{r}\Big]\otimes\mathbb{1}_{\mathcal{B}} = \Big[\sigma_x r_{1x}+\sigma_y r_{1y}+\sigma_z r_{1z}\Big]\otimes\mathbb{1}_{\mathcal{B}}$$

$$\widetilde{\sigma}_{\vec{r}_2}(\mathcal{B}) = \mathbb{1}_{\mathcal{A}}\otimes\sigma_{\vec{r}_2}(\mathcal{B}) = \mathbb{1}_{\mathcal{A}}\otimes\Big[\sigma(\mathcal{B})\cdot\widehat{r_2}\Big] = \mathbb{1}_{\mathcal{A}}\otimes\Big[\sigma_x r_{2x}+\sigma_y r_{2y}+\sigma_z r_{2z}\Big].$$

He also assumed that the measurement outcome of quibit $\mathcal{B}$ was independent of the orientation $\vec{r}_1$ where qubit $\mathcal{A}$ is measured (hypothesis of locality). Therefore, there exist two functions $M_{\mathcal{A}}(\vec{r}_1,\lambda)$ and $M_{\mathcal{B}}(\vec{r}_2,\lambda)$, which correspond to both measurements outcomes, with values

$$M_{\mathcal{A}}(\vec{r}_1,\lambda) = \pm 1, \qquad M_{\mathcal{B}}(\vec{r}_2,\lambda) = \pm 1. \tag{3.8}$$

(the latter equation can be seen as an hypothesis of reality). In particular, both functions satisfy the desired result if $\vec{r}_1 = \vec{r}_2$:

$$M_{\mathcal{A}}(\vec{r}_1,\lambda) = -M_{\mathcal{B}}(\vec{r}_1,\lambda), \quad \forall\lambda. \tag{3.9}$$

Nevertheless, if $p(\lambda)$ is the probability distribution for the hidden variable, with $p(\lambda\geq 0)$ and $\int p(\lambda)d\lambda = 1$, the average of the product of both outcomes should be

$$\mathcal{P}(\vec{r}_1,\vec{r}_2) = \int p(\lambda)M_{\mathcal{A}}(\vec{r}_1,\lambda)M_{\mathcal{B}}(\vec{r}_2,\lambda)d\lambda \tag{3.10}$$

and

$$\mathcal{P}(\vec{r}_1,\vec{r}_2) = -\int p(\lambda)M_{\mathcal{A}}(\vec{r}_1,\lambda)M_{\mathcal{A}}(\vec{r}_2,\lambda)d\lambda. \tag{3.11}$$

Considering another unit vector $\vec{r}_2'$ and considering that the three integers $M_{\mathcal{A}} = \pm 1$ satisfy

$$M_{\mathcal{A}}(\vec{r}_1)\Big[M_{\mathcal{A}}(\vec{r}_2) - M_{\mathcal{A}}(\vec{r_2}')\Big] \equiv \Big[1 - M_{\mathcal{A}}(\vec{r}_2)M_{\mathcal{A}}(\vec{r_2}')\Big], \tag{3.12}$$

and after some algebraic manipulation, the following Bell inequality is obtained:

$$|\mathcal{P}(\vec{r}_1,\vec{r}_2) - \mathcal{P}(\vec{r}_1,\vec{r_2}')| \leq 1 + \mathcal{P}(\vec{r}_2,\vec{r_2}'). \tag{3.13}$$

The last inequality is called *Bell inequality* and it is important to notice that there are some quantum states in which a quantum machanical system violates them, just because of the existence of non-classical correlation. This correlation of quantum nature, induced particular states as $|\psi_T\rangle$ that is know

as Bell state that is maximally entangled. For such a state, if the vector $\vec{r}_1$ and $\vec{r}_2$ are orthogonal and $\vec{r_2}'$ lies between them at 45° we have

$$\mathcal{P}(\vec{r}_1, \vec{r}_2) = 0, \mathcal{P}(\vec{r}_1, \vec{r_2}') = \mathcal{P}(\vec{r}_2, \vec{r_2}') = -\frac{1}{\sqrt{2}}. \tag{3.14}$$

The Bell inequality is thus violated, since

$$\frac{\sqrt{2}}{2} \not\leq 1 - \frac{\sqrt{2}}{2}. \tag{3.15}$$

The violation of this inequality not only implies that QM is a non–local theory, but it also says that there not exist a local realistic theory that is probabilistically equivalent to QM. Moreover Aspect et al. experiments in 1982 demonstrated that nature is non–local and that hidden variables don't exist. As a consequence, EPR argument is not acceptable because of its condition of locality, and QM is a complete theory. However, an analysis of the measurement process tells us that the existence of these of non-classical correlations does not imply a violation of causality principle, as EPR stated.

3.3 Relations among the compound system and its subsystems

Our main aim in this section is to discuss the relations among a compound physical system and its subsystems, but first let us spend some words on the notations we shall use on these topics.

In the following, we use $|\psi_s\rangle$ to identify a product or separable pure state and ρ_s for the correspondent density operator. Anologously, we use $|\psi_e\rangle$ and ρ_e when refering to an entangled state and its density operator, respectively. Hence, let us associate with the product state $|\psi_s\rangle$ the density operator

$$\rho_s = |\psi_s\rangle\langle\psi_s| = |\phi\rangle|\chi\rangle\langle\phi|\langle\chi| \equiv |\phi, \chi\rangle\langle\phi, \chi|, \tag{3.16}$$

and with the entangled state the density operator

$$\rho_e = |\psi_e\rangle\langle\psi_e| = \sum_{ij} \sqrt{p_i}\sqrt{p_j}|\phi_i(A)\rangle|\chi_i(B)\rangle\langle\phi_j(A)|\langle\chi_j(B)| \equiv$$

$$\equiv \sum_{ij} \sqrt{p_i}\sqrt{p_j}|\phi_i(A), \chi_i(B)\rangle\langle\phi_j(A), \chi_j(B)|. \tag{3.17}$$

Once we have expressed the global state in terms of the biorthogonal decomposition, it is possible to obtain some informations on the subsystems.

For example, if we are interested in predicting expectation values or probabilities of outcomes for measurements performed on subsystem A (B), we only need the reduced density operator

$$\rho_A = \mathcal{T}r_B\rho \qquad \Big(\rho_B = \mathcal{T}r_A\rho\Big). \tag{3.18}$$

We can shown that if the compound system is in a separable pure state, the subsystems are in a pure state. Indeed, if $|\psi_s\rangle = |\phi,\chi\rangle$ is the ket associated with the separable state, its density operator is $\rho_s = |\phi,\chi\rangle\langle\phi,\chi|$. Hence, in order to obtain information on the subsystem A we make the partial trace as the following:

$$\rho_A = \mathcal{T}r_B\rho_s = \sum\langle\chi_j(B)|\rho|\chi_j(B)\rangle = |\phi\rangle\langle\phi|, \tag{3.19}$$

where $\{\chi_j(B)\}_{j\in\mathbb{N}}$ is an orthonormal basis on the Hilbert space $\mathscr{H}_B$.

Moreover, one can prove that if the compound system is in an entangled pure state, the subsystems are in a mixed state. Indeed, if the entangled state is represented by $|\psi_e\rangle = \sum_{i>1}\sqrt{p_i}|\phi_i(A)\rangle|\chi_i(B)\rangle$, then the corresponding density operator is $\rho_e = \sum_{ij}\sqrt{p_i}\sqrt{p_j}|\phi_i(A),\chi_i(B)\rangle\langle\phi_j(A),\chi_j(B)|$. Hence, by making the partial trace with respect to system B, we obtain

$$\rho_A = \mathcal{T}r_B\rho_e =$$

$$= \sum_l\langle\chi_l(B)|\rho|\chi_l(B)\rangle = \sum_{ijl}\sqrt{p_i}\sqrt{p_j}\langle\chi_l(B)|\phi_i(A)\chi_i(B)\rangle\langle\phi_j(A)\chi_j(B)|\chi_l(B)\rangle =$$

$$= \sum_{ijl}\sqrt{p_i}\sqrt{p_j}\delta_{li}\delta_{lj}|\phi_i(A)\rangle\langle\phi_j(A)| = \sum_l p_l|\phi_l(A)\rangle\langle\phi_l(A)|. \tag{3.20}$$

A similar result can be obtained by tracing out with respect to system A In other words, the vector $|\psi\rangle$ represents a product state of the compound system if and only if the corresponding reduced density operators represent pure states. If $|\psi\rangle$ is an entangled state, the corresponding reduced density operators must correspond to mixed states.

Hence, if we want to measure the degree of entanglement we can calculate the degree of mixedness of the corresponding reduced density operator (or matrix) [93].

3.4 Entropy and its rule in information theory

We have seen that the mixedness of the reduced density operators is linked to the entanglement of the corresponding state. This is a consequence of the

fact that an entangled state gives rise to correlations and if we only observe one subsystems we lose information about these correlations, as it results from the fact that we effectively have a mixed state.

Since the *von Neumann entropy* is of particular significance for describing randomness of a state and mixedness of density operators, in this paragraph we deald with the concept of *entropy*.

The highway of the development of entropy is marked by many great names as Clausius, Boltzmann, von Neumann, Shannon, Jaynes and several others.

The word "entropy" was created by Rudolf Clausius according to which the change of entropy of a system is obtained by adding the small portions of heat quantity received by the system divided by the absolute temperature during the heat absorption. This definition is satisfactory from a mathematical point of view and gives nothing other than an integral in precise mathematical terms. Clausius postulated that the entropy of a closed system cannot decrease, which is generally referred to as the second law of thermodynamics. Nevertheless, he did not provide any heuristic argument to support the law. In 1877, the concept of entropy was really clarified by Ludwig Boltzmann, whose great discovery was the celebrated formula

$$S = k_B \ln W, \tag{3.21}$$

where k_B is the Boltzmann constant ($k_B = 1.38 * 10^{-16}$ erg/K). It established the connection between the variable of the state, "entropy", which had been derived from phenomenological considerations, and the "amount of chaos" (or disorder) of a system, which, more precisely, means the number of microstates which have the same prescribed macroscopic properties (this number is known as "thermodynamical probability" and is commonly representad by the letter W).

In 1927, von Neumann generalized the classical expression of Boltzmann to quantum mechanics. Entropy is not an observable, and there isn't an operator with the property that its expectation value in some state would be its entropy. It is rather a function of a state. If the state is described by the density matrix ρ, its entropy is defined by

$$S(\rho) = -Tr\rho \ln \rho, \tag{3.22}$$

in which $k_B = 1$ which corresponds to measuring the temperature in ergs instead of Kelvin, the entropy becomes dimensionless. It is important to note

that any density matrix ρ can be diagonalized, that is, it can be represented in some orthonormal basis, by a matrix of the form

$$\rho = \begin{pmatrix} p_1 & 0 & \cdots & 0 \\ 0 & p_2 & \cdots & 0 \\ 0 & 0 & p_3 & \cdots \\ \vdots & \vdots & \vdots & \vdots \\ 0 & 0 & \cdots & p_N \end{pmatrix}, \tag{3.23}$$

where $p_i \geq 0$ and $\sum_{i=1}^{N} p_i = 1$. By inserting Eq. (3.23) in Eq. (3.22) we thus obtain the following for the von Neumann entropy: $(\rho) = -\sum p_i \ln p_i$, where for definition we assume $0 \ln 0 = 1$. The coefficients P_i are the probabilities of finding the system in the corresponding pure state. If we consider N copies of the same system, the Hilbert space that describes the resulting system is

$$\mathcal{H}_{TOT} = \underbrace{\mathcal{H} \otimes \mathcal{H} \otimes \cdots \otimes \mathcal{H}}_{N\ times}, \tag{3.24}$$

where $\mathcal{H}$ is the Hilbert space of the original system. In this new system there are microstates of the form $|1\rangle \otimes |2\rangle \cdots$, where $|1\rangle$ occurs $p_1 N$ times, $|2\rangle$ $p_2 N$ times, and so on. All these microstates have the same weight. According to Boltzmann one obtains for the entropy $\ln W_N$ (with $W_N = N!/(p_1 N)!(p_2 N)! \cdots$). The corresponding portion for one system is $(1/N) \ln W_N$, which goes to $S(\rho)$ as $N \to \infty$. In 1943, after Boltzmann and von Neumann, Shannon initiated the interpretation of the quantity $-\sum_i p_i \log p_i$ as "uncertainty measure" or "information measure". He posed a problem in the following way:

"Suppose we have a set of possible events whose probabilities of occurence are $p_1, p_2, \cdots, p_N$. These probabilities are known but that is all we know concerning which event will occur. Can we find a measure of how much "choice" is involved in the selection of the event or how uncertain we are of the outcome?"

Denoting such a measure by $S(p_1, p_2, \cdots, p_N)$ he listed three very reasonable requirements which should be satisfied. He concluded that the only H satisfying the three assumptions is of the form

$$S = -K \sum_{i=1}^{N} p_i log p_i, \tag{3.25}$$

where K is a positive constant. For S he used different names such as information, uncertainty and entropy. Many years later Shannon said

"My greatest concern was what to call it. I thought of calling it 'information', but the word was overly used, so I decided to call it 'uncertainty'. When I discussed it with John von Neumann, he had a better idea. Von Neumann told me, 'You should call it entropy, for two reasons. In the first place your uncertainty function has been used in statistical mechanics under that name, so it already has a name. In the second place, and more important, nobody knows what entropy really is, so in a debate you will always have the advantage'."

Shannon's postulates were transformed later into the following axioms:

1. Continuity: $S(p, 1-p)$ is a continuous function of p.

2. Symmetry: $S(p_1, p_2, \cdots, p_N)$ is a symmetric function of its variables.

3. Recursion: For every $0 \leq \lambda < 1$ the following recursion holds

$$S\Big(p_1, \cdots, p_{N-1}, \lambda p_N, (1-\lambda)p_N\Big) = S(p_1, \cdots, p_N) + p_N S(\lambda, 1-\lambda).$$

These axioms determine a function S up to a positive constant factor. Excepting the above story about a conversation between Shannon and von Neumann, we do not know about any mutual influence. Shannon was interested in communication theory and von Neumann's thermodynamical entropy was in the formalism of quantum mechanics. Von Neumann himself never made any connection between his quantum mechanical entropy and information. The concept that entropy is a mesure of our ignorance about a given physical was recognized very early, however Boltzmann was also aware of it.

The mathematical theory of information originally was intended as a theory of communication. The simplest problem it deals with is the following: take any message, for instance consisting of word or of digits. One can represent it as a sequence of binary dogits and thus, if the length of the "word" is n, one needs n digits to characterize it. The set E_n of all words of lenght n contains 2^n elements, therefore the amount of information needed to characterize one element of its is $\log_2 N$, where N is the number of elements of E_N and it is $N = 2$. Elaborating on this little bit, one arrives at the result that the amount of information which is needed to characterize an element of any set of power N is $\log_2 N$. Moreover, let E be a union $E_1 \bigcup \cdots \bigcup E_k$ of pairwise disjoint sets, N_i is the number of elements of E_i. Let $p_i = N - i/N$, $n = \sum N_i$. If one knows that an element of E belongs

to some E_i, one needs $\log_2 N_i$ additional information in order to determine it completely. Hence the average amount of information need to determine an element, provided that one already knows to which E_i it belongs, is

$$\sum (N_i/N) \log_2 N_i = \sum p_i \log_2 N p_i = \sum p_i \log_2 p_i + \log_2 N.$$

The quantity $\log_2 N$ is the information that is needed if one does not know to which E_i a given element belongs, hence the corresponding average lack of information is

$$-\sum p_i \log_2 p_i. \tag{3.26}$$

This is usually called Shannon's formula, although it was discovered by Wiener independently.

Eq. (3.26) is very important because if the set E is considered as a set of N measurements, and the p_i are the probabilities of finding the system in the pure state $|i\rangle$, then, a part for an irrelevant factor $\ln 2$, Shannon's expression equals the definition of entropy.

By means of information theory it is possible to rephrase the well–known maximum entropy principle as in the following: suppose that for some system you know only a few, macroscopic quantities, and you have no further knowledge of it. Then the system is expected to be in the state with maximal entropy, because if it were in a state with lower entropy it would also contain more information than previously specified; it is the so–called *Jaynes' principle*, due to Jaynes in 1957.

Chapter 4

Entanglement of electrons in interacting molecules

Entanglement is a concept commonly used with reference to the existence of certain correlations in quantum systems that have no classical interpretation and it holds a fundamental role in quantum information theory. Starting from the Collin's conjecture, that is, the correlation energy in molecular systems is proportional to their entropy, we have interpreted the degree of entanglement as an evaluation of correlation energy. Entanglement is in fact a physical observable directly measured by the von Neumann entropy of the system. This concept is used in order to give a physical meaning to the electron correlation energy, which is defined as the difference between the total energy of a given molecular system, with respect to the one obtained with the Hartree–Fock approximation method. We have made a measurement of electron entanglement and compared with electron correlation energy in two different examples of bipartite systems, as Hydrogren molecule and the dimer of ethylene, where each hydrogen atom or each ethylene molecule, respectively, can be considered a qubit. Changing the relative orientation and distance of the molecules of the dimer, we have found the configuration corresponding to maximum entanglement [94], [95].

4.1 Usefulness of entanglement

Entanglement is the name given by Schrödinger to the nonlocal correlations responsible for violations of the Bell inequalities [96]. The potential usefulness of this property has been demonstrated in a variety of applications,

such as quantum teleportation [97], quantum key distribution [98], quantum cryptography [99], and it is a useful resource to accelerate some quantum processes as, for example, the factorization in Shor's algorithm or to enhance the mutual information of memory channels.

The quantum information community devoted a lot of efforts to analyze entanglement theoretically and experimentally. For example, Machiavello *et al.* [100] considered a different class of channels, in which correlated noise acts on consecutive uses of channels. They showed that higher mutual information can be achieved above a certain memory threshold, by entangling two consecutive uses of the channel. Banaszek *et al.* [101] implemented Machiavello *et al.* suggestion experimentally. They shown how entanglement can be used to enhance classical communication over a noisy channel. In their setting, the introduction of entanglement between two photons is required in order to maximized the amount of information that can be encoded in their joint polarization degree of freedom.

Schliemann proposed an idea [102], extended by other outhors [103], [104], to make a measurement of the degree of entanglement. He, in fact, suggested to use a density matrix in the spatial coordinates and to compute the von Neumann entropy. Such an approach is based on an analogous of the Schmidt decompostion for state vectors of two fermionic particles: through an unitary transformation the antisymmetric wave function is expressed into a basis of Slater determinants with a minimum number of nonvanishing terms. This number, known as Slater rank, is a criterion to identify whether a system is entangled or not, which involves the evaluation of the von Neumann entropy of one particle reduced density matrix. In order to exploit entanglement in quantum computation also more complex molecules are studied. For example, the researchers of Hahn–Meitner–Institut are working on the realization of molecular quantum computers whose quantum bits could be formed by fullerenes with a single nitrogen or phosphorus atom trapped inside.

For this reason, it is important to investigate the properties of some molecules and the interaction among them. A study of this kind is carried out in this chapter. Here, the starting point is the so–called Collin's conjecture [105], that is, the correlation energy in molecular systems is proportional to their entropy. This conjecture was confirmed by numerical evidence by Ramirez *et al.* [106] and taken up by Huang and Kais in [104] who interpreted the degree of entanglement as an evaluation of correlation

energy. Entanglement is in fact a physical observable directly measured by the von Neumann entropy of the system. This concept is used in order to give a physical meaning to the electron correlation energy, which is not directly observable since it is defined as the difference between the total energy of a given molecular system, with respect to the one obtained with the Hartree–Fock approximation method. The Hartree–Fock method, in fact, is typically used to solve Schrödinger equation for a multi–electron atom or molecule described in the fixed–nuclei approximation (Born–Oppenheimer approximation) by the electronic molecular Hamiltonian and the calculation of the error due to this approximation is a major problem in many–body theory and a vast amount of work has been done on this subject [107].

In this work, we make a measurement of electron entanglement in two different examples of bipartite systems, as H_2 molecule and the dimer of ethylene, where each hydrogen atom or each ethylene molecule, respectively, can be considered a qubit. In this chapter, firstly, we decide the method we use to make a measurement of entanglement comparing the von Neumann entropy of the reduced density matrix $S(\rho_1)$ and the von Neumann entropy of the density matrix $S(\rho)$ for the H_2 molecule. After, fixed that the most convenient method to adopt is the second, $(S(\rho))$, we analyze a dimer of ethylene. Using the Klein's inequality for a bipartite system, we define the interaction electron entanglement in order to study the degree of entanglement between the two molecules of the dimer then, we compare it with the interaction electron correlation.

The structure of the present chapter is the following: in §4.2 we briefly resume what entanglement is [108] (equivalently, when a state is separable or entangled [109]) and why we choose the von Neumann entropy to make an estimate of the degree of entanglement. In §4.3 we first analyze a dimer of ethylene considering it as a multielectrons system, calculate the correlation energy, and then compare it with the entanglement, as a function of the distance between the two molecules. In §4.4 we introduce a new quantity, the *interaction electron entanglement*, which is defined as $S_{int} = S[2C_2H_4] - 2S[C_2H_4]$, in order to obtain the entanglement between the two molecules of the dimer. Then, we change the relative orientation and the distance between the molecules, in order to obtain the configuration corresponding to maximum entanglement. In this way, the system can be considered bipartite and each molecule can be seen as a qubit for an application to quantum computing. In §4.5 we explain some computational details describing the

package we use and how we prepare the input for the compound systems that we analyzed. Finally, in §4.6 some comments and results are discussed.

4.2 A measurement of entanglement

As a simple bipartite system, let us consider the H_2 molecule, whose Hilbert space can be represented by:

$$\mathscr{H} = \Big[\mathscr{L}^m(1) \otimes \mathscr{S}^2(1)\Big] \otimes \Big[\mathscr{L}^m(2) \otimes \mathscr{S}^2(2)\Big] = \mathscr{C}^{2m}(1) \otimes \mathscr{C}^{2m}(2), \quad (4.1)$$

where $\mathscr{L}$ and $\mathscr{S}$ represent the orbital and the spin space, respectively; in brackets we denote one of the two electrons while the index represents the dimension of the space.

In the occupation number representation [110] ($n_1\uparrow, n_1\downarrow, n_2\uparrow, n_2\downarrow, \ldots, n_m\uparrow, n_m\downarrow$) the subscripts denote the spatial orbital index and with this notation let us introduce an orthonormal basis for each space $\mathscr{C}^m$:

$$\left\{\begin{array}{c} |n_1\uparrow\rangle \\ |n_1\downarrow\rangle \\ |n_2\uparrow\rangle \\ |n_2\downarrow\rangle \\ \vdots \\ |n_m\uparrow\rangle \\ |n_m\downarrow\rangle \end{array}\right\}_{(1)} \otimes \left\{\begin{array}{c} |n_1\uparrow\rangle \\ |n_1\downarrow\rangle \\ |n_2\uparrow\rangle \\ |n_2\downarrow\rangle \\ \vdots \\ |n_m\uparrow\rangle \\ |n_m\downarrow\rangle \end{array}\right\}_{(2)} \quad (4.2)$$

A pure two-electron state $|\Psi\rangle$ can be written in this representation as

$$|\Psi\rangle = \sum_{a=1}^{m}\sum_{b=1}^{m} \omega_{a,b} c_a^\dagger c_b^\dagger |0\rangle, \quad (4.3)$$

where $|0\rangle$ is the vacuum state, the coefficients $\omega_{a,b}$ satisfy, accordingly to Pauli exclusion principle the following requests:

$$\left\{\begin{array}{l} \omega_{a,b} = -\omega_{b,a} \\ \omega_{i,i} = 0, \end{array}\right. \quad (4.4)$$

and $c^\dagger$ and c are the creation and annihilation operators of single–particle states, respectively, whose action on the vacuum state is

$$c_a^\dagger c_b^\dagger |0\rangle = |ab\rangle, \quad a, b \in \{1, 2, 3, 4, \ldots, 2m\}$$

$$\begin{array}{ll} 1 \equiv |n_1\uparrow\rangle & 2 \equiv |n_1\downarrow\rangle \\ 3 \equiv |n_2\uparrow\rangle & 4 \equiv |n_2\downarrow\rangle \\ \vdots & \vdots \\ 2m-1 \equiv |n_m\uparrow\rangle & 2m \equiv |n_m\downarrow\rangle \end{array} \quad (4.5)$$

The coefficients $\omega_{a,b}$ can be calculated by using the configuration interaction method [111], [112]. In particular, for H_2 molecule we use configuration interaction single–double (CISD) method that is limited to single and double excitations:

$$|\Psi^{CISD}\rangle = c_0|\psi_0\rangle + \sum_{ar} c_a^r|\psi_a^r\rangle + \sum_{a<b,r<s} c_{a,b}^{r,s}|\psi_{a,b}^{r,s}\rangle, \tag{4.6}$$

where $|\psi_0\rangle$ is the ground state Hartree–Fock wave function, c_a^r is the coefficient for single excitation from orbital a to r, and $c_{a,b}^{r,s}$ is the double excitation from orbital a and b to r and s. In the occupation number representation, the CISD wave function is given by

$$|\Psi\rangle = c_0|1_1 1_2 0_3 0_4 \ldots\rangle + c_1^3|0_1 1_2 1_3 0_4 \ldots\rangle + c_2^4|1_1 0_2 0_3 1_4 \ldots\rangle + c_{1,2}^{3,4}|0_1 0_2 1_3 1_4 \ldots\rangle + \cdots \tag{4.7}$$

where each "1" represents the presence of the electron and the subscript represents the site where the electron is [113].

In order to realize whether the state of the compound system is entangled or not, we have to construct the corresponding reduced density matrix. Indeed, the vector $|\psi\rangle$ represents a product state of the compound system if and only if the corresponding reduced density operators represent pure states (equivalently, $|\psi\rangle$ is an entangled state if and only if the corresponding reduced density operators formally represent mixed states). Hence, if we want to measure the degree of entanglement we can calculate the degree of mixedness of the corresponding reduced density operator (or matrix) [114]. This is a consequence of the fact that an entangled state gives rise to correlations whose information is lost if we only observe the subsystems, as it results from the fact that we effectively have a mixed state.

Of particular significance for describing randomness of a state and mixedness of density operators is the *von Neumann entropy*, defined as

$$S(\rho) = -\mathcal{T}r(\rho log_2 \rho). \tag{4.8}$$

It is important to note that ρ is a non–negative trace class operator, while S is not. In analogy with classical entropy, S measures the amount of randomness in the state ρ. More precisely, the entropy S is zero if and only if the state is pure, and it is maximized when $S(\rho) = log_2 d$, where d is the dimension of the Hilbert space. In other words, the more mixed is the reduced density operator, the more entangled is the original state and this result can be seen as a justification for the use of entropy as a measurement

of quantum entanglement. Thus, the entanglement of a pure state of a pair of quantum systems can be obtained as entropy of either member of the pair, consequently, in order to calculate the degree of electron entanglement in the H_2 molecule we have to calculate the von Neumann entropy of the density matrix reduced with respect to an electron. Starting from the density matrix $\rho = |\Psi^{\mathrm{CISD}}\rangle\langle\Psi^{\mathrm{CISD}}|$, we obtain the reduced density matrix by making the partial trace relative to all the occupation numbers except $n_1\uparrow$ (see Appendix A)

$$\rho_1^{\mathrm{CISD}} = Tr_{\substack{n_i\uparrow, n_j\downarrow \\ \left\{ \begin{smallmatrix} 1 < i \leq m \\ 1 \leq j \leq m \end{smallmatrix} \right.}} \rho^{\mathrm{CISD}} =$$

$$= \sum_{\substack{n_i\uparrow = 0,1 \\ n_j\downarrow = 0,1}} \langle n_1\downarrow, n_2\uparrow, n_2\downarrow, \ldots, n_m\uparrow, n_m\downarrow |\rho| n_1\downarrow, n_2\uparrow, n_2\downarrow, \ldots, n_m\uparrow, n_m\downarrow\rangle$$

$$\rho_1^{CISD} = \begin{pmatrix} \sum_{i=1}^{m-1} |c_1^{2i+1}|^2 + \sum_{i,j=1}^{m-1} |c_{1,2}^{2i+1,2j+2}|^2 & 0 \\ 0 & |c_0|^2 + \sum_{i=1}^{m-1} |c_2^{2i+2}|^2 \end{pmatrix}. \tag{4.9}$$

The von Neumann entropy of the reduced density matrix ρ^{CISD} represents the degree of entanglement:

$$S\Big(\rho_1^{CISD}\Big) = -Tr\Big(\rho_1^{CISD} log_2 \rho_1^{CISD}\Big) =$$

$$= -\Big(\sum_i^{m-1} |c_1^{2i+1}|^2 + \sum_{i=1}^{m-1} |c_{1,2}^{2i+1,2i+2}|^2\Big) log_2\Big(\sum_i^{m-1} |c_1^{2i+1}|^2 + \sum_{i=1}^{m-1} |c_{1,2}^{2i+1,2i+2}|^2\Big) +$$

$$-\Big(|c_0|^2 + \sum_{i=1}^{m-1} |c_2^{2i+2}|^2\Big) log_2\Big(|c_0|^2 + \sum_{i=1}^{m-1} |c_2^{2i+2}|^2\Big). \tag{4.10}$$

In order to make a generalization of this method to multipartite systems, we decide to measure the degree of entanglement as the von Neumann entropy of the density matrix corresponding to the compound system:

$$S\Big(\rho\Big) = -Tr\Big(\rho log_2 \rho\Big) = -\frac{1}{2}\Big(\sum \alpha_i log_2 \alpha_i + \sum \beta_i log_2 \beta_i\Big), \tag{4.11}$$

where α_i and β_i are the so called *Natural Spin Orbitals* (the eigenvalues of ρ). We compare the behaviours of the entanglement obtained with the CISD coefficients method or with the Natural Spin Orbital method, calculated as a function of internuclear distance R.

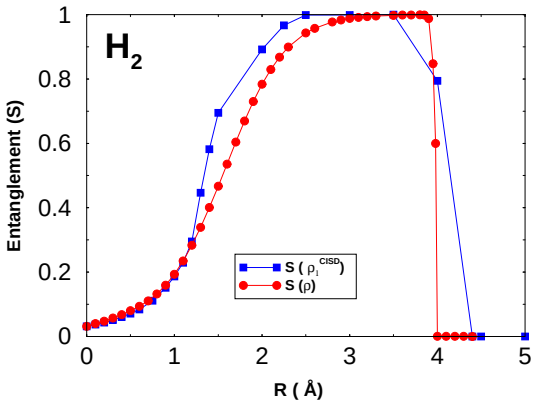

Figure 4.1: *The figure shows the degree of entanglement in the Hydrogen molecule calculated as the von Neumann entropy of the reduced density matrix with respect to an electron* ($S(\rho_1^{CISD})$) *and as the von Neumann entropy of the density matrix* ($S(\rho)$).

In Figure 4.1 we show that the entanglement calculated as the von Neumann entropy of the reduced density matrix $S(\rho_1^{CISD})$ has a similar behaviour as the entanglement calculated as the von Neumann entropy of the density matrix $S(\rho)$ of the compound system. In particular, at small internuclear distances, the two curves representing the entropies overlap, while outside the bond region, they give different results though their behaviours are similar. Since we are interested to a qualitative course of entanglement and to the search of its maximum value, we neglect the above differences and choose to adopt the Natural Spin Orbital method in order to investigate more complicated systems.

4.3 Entanglement as a measurement of electron correlation

Our main aim in this Section is to show that entanglement can be interpreted as a measure of the electron correlation [115], [116], [117]. Entanglement, in fact, is a physical observable directly measurable by the von Neumann entropy of the system. On the contrary, the electron correlation energy is not directly observable, since it is defined as the difference between the exact total energy of a given molecular system, with respect to the one prescribed

by the Hartree–Fock approximation method, that is

$$E_c = E_{exact}^{Sch} - E_{HF}. \tag{4.12}$$

The correlation energy is the energy recovered by fully allowing the electrons to avoid each other and Hartree–Fock method improperly treats interelectron repulsions in an averaged way. In other words, the exact wave function for a system of many interacting electrons is never a single determinant or a simple combination of a few determinants. The corresponding error is due to the correlations that are the analogue of the quantum entanglement in separated systems and are essential for quantum information processing in nonseparated systems.

Since in [104] the authors discussed the formation of H_2 molecule, showing a qualitative agreement between the entanglement and the correlation energy as functions of nucleus-nucleus distance, let us generalize the argument proposed above to more complex molecules, as a dimer of ethylene.

4.3.1 Hydrogen molecule

Entanglement is a physical observable measured by the von Neumann entropy and this concept gives a physical meaning to the electron correlation energy in structures of interacting electrons. The electron correlation, in fact, is not directly observable, since it is defined as the difference between the exact ground state energy of the many electrons Schrödinger equation and the Hartree–Fock energy. Hence, we want to investigate whether entanglement can be considered as an estimation of correlation energy.

In this framework, entanglement (S) and correlation energy (E_c) are calculated respectively by Eq. (4.10) and Eq. (4.12). the obtained behaviours are represented in Figure 4.2 as functions of nucleus–nucleus separation.

Even if, in order to represent correlation energy and entanglement, we use two different scales, in Figure 4.2 we can see that entanglement has a small value in the united atom limit after it is growing for small distances till it arrives at a maximum value then it decreases till it assumes zero value at the separated atom limit and it is exactly the progress of the correlation curve.

In order to compare the entropy S with the electron correlation energy E_c, we rescale S with the parameter α_{min} calculated with the procedure illustrated in the following.

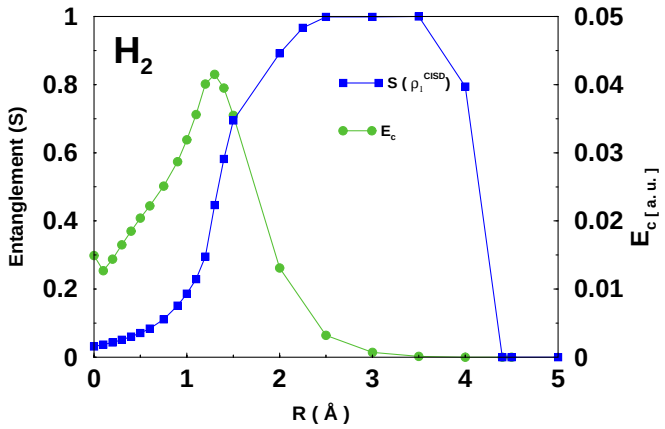

Figure 4.2: *Comparison between the entanglement, calculated by the von Neumann entropy of the reduced density matrix, and the electron correlation energy in the Hydrogen molecule.*

Let us introduces the quantity Δ defined as

$$\Delta_\alpha = E_c - \alpha S_{vN} \tag{4.13}$$

and minimize the mean sqared deviation

$$I[\alpha] = \int \Delta_\alpha^2 \, dR, \tag{4.14}$$

where the integration variablr is the interatomic distance R.

The minimizing parameter α_{min} is the one that satisfies the condition

$$\frac{\delta I[\alpha]}{\delta \alpha} = 0. \tag{4.15}$$

Consequently

$$\alpha = \frac{\int E_c S_{vN} \, dR}{\int S_{vN}^2 \, dR} \approx 0.009. \tag{4.16}$$

Once we have found the parameter α_{min}, the corresponding $\Delta_{\alpha_{min}}$,

$$\Delta_{\alpha_{min}} = E_c - \alpha_{min} S_{vN}, \tag{4.17}$$

allows us to answer to the following question about the analysis of H_2 molecule. We want to know if the quantity $\Delta_{\alpha_{min}}$ in Eq. (4.17) has a more concrete physical meaning, in particular whether the minimizing parameter α_{min} and the vanishing point of $\Delta_{\alpha_{min}}$ does possess any physical meaning.

In Figure 4.3 it is shown $\Delta_{\alpha_{min}}$ as a function of nucleus–nucleus distance: it is important to note that the vanishing point of $\Delta_{\alpha_{min}}$ is nearby $R \approx 2$ Å that corresponds to the equilibrium configuration of the Hydrogen molecule.

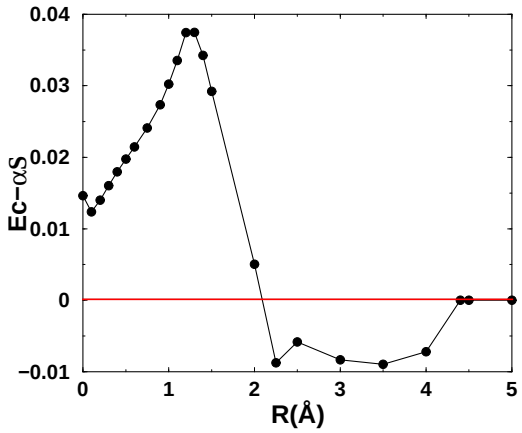

Figure 4.3: $\Delta_{\alpha_{min}}$ *for the* H_2 *molecule as a function of nucleus–nucleus distance.*

4.3.2 Dimer of ethylene

Once we have setted the distance between the molecular planes, we calculate the electron correlation energy of the dimer by the procedure described in §4.2. For the same configuration, we calculate the degree of entanglement with the Natural Spin Orbitals method. We repeate the same procedure changing the distance between the planes or, once we have fixed this distance, we make a rotation as in picture and the results are in the first and in the second panel of Figure 4.4 respectively.

As we can see from the above picture, the entropy (S) and the correlation energy (E_c) have a comparable behaviour, although we use two different scales to represent these two quantities. In fact, when we plot them as functions of the plane distance, the two curves quickly decrease till $R = 4.5$ Å, moreover for bigger distances, both of them decrease more slowly. When we set the distance at $R = 3.5$ Å and change the mutual orientation of the molecules on their planes, we can see that both the entanglement and correlation energy decrease when the rotation angle grows up. The reason of this fact is that when a rotation of a molecule on its plane is made, the bigger is the rotation angle, the small becomes the superposition of the external orbitals of the two molecules. Consequently, the electron entanglement and the correlation energy decrease as it is shown in Figure 4.4.

The above reasonings suggest us to interpret the entanglement as an efficient instrument to evaluate the electronic correlation energy, not only for H_2 molecule [104], but also for some bigger systems.

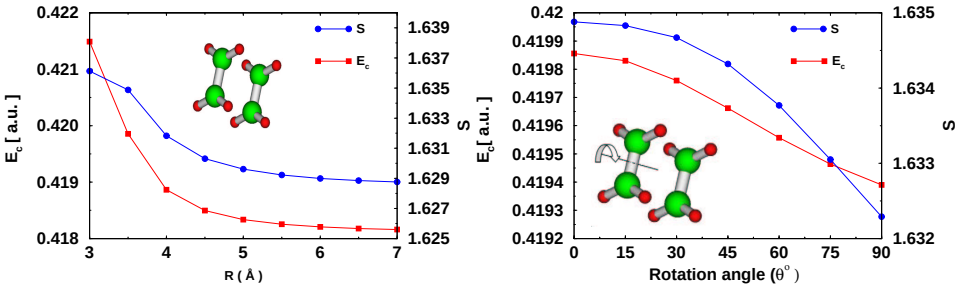

Figure 4.4: *A comparison between entanglement and correlation energy in the dimer of ethylene, calculated by changing the mutual distance of the molecules (left panel) with molecules in a face to face orientation and by changing the relative orientation (right panel, the molecules are parallel at R=3.5 Å).*

4.4 Results: interacting molecules

The study of the degree of electronic entanglement that we have made in this thesis is a useful resource for quantum computers whose input states are constructed in order to be maximally entangled. In this way, it is possible to obtain an exponential speed–up of quantum computation over classical computation. Therefore, the main aim of this work, is to analyze a dimer of ethylene, which represents the simplest organic conjugate system, in order to find the configuration corresponding to a maximum degree of entanglement between the two molecules. Thus we have to consider the compound system as a bipartite system where each molecule can be seen as a qubit and, consequently, calculate the degree of the entanglement due to the interaction of the molecules only, thus neglecting the internal interaction of each molecule.

In order to realize our goal we utilize the well known fact in quantum chemistry that the correlation energy between the two molecules of ethylene can be obtained as the difference between the correlation energy due to the interaction of all the electrons in the compound systems and the correlation energy of the electrons in each molecule, *i.e.*,

$$E_c^{int} = E_c[2C_2H_4] - 2E_c[C_2H_4]. \tag{4.18}$$

Let us now observe in Figure 2a that when the distance between the two C_2H_4 molecules is infinite, we can consider them as two separated subsystems of the compound system dimer, which we denote by $2C_2H_4$, since

they are uncorrelated. In this case, we have that $\rho[2C_2H_4] = \rho[C_2H_4] \otimes \rho[C_2H_4]$, thus, by using the definition of von Neumann entropy, we have that $S(\rho[2C_2H_4]) = 2S(\rho[C_2H_4])$. In the general case, *i. e.*, for finite discances, the Klein's inequality holds, that is,

$$S(\rho[2C_2H_4]) > S(\rho[C_2H_4]) + S(\rho[C_2H_4]) = 2S(\rho[C_2H_4]). \tag{4.19}$$

We thus define the *interaction electron entanglement* ($S_{(int)}$) as

$$S_{(int)} = S(\rho[2C_2H_4]) - 2S(\rho[C_2H_4]). \tag{4.20}$$

Then, we make a study of the degree of the interaction electron entanglement in the dimer of ethylene by changing the relative orientation and distance of the molecules. The results obtained are reported in Figure 4.5, where it is shown the degree of interaction electron entanglement as a function of the rotation angle (in (b) and (c)) and as a function of molecular distance (in (d)) calculated in a face to face configuration. We can see that, for $R < 3.1$ Å, S_{int} grows up with the increasing of the molecular distance and the maximum value of this function moves from a rotation angle $\theta = 50°$ to $\theta = 30°$ and in general, the closer are the molecules the smaller is the rotation we would make to obtain the maximum value of S_{int}. Instead, for $R > 3.1$ Å, S_{int} decreases with the increasing of R, and becomes less sensible to the rotation angle since the molecules are more and more uncorrelated. In order to confirm this behaviour, we plot S_{int} as a function of R for different torsion angles, in the Figure 4.5(d). It is evident that the configuration obtained setting $R = 3.1$ Å is the critical configuration. Indeed, for smaller distances, the entropy increases, while for bigger distances, it decreases with the increasing of R. Moreover, for $R = 5.5$ Å, the correlation between the two molecules is approximatively zero indipendently of the rotation angle.

4.5 Computational details

In order to calculate the CISD coefficients of the wave function, or equivalently, the entries of the reduced density matrix ρ_1^{CISD} and to found the eigenvalues of the density matrix, the so called Natural Spin Orbitals, we use the package *Gaussian 03* [118]. In the calculation concerning the dissociation of the H_2 molecule, we expand the wave function with a Configuration Interaction Single Double method. For this system, all the possible excitations are the single or the double ones, hence the CISD method represents a

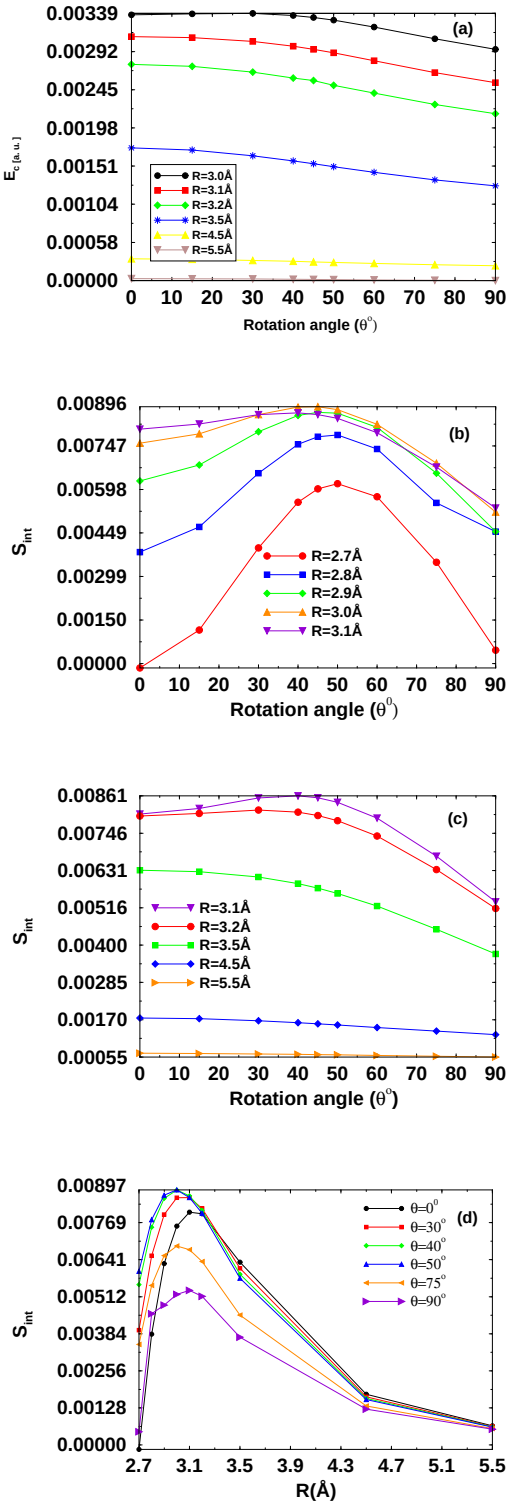

Figure 4.5: *Interaction electron correlation (in (a)) and interaction electron entanglement for the dimer of ethylene as function of rotation angle, calculated for different molecular planes distances (R) in a face to face configuration (in (b) and (c)). The same results for entanglement are plotted as function of molecular distances for different rotation angles (in (d)).*

Full Configuration Interaction (FCI) method. In the study of the dimer of ethylene, we expand the wave function with a Coupled Cluster Single Double (CCSD) method [119], [120]. This is a numerical tecnique used for describing many–body systems and has the property of describing coupled two–body electron correlation effects. The CCSD method is an excitation truncated Coupled Cluster (CC) method constructed in an exponential approach by including only the desired excitation operators (single and double); hence it cannot be considered a FCI-like method. However it can describe the interaction of separated molecules better than CISD [112]. For both systems, the input is prepared with an Unrestricted Hartree-Fock (UHF) calculation. In fact, the UHF description of bond breaking in H_2 gives the proper dissociation products, while the Restricted Hartree-Fock (RHF) description of H_2 gives unrealistic ones. In the following we show that, in order to study the dissociation of H_2 molecule, the electron correlation energy must be defined by UHF appoximation as $|E_{corr}| = |E_{exact} - E_{UHF}|$. In fact, at short internuclear distances the RHF and UHF wave functions are identical but at large distances, outside the bond region, only UHF reproduces the correct progress of correlation energy of H_2 that must be zero when the two atoms are distant and each electron cannot interfere with the other (Figure 4.6). The correlation energy in Eq. (4.12) is defined in terms of a complete one–electron basis. In practice, however, an incomplete basis must be used for the calculation of the correlation energy. The term *correlation energy* is that used to denote the energy obtained from Eq. (4.12) in a given one–electron basis.

The correlation energy usually increases in magnitude with the size of the orbital basis, since a small basis does not have the flexibility required for an accurate representation of correlation effects.

In order to confirm this theory, we analyze four different kinds of basis sets known in the literature as $3-21G$, $6-31G$, $6-31G^{**}$, $6-31{+}{+}G^{**}$ and we note, as it is represented in Figure 4.7, that the more increase the bases used the bigger becomes the contribute to correlation energy.

The basis sets $3-21G$ and $6-31G$ use $1s$, $2s$ and $1p$ atomic orbitals hence their contributions to the correlation energy are approximatively the same. The basis set $6-31G^{**}$ instead includes the orbital $1d$, while $6-31{+}{+}G^{**}$ uses the same orbitals but these are more diffuse. Hence, we can see that the energy correlation obtained with these two bases is bigger than the one obtained with the first basis sets. It is however important to note that at

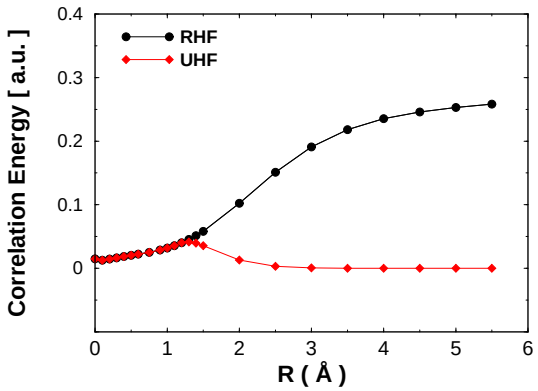

Figure 4.6: *The figure reports the electron correlation as a function of the internuclear distance R of the H_2 molecule using Gaussian basis set 3-21G with package Gaussian. The comparison between correlation energy calculated as $|E_{corr}| = |E_{exact} - E_{RHF}|$ and calculated as $|E_{corr}| = |E_{exact} - E_{UHF}|$ is showed.*

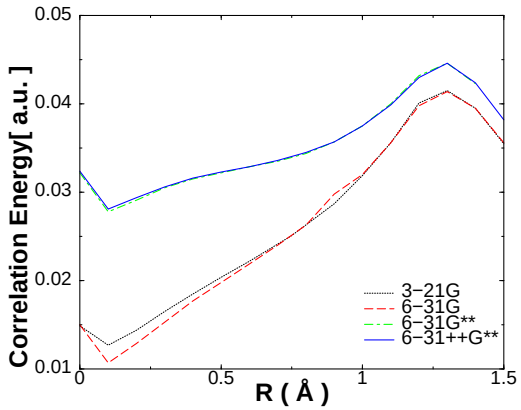

Figure 4.7: *A comparison of correlation energy calculated with four different basis sets.*

short internuclear distances the correlation energy strongly depends on the size of orbital basis whereas at large distances, outside the bond region, all four courses become approximatively the same.

After the above preliminary study of basis sets we decide to use the smallest basis set $(3-21G)$. This choice allows us to reduce drastically the computational cost, which constitutes an enormus advantage in the study of other systems, in particular more complex molecules.

4.6 Conclusions

In this paper, we have analyzed and elaborated the suggestion in [104] that the entanglement can be used as an alternative estimation of the electron correlation in quantum chemistry calculations.

We have, firstly, compared the degree of entanglement in the dissociation process of H_2 molecule calculated as the von Neumann entropy of the reduced density matrix $S(\rho_1)$, as in [104], with the one calculated by the entropy of the density matrix of the compound system $S(\rho)$. The two behaviours obtained in this way are shown to be similar, hence, we have choosen to adopt $S(\rho)$ for a qualitative estimation of entanglement in more complex systems. Then, we have verified that the electron correlation energy for a dimer of ethylene is well reproduced by the entanglement $S(\rho)$ for different configurations of the system, as it has been shown in Figure 4.4.

Analyzing interacting molecules, we have introduced the interaction electron entanglement in order to calculate the only entanglement due to the interaction of the two molecules without their internal correlations. As it has been shown in Figure 4.5, there are configurations that maximize the degree of entanglement. This study of the degree of electronic entanglement is a useful resource for quantum computers whose input states are constructed in order to be maximally entangled.

Chapter 5

Entanglement, interferometry and statistics

5.1 Hong–Ou–Mandel interferometry

In this chapter we are going to describe the Hong–Ou–Mandel interferometer in each its part: *twin–beam* source, 50/50 beam splitter and photodetectors.

Taking into account an interesting paper by Giovannetti [121], we discuss a Hong–Ou–Mandel interferometer setup where the two particles entering the interferometer obey generalized quantum statistics.

5.1.1 A twin–beam source

The source of the light is a nonlinear crystal that is pumped with a monochromatic laser with frequency ω_0. The laser radiaton goes through the crystal and emerges with the same frequency ω_0, but a small part of it is subjected to a *down conversion* process: some photons excite some atoms, hence each atom emits a pair of photons with frequency ω_1 and ω_2 such that $\omega_1 + \omega_2 = \omega_0$. It is important to note that the previous one is the only constraint for the frequencies of the photons emitted by down conversion process.

Moreover, it is possible to choose the crystal in a such way that the emitted photons have two different polarizzations. In this way, one can reproduce the two separated beam that one need in the Hong–Ou–Mandel interferometer.

The wave function coming out of the crystal consists of two terms:

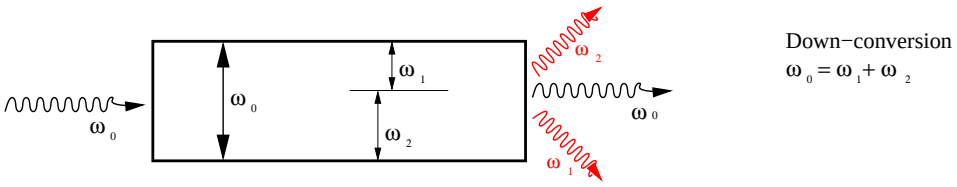

Figure 5.1: *A twin–beam source. A monocromatic laser with frequency ω_0 is pumped on a nonlinear crystal. The laser radiaton goes through the crystal and emerges with the same frequency ω_0, but a small part of it is subjected to a down conversion process, consequently two photons are emitted with frequency ω_1 and ω_2 such that $\omega_1 + \omega_2 = \omega_0$.*

- the first one is $|0\rangle$ that describes the being missing of a down conversion process and it is relative to the emission of a photon with frequency ω_0;

- the second one gives a small contribute to the wave function and takes into account the down conversion process.

  This is $\sum_{k_1,k_2} \phi(k_1,k_2) a_1^\dagger(k_1) a_2^\dagger(k_2)|0\rangle$, where:

  $\phi(k_1,k_2)$ describes the scattering in the crystal, in fact it is the two–photon spectral amplitude which satisfies the normalization condition $\sum_{k_1,k_2} |\phi(k_1,k_2)|^2 = 1$;

  $a_1(k)$ and $a_2(k)$ are the photonic annihilation operator associated with the kth mode of the path A_1 or A_2, respectively, which obey the following standard bosonic commutation relations:

$$[a_j(k), a_{j'}(k')] = 0; \quad [a_j(k), a_{j'}^\dagger(k')] = \delta_{jj'}\delta_{kk'}; \tag{5.1}$$

  $|0\rangle$ is the vacuum state.

Hence, the wave function $|\Psi\rangle$ that describes the two–particle state entering in the beam splitter of the Hong–Ou–Mandel interferometer is

$$|\Psi\rangle = |0\rangle + \underbrace{\sum_{k_1,k_2} \phi(k_1,k_2) a_1^\dagger(k_1) a_2^\dagger(k_2)|0\rangle}_{|\psi\rangle} . \tag{5.2}$$

5.1.2 A 50/50 beam splitter

The process in the beam splitter has a scattering dynamics. Photons with different frequencies propagate on the paths 1 and 2 and there is a probability that these photons are transmitted or reflected with the same entering frequency. In this context, each photon is subjected to an autonomus scattering process. First of all, we consider the relations between entering and

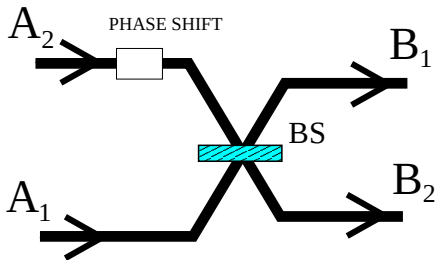

Figure 5.2: *A 50/50 beam splitter.*

coming out field. If we represent with $a_1(k)$ and $a_2(k)$ the entering photons and with $b_1(k)$ and $b_2(k)$ the coming out ones, the following relations:

$$b_1(k) = \frac{a_1(k) + e^{i\varphi_k} a_2(k)}{\sqrt{2}}; \quad b_2(k) = \frac{a_1(k) - e^{i\varphi_k} a_2(k)}{\sqrt{2}} \tag{5.3}$$

hold. It is easy to check that $b_1(k)$ and $b_2(k)$, that are built starting from bosonic operators, satisfy the bosonic commutation relations. In fact:

$$[b_1(k), b_2(k)] = \left[\frac{a_1(k) + a_2(k)}{\sqrt{2}}, \frac{a_1(k) - a_2(k)}{\sqrt{2}}\right] =$$

$$\left[\frac{a_1(k)}{\sqrt{2}}, \frac{a_1(k) - a_2(k)}{\sqrt{2}}\right] + \left[\frac{a_2(k)}{\sqrt{2}}, \frac{a_1(k) - a_2(k)}{\sqrt{2}}\right] = 0. \tag{5.4}$$

Within the interferometer, the photons on path 2 undergo phase–shift transformations introduced through controllable delays (the phase shift is depicted with a withe box in Figure 5.2) which transforms $a_2(k)$ into $a_2(k)e^{i\varphi}$.

Let us consider the different configuration on the beam splitter.

a) A photon entering in the beam splitter with frequency ω_k.

   If the photon follows the path 1 the input state is $a_1^\dagger|0\rangle$, while, from Eq. (5.3), the output state is $\frac{b_1^\dagger(k)+b_2^\dagger(k)}{\sqrt{2}}|0\rangle$. If the photon follows the path 2, the input state becomes $a_2^\dagger(k)$ and the output one becomes $\frac{b_1^\dagger(k)-b_2^\dagger(k)}{\sqrt{2}}|0\rangle$.

By a classical point of view, there is the same probability that the photon is emitted from path 1 or path 2.

b) Two photons entering in the beam splitter with the same frequency ω_k. In this case, the input state is $a_1^\dagger(k)a_2^\dagger(k)|0\rangle$; the output state is:

$$\Big(\frac{b_1^\dagger(k)+b_2^\dagger(k)}{\sqrt{2}}\Big)\Big(\frac{b_1^\dagger(k)-b_2^\dagger(k)}{\sqrt{2}}\Big)|0\rangle = \frac{1}{2}[b_1^\dagger(k)b_1^\dagger(k) - b_2^\dagger(k)b_2^\dagger(k)]|0\rangle$$

In this case, where the input particles are bosons, the only possible output configuration is the so–called *bunching configuration*. This is a consequence exclusively of the input (bosonic) particle statistics.

c) Two photons entering in the beam splitter with different frequencies: $\omega_k \neq \omega_{k'}$.

The input state is $a_1^\dagger(k)a_2^\dagger(k')|0\rangle$, the output state is:

$$\Big(\frac{b_1^\dagger(k)+b_2^\dagger(k)}{\sqrt{2}}\Big)\Big(\frac{b_1^\dagger(k')-b_2^\dagger(k')}{\sqrt{2}}\Big)|0\rangle =$$

$$\frac{1}{2}[b_1^\dagger(k)b_1^\dagger(k') - b_1^\dagger(k)b_2^\dagger(k') + b_2^\dagger(k)b_1^\dagger(k') - b_2^\dagger(k)b_2^\dagger(k')]|0\rangle.$$

The two photons with different frequencies propagate themselves independently each others.

5.1.3 Photodetectors

In the prototypical Hong–Ou–Mandel interferometer, behind the beam splitter, there are two photodetectors, one for each possible path of the coming out photon. Let us describe the measurement procedure in correspondence

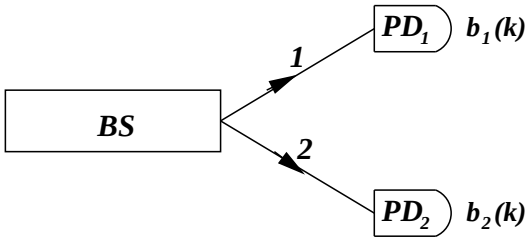

Figure 5.3: *A scheme of the two photodetectors that mesure coincidence counts after the beam splitter, and $b_1(k)$ and $b_2(k)$ represent the bosonic fields.*

of a photodetector: the two optical phat interfere at the 50/50 beam splitter, where the photocoincidence $\mathcal{C}_{12}$ is measured at the output ports.

5.2 Detection of entanglement in input states

5.2.1 Bosons

Let us calculate the coincidence parameter $\mathcal{C}_{12}$ on the state $|\Psi\rangle$ in Eq. (5.2):

$$\mathcal{C}_{12} = \langle 0|N_1N_2|0\rangle + \langle 0|N_1N_2|\psi\rangle + \langle \psi|N_1N_2|0\rangle + \langle \psi|N_1N_2|\psi\rangle = \langle \psi|N_1N_2|\psi\rangle, \tag{5.5}$$

where, for $j = 1, 2$, N_j is the total photon number operator of the B_j output port:

$$N_j = \sum_k n_j(k), \tag{5.6}$$

with $n_j(k) = b_j^\dagger(k)b_j(k)$ being the number operator of the kth mode. If we calculate explicitly the matrix element $\langle \psi|N_1N_2|\psi\rangle$, we obtain:

$$\langle \psi|N_1N_2|\psi\rangle = \sum_{kk'} \langle \psi|b_1^\dagger(k)b_1(k)b_2^\dagger(k')b_2(k')|\psi\rangle =$$

$$= \sum_{kk'} \langle \psi|b_1^\dagger(k)b_2^\dagger(k') \underbrace{\left[b_1^\dagger(k)b_2(k')|\psi\rangle\right]}_{\propto|0\rangle} \tag{5.7}$$

The term in brackets $\left[b_1^\dagger(k)b_2(k')|\psi\rangle\right]$ is proportional to the vacuum state by the factor $\mathcal{F}_\psi(k,k')$

$$b_1^\dagger(k)b_2(k')|\psi\rangle = \mathcal{F}_\psi(k,k')|0\rangle.$$

By making the product scalar with the vacuum state:

$$\mathcal{F}_\psi(k,k') = \langle 0|b_1(k)b_2(k')|\psi\rangle.$$

Hence, once we have manipulated the left side of Eq. (5.7) in the same way, this equation becomes:

$$\langle \psi|N_1N_2|\psi\rangle = \sum_{kk'} \langle 0|\mathcal{F}_\psi^\star(k,k')\mathcal{F}_\psi(k,k')|0\rangle = \sum_{kk'} |\mathcal{F}_\psi(k,k')|^2 =$$

$$\sum_{kk'} \left|\langle 0|b_1(k)b_2(k')|0\rangle\right|^2. \tag{5.8}$$

If we introduce the following quantity

$$\omega = \sum_{kk'} \phi(k_1,k_2)\phi^\star(k_2,k_1)e^{i(\varphi_{k_1}-\varphi_{k_2})}, \quad \omega \in [-1,1], \tag{5.9}$$

the photocoincidence counts parameter $\mathcal{C}_{12}$ becomes:

$$\mathcal{C}_{12} = \frac{1-\omega}{2}. \tag{5.10}$$

It is important to note that, for a suitable choice of the delays φ_k and of the two–photon spectral amplitude $\phi(k_1, k_2)$ (remenbering its normalization condition), the real quantity ω can take any values in the interval $[-1, 1]$. Correspondingly, $\mathcal{C}_{12}$ can take values over the interval $[0, 1]$.

In the following, we briefly sketch the proof of Eq. (5.10):

$$\mathcal{C}_{12} = \sum_{kk'} \Big| \langle 0|b_1(k)b_2(k')|\psi\rangle \Big|^2 =$$

$$\sum_{kk'} \Big| \langle 0|b_1(k)b_2(k') \Big[\sum_{k_1 k_2} \phi(k_1,k_2) a_1^\dagger(k_1) a_2^\dagger(k_2) e^{i(\varphi_{k_1}-\varphi_{k_2})}|0\rangle \Big] \Big|^2. \tag{5.11}$$

Let us calculate only the quantity $\langle 0|b_1(k)b_2(k')|\psi\rangle$:

$$\sum_{k_1 k_2} \frac{\phi(k_1 k_2) e^{i(\varphi_{k_1}-\varphi_{k_2})}}{2} \langle 0|b_1(k_1)b_2(k')[b_1^\dagger(k_1)+b_2^\dagger(k_2)][b_1^\dagger(k_1)-b_2^\dagger(k_2)]|0\rangle. \tag{5.12}$$

Let us calculate each terms separately

- $$\underbrace{\langle 0|b_1(k)b_2(k')}_{\langle 2,k';1,k|} \underbrace{b_1^\dagger(k_1)b_1^\dagger(k_2)|0\rangle}_{|1,k_1;1,k_2\rangle} = 0 \tag{5.13}$$

- $$\underbrace{-\langle 0|b_1(k)b_2(k')}_{\langle 2,k';1,k|} \underbrace{b_1^\dagger(k_1)b_2^\dagger(k_2)|0\rangle}_{|1,k_1;2,k_2\rangle} = -\delta_{k,k_1}\delta_{k',k_2} \tag{5.14}$$

- $$\underbrace{\langle 0|b_1(k)b_2(k')}_{\langle 1,k;2,k'|} \underbrace{b_2^\dagger(k_1)b_1^\dagger(k_2)|0\rangle}_{|2,k_1;1,k_2\rangle} = \delta_{k',k_1}\delta_{k,k_2} \tag{5.15}$$

Hence:

$$\langle 0|b_1(k)b_2(k')|\psi\rangle = \sum_{k_1 k_2} \frac{1}{2}\phi(k_1 k_2) e^{i(\varphi_{k_1}-\varphi_{k_2})} \Big\{ -\delta_{k,k_1}\delta_{k'k_2} + \delta_{k'k_1}\delta_{k_1 k_2} \Big\} =$$

$$= \frac{1}{2}\Big\{ -\phi(kk')e^{i(\varphi_k-\varphi_{k'})} + \phi(k'k)e^{-i(\varphi_k-\varphi_{k'})} \Big\}. \tag{5.16}$$

Adopting the substitutions $k \to k_1$ and $k' \to k_2$, we calculate the following quantity:

$$\Big(\langle |b_1(k_1)b_2(k_2)|\psi\rangle\Big)^\star = \frac{1}{2}\Big\{ -\phi^\star(k_1,k_2)e^{-i(\varphi_{k_1}-\varphi_{k_2})} + \phi^\star(k_2,k_1)e^{i(\varphi_{k_1}-\varphi_{k_2})} \Big\}. \tag{5.17}$$

Finally, inserting Eq. (5.16) and Eq. (5.17) in Eq. (5.11), the parameter $\mathcal{C}_{12}$ becomes:

$$\mathcal{C}_{12} = \frac{1}{4}\Big\{ \sum_{k_1 k_2} \phi(k_1,k_2)\phi^\star(k_1,k_2) - \sum_{k_1 k_2} \phi(k_1,k_2)\phi^\star(k_1,k_2)e^{2i(\varphi_{k_1}-\varphi_{k_2})} -$$

$$- \sum_{k_1 k_2} \phi(k_2,k_1)\phi^\star(k_1,k_2)e^{-2i(\varphi_{k_1}-\varphi_{k_2})} + \sum_{k_1 k_2} \phi(k_2,k_1)\phi^\star(k_2,k_1)\Big\} =$$

$$= \frac{1}{2} - \frac{1}{2}\Big\{ \sum_{k_1 k_2} \Big(\phi(k_1 k_2)\phi^\star(k_1 k_2)e^{2i(\varphi_{k_1}-\varphi_{k_2})} + \phi(k_2 k_1)\phi^\star(k_2 k_1)e^{-2i(\varphi_{k_1}-\varphi_{k_2})}\Big)\Big\} =$$

$$\frac{1-\omega}{2}.$$

Hong–Ou–Mandel interferometer allows one to detect the presence of entanglement in two–photon input state.

In fact, we consider the case in which the wave function Ψ in Eq. (5.2) is separable with respects the two paths A_1 and A_2. In this case, the spectral amplitude can be written $\phi(k_1,k_2) = \phi_1(k_1)\phi_2(k_2)$ and the function ω in Eq. (5.9) becomes, for separable states,

$$\omega = \omega_{sep} \equiv \Big| \sum_k \phi_1^\star(k)\phi_2(k)e^{i\varphi_k} \Big|^2 \geq 0. \tag{5.18}$$

Consequently, for separable states, the coincidence counts $\mathcal{C}_{12sep}$ can assume the maximum value 1/2:

$$\mathcal{C}_{12sep} = \frac{1-\omega_{sep}}{2} \in [0, 1/2]. \tag{5.19}$$

Therefore, we can use $\mathcal{C}_{12}$ as an entanglement witness for two–photon input states. Indeed, it is sufficient to repeat the coincidence measurement for different values of the controllable delay.

5.2.2 Fermions

The fermionic counterpart of the Hong–Ou–Mandel interferometer is proposed in [122]. It is important to note that such an interferometer, having as input particles two fermions, can be described in a similay way, in other words, we can use the two-particle input state introduced in Eq. (5.2) by simply replacing bosonic commutation rules in Eq. (5.1) with their fermionic counterpart:

$$\{a_j(k), a_{j'}(k')\} = 0, \quad \{a_j(k), a_{j'}^\dagger(k')\} = \delta_{jj'}\delta_{kk'}, \tag{5.20}$$

where $\{r, s\} = rs + sr$ is the anticommutator of the operators r and s. Hence, with new particle statistics, Eq. (5.10) for the photocoincidence counts $\mathcal{C}_{12}$ is replaced by

$$\mathcal{C}_{12} = \frac{1+\omega}{2}, \tag{5.21}$$

with ω as in Eq. (5.9). In the fermionic case, we can verify that among the two-particle state $\Psi\rangle$ of Eq. (5.2), only the entangled one can have $\mathcal{C}_{12} < 1/2$; separable states always stay upon the $1/2$ threshold.

Of particular phisycal relevance is the fact that the sign difference between Eq. (5.10) and Eq. (5.21) implies that separable states of fermions are forced to have $\mathcal{C}_{12}$ greater than or equal to $1/2$, while separable states of bosons have $\mathcal{C}_{12}$ smaller than or equal to $1/2$ (in Figure 5.4 there is a pictorial representation of $\mathcal{C}_{12}$ as a function of interferometric delay.) This phenomenon can be interpreted in terms of the different bouncing and antibouncig attitudes of Bose and Fermi statistics.

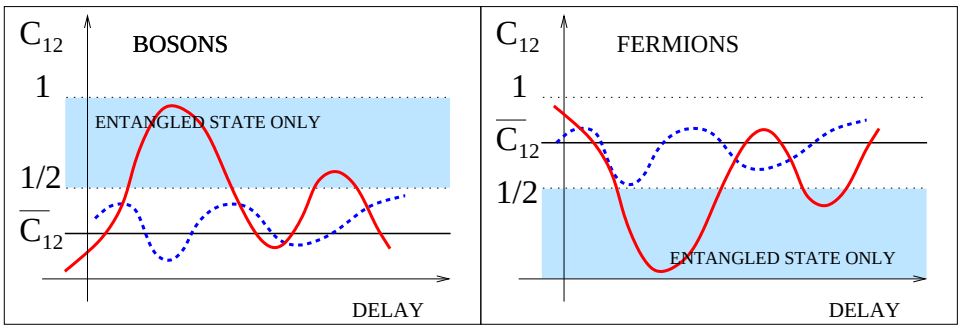

Figure 5.4: *Scheme of the dependence of coincidence counts $\mathcal{C}_{12}$ upon the interferometric delay φ_k in the Hong–Ou–Mandel interferometer. On the left we depicted the bosonic case. Among the two–particle states $|\Psi\rangle$ of Eq. (5.2) the separable one (represented by dotted curve) always have $\mathcal{C}_{12} < 1/2$. The only state that can have $\mathcal{C}_{12} > 1/2$ are the entangled one (represented by continuous curve). On the right we depicted the fermionic analogue case. The area which is not accessible to separable states is the region below $1/2$.*

5.3 Intermediate statistics: quons

In this section a *Gedankenexperiment* is analyzed where the particles entering the HOM interferometer are assumed to be quons. These have been introduced by Greenberg as an example of continuous interpolation between

Bose and Fermi algebras. We will use them to describe the sharp transition from the left part to the right part of Figure 5.4 in terms of a continuous deformation of the particle statistics.

For $q \in [-1, 1]$ the quon algebra is obtained by replacing Eqs. (5.1) and (5.20)with the identity

$$a_j(k)a^\dagger_{j'}(k') - qa^\dagger_{j'}(k')a_j(k) = \delta_{jj'}\ \delta_{kk'}. \tag{5.22}$$

For $|q| < 1$, Eq. (5.22) can be used to define a valid non-relativistic field theory but poses serious problems in deriving a reasonable relativistic quantum field theory. A proper Fock-like representation can be derived upon enforcing the vacuum condition

$$a_j(k)|\emptyset\rangle = 0 \tag{5.23}$$

for all j and k. In particular, it can be shown that for $|q| < 1$ the squared norms of all vectors made by polynomials of $a^\dagger_j(k)$ acting on the vacuum state $|\emptyset\rangle$ are strictly positive. For $q = 1$ and $q = -1$ instead the squared norms are never negative and nullify for those configurations which are, respectively, totally symmetric and totally antisymmetric under permutations. This allows us to recover the Bosonic and Fermionic statistics as limiting cases of Eq.(5.22) without explicitly imposing the conditions in Eqs. (5.1) and (5.20), respectively. Of particular interest is also the $q = 0$ case whose statistics can be interpret [123] as a quantum version of the Boltzmann statistics, based on a system of identical particles having infinite number of internal degree of freedom.

The possibility of defining a proper Fock-like structure for the quon algebra (5.22) implies the existence of number operators $n_j(k)$ which satisfy the standard commutation relations

$$\left[n_j(k), a_{j'}(k')\right] = -\delta_{jj'}\ \delta_{kk'}\ a_j(k) \tag{5.24}$$

and which reduce to $a^\dagger_j(k)a_j(k)$ in the Bosonic and Fermionic limits.

In the following we will adopt a pragmatic point of view assuming that the equations of the previous section yield a legitimate description of our quon HOM interferometer. This is in part justified by the fact that the input-output relations Eq. (5.3) map the quon annihilation operators $a_j(k)$ into annihilation operators $b_j(k)$ which still satisfy the quon algebra Eq. (5.22) and the vacuum condition (5.23). The only technical problem of our

approach comes from the fact that for $|q| < 1$ Eq. (5.5) is not necessarily a real quantity. Consequently we replace the product $N_1 N_2$ with its Hermitian part, i.e.

$$\mathcal{C}_{12} \equiv \langle \Psi | \frac{N_1 N_2 + N_2 N_1}{2} | \Psi \rangle = \Re e \, \langle \Psi | N_1 N_2 | \Psi \rangle \; . \tag{5.25}$$

The right hand side term of Eq. (5.25) can now be computed by inverting the transformation (5.3) and expressing the input state $|\Psi\rangle$ of Eq.(5.2) in terms of the operators $b_j(k)$. With the help of the relations (5.24) and (5.22) and using the vacuum condition (5.23) one can then verify (see Appendix B) that the quon "coincidence counts" of the q-algebra are,

$$\mathcal{C}_{12}(q) = \frac{1 - q\, w}{2} \tag{5.26}$$

with w as in Eq. (5.9). Analogously one can verify that for normalized input states the condition $\sum |\phi(k_1, k_2)|^2 = 1$ still holds and that the average number $i_{1,2}$ is equal to 1 for all q. As expected, for $q = \pm 1$ Eq. (5.26) reduces to the Bosonic and Fermionic case. More interestingly for $q = 0$, $\mathcal{C}_{12}(q)$ does not depend upon the two-particle input state $|\Psi\rangle$ and has constant value $1/2$. This is exactly what one would expect from a classical model of the interferometer confirming the Boltzmann interpretation [123] of the $q = 0$ algebra.

Taking into account that for generic input state one has $w \in [-1, 1]$ the following bounds can be derived:

$$\frac{1 - q}{2} \leq \mathcal{C}_{12}(q) \leq \frac{1 + q}{2} \quad q \in [0, 1]; \tag{5.27}$$

$$\frac{1 + q}{2} \leq \mathcal{C}_{12}(q) \leq \frac{1 - q}{2} \quad q \in [-1, 0]. \tag{5.28}$$

On the other hand for factorizable amplitudes $\phi(k_1, k_2)$, the function w obeys Eq. (5.18). Therefore for these states one has

$$\frac{1 - q}{2} \leq \mathcal{C}_{12}(q) \leq \frac{1}{2} \quad q \in [0, 1]; \tag{5.29}$$

$$\frac{1}{2} \leq \mathcal{C}_{12}(q) \leq \frac{1 - q}{2} \quad q \in [-1, 0]. \tag{5.30}$$

The above constraints have been plotted in Figure 5.5. They indicate that the transition from the Bosonic regime to the Fermionic regime is characterized by a critical point at $q = 0$. Here the values $\mathcal{C}_{12} > 1/2$ which for $q > 0$ were pertinent to non factorizable input states $|\Psi\rangle$, become accessible to factorizable configurations. At the same time, however the values

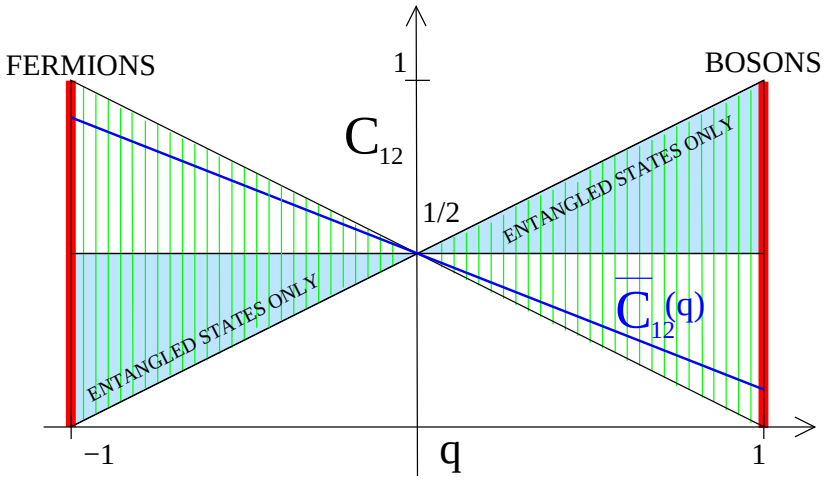

Figure 5.5: *Plot of the maximum and minimum values of $\mathcal{C}_{12}$ of Eq. (5.26) allowed for a two–particle quon state as a function of the parameter q of the quon algebra. The shaded region represents the allowed values in Eqs. (5.27) and (5.28) of $\mathcal{C}_{12}$. According Eqs. (5.29) and (5.30), the gray region is accessible only to non factorizable input configurations. For $q = 1$ and $q = -1$ the boundaries coincide with those of Bosonic and Fermionic case respectively. It is interesting to note that the Boltzmann statistics $q = 0$ admits only the value* $1/2$.

$\mathcal{C}_{12} < 1/2$ become inaccessible to them. Following the discussion of the previous section this effect can be interpreted as a continuous transition from a bouncing behavior to an anti-bouncing behavior with $q = 0$ corresponding to the classical "neutral" point.

5.4 Future Developments

Starting from these considerations and these results about entanglement of fermions, bosons or quons, we want to extend our theoretical scheme in order to detect the presence of entanglement in states of other particles, the so–called exotic quasiparticles. We want to analyze particles, or "paraparticles", obeying intermediate statistics, as anyons, interpolating between bosons and fermions.

Indeed, a probable line of our future research can deal with the study of entanglement, based on the coincidence counts parameter, for paraparticles that obey to intermediate statistics and that are defined by means of

the algebra satisfied by their creation and annihilation operators in Fock representation.

Appendix A

The reduced density matrix of Eq. (4.9)

The aim of this appendix is clarifying how one can calculate the reduced density matrix as that one we propose in Eq. (4.9). In order to semplify the calculations, we consider two electrons in a two–levels system. Let us introduce the Hilbert space (4.1) with $m = 2$,

$$\mathscr{H} = \left[\mathscr{L}^2(1) \otimes \mathscr{S}^2(1)\right] \otimes \left[\mathscr{L}^2(2) \otimes \mathscr{S}^2(2)\right] = \mathscr{C}^4(1) \otimes \mathscr{C}^4(2), \qquad \text{(A.1)}$$

where $\mathscr{L}$ and $\mathscr{S}$ represent the orbital and the spin space, respectively; in brackets we denote one of the two electrons and the apex represents the dimension of the space. An orthonormal basis for each space $\mathscr{C}^4$ in the occupation number representation $(n_1\uparrow, n_1\downarrow, n_2\uparrow, n_2\downarrow)$ is

$$\left\{ \begin{array}{l} |n_1\uparrow\rangle \\ |n_1\downarrow\rangle \\ |n_2\uparrow\rangle \\ |n_2\downarrow\rangle \end{array} \right\} \otimes \left\{ \begin{array}{l} |n_1\uparrow\rangle \\ |n_1\downarrow\rangle \\ |n_2\uparrow\rangle \\ |n_2\downarrow\rangle \end{array} \right\}. \qquad \text{(A.2)}$$

A pure two-electron state $|\Psi\rangle$ in this case can be written as

$$|\Psi\rangle = \sum_{a=1}^{4}\sum_{b=1}^{4} \omega_{a,b} c_a^\dagger c_b^\dagger |0\rangle, \qquad \text{(A.3)}$$

where $|0\rangle$ is the vacuum state, the coefficient ω, accordingly to Pauli exclusion principle, satisfies the following requests:

$$\left\{ \begin{array}{l} \omega_{a,b} = -\omega_{b,a} \\ \omega_{i,i} = 0, \end{array} \right. \qquad \text{(A.4)}$$

and $c^\dagger$ and c are the creation and annihilation operators of single–particle states, respectively whose action on the vacuum state is

$$c_a^\dagger c_b^\dagger|0\rangle = |ab\rangle, \quad a,b \in \{1,2,3,4\} \qquad \begin{array}{ll} 1 \equiv |n_1\uparrow\rangle & 3 \equiv |n_2\uparrow\rangle \\ 2 \equiv |n_1\downarrow\rangle & 4 \equiv |n_2\downarrow\rangle. \end{array}$$

Let us now consider the four sites instead of the two particles: they are single particle sites consequently they have no particle or one. Since our aim is having some informations about the n_1 we proceed making the partial trace of the density operator ρ with respect to $n_2\uparrow$ and $n_2\downarrow$ that is,

$$\rho_{n_1} = Tr_{n_2}\rho = \sum_{\substack{n_2\uparrow=0,1 \\ n_2\downarrow=0,1}} \langle n_2\uparrow, n_2\downarrow|\rho|n_2\uparrow, n_2\downarrow\rangle =$$

$$= \langle 00|\rho|00\rangle + \langle 01|\rho|01\rangle + \langle 10|\rho|10\rangle + \langle 11|\rho|11\rangle. \tag{A.5}$$

Let us calculate each matrix element separately.

The first one is

$$\langle 00|\rho|00\rangle = \sum_{a,b=1}^{4}\sum_{a',b'=1}^{4} \omega_{a,b}\omega^*_{a',b'}\langle 00|c_a^\dagger c_b^\dagger|0\rangle\langle 0|c_{b'}c_{a'}|00\rangle \tag{A.6}$$

where a, b, a' and b' assume the values $1,2,3,4$ and they represent the four sites of the two levels system that we are studying. Moreover, since we make the inner product with $\langle 00|$ and $|00\rangle$, the only elements of the sum with a nonzero contribution are $|1100\rangle$[1] thus they correspond to $\omega_{1,2}$ and $\omega_{2,1}$:

$|1100\rangle$: $|n_1\uparrow\rangle \otimes |n_1\downarrow\rangle \to \omega_{12}$

$|n_1\downarrow\rangle \otimes |n_1\uparrow\rangle \to \omega_{21}$.

Hence

$$\langle 00|\rho|00\rangle = \sum_{a,b=1}^{2}\sum_{a',b'=1}^{2} \omega_{a,b}\omega^*_{a',b'}\langle 00|c_a^\dagger c_b^\dagger|0\rangle\langle 0|c_{b'}c_{a'}|00\rangle. \tag{A.7}$$

Making explicit the sum and using the fact that $\omega_{ii} = 0$, it becomes:

$$\langle 00|\rho|00\rangle = \omega_{1,2}\omega^*_{1,2}\langle 00|c_1^\dagger c_2^\dagger|0\rangle\langle 0|c_2c_1|00\rangle + \omega_{2,1}\omega^*_{1,2}\langle 00|c_2^\dagger c_1^\dagger|0\rangle\langle 0|c_2c_1|00\rangle +$$

$$+\omega_{1,2}\omega^*_{2,1}\langle 00|c_1^\dagger c_2^\dagger|0\rangle\langle 0|c_1c_2|00\rangle + \omega_{2,1}\omega^*_{2,1}\langle 00|c_2^\dagger c_1^\dagger|0\rangle\langle 0|c_1c_2|00\rangle. \tag{A.8}$$

[1] In all these calculations, each vector with four components has the first and the second entries corresponding with each two sites of n_1 level and the third and fourth entries corresponding with n_2 level. Hence the ket $|1100\rangle$, for example, represents two electrons on the level n_1 and no one on the level n_2.

The action of the creation and distruction operators on the vacuum state produces some states such as $\pm|n_1\uparrow n_1\downarrow\rangle$ and $\pm|n_1\downarrow n_1\uparrow\rangle$ where the double sign depends on the order of the operators. Using no more the representation refering to fermions but the one refering to the sites all these states can be represented with $\pm|1100\rangle$ so Eq (A.8) becomes:

$$\langle 00|\rho|00\rangle = \omega_{1,2}\omega^*_{1,2}\langle 00|1100\rangle\langle 1100|00\rangle - \omega_{2,1}\omega^*_{1,2}\langle 00|1100\rangle\langle 1100|00\rangle+$$

$$-\omega_{1,2}\omega^*_{2,1}\langle 00|1100\rangle\langle 1100|00\rangle + \omega_{2,1}\omega^*_{2,1}\langle 00|1100\rangle\langle 1100|00\rangle. \qquad (A.9)$$

Using the orthogonality, we obtain:

$$\langle 00|\rho|00\rangle = 4|\omega_{12}|^2|11\rangle\langle 11|. \qquad (A.10)$$

Let us analyze the second matrix element:

$$\langle 01|\rho|01\rangle = \sum_{a,b=1}^{4}\sum_{a',b'=1}^{4}\omega_{a,b}\omega^*_{a',b'}\langle 01|c^\dagger_a c^\dagger_b|0\rangle\langle 0|c_{b'}c_{a'}|01\rangle. \qquad (A.11)$$

Since we make the inner product with $\langle 01|$ and $|01\rangle$, the only elements of the sum with a nonzero contribution are $|1001\rangle$ and $|0101\rangle$ thus they correspond to $\omega_{1,4}$, $\omega_{4,1}$ and $\omega_{2,4}$, $\omega_{4,2}$:

$$\begin{aligned}
|1001\rangle: &\quad |n_1\uparrow\rangle\otimes|n_2\downarrow\rangle \to \omega_{14}\\
&\quad |n_2\downarrow\rangle\otimes|n_1\uparrow\rangle \to \omega_{41}\\
|0101\rangle: &\quad |n_1\downarrow\rangle\otimes|n_2\downarrow\rangle \to \omega_{24}\\
&\quad |n_2\downarrow\rangle\otimes|n_1\downarrow\rangle \to \omega_{42}.
\end{aligned}$$

Hence

$$\langle 01|\rho|01\rangle = \sum_{a,b=1,2,4}\sum_{a',b'=1,2,4}\omega_{a,b}\omega^*_{a',b'}\langle 01|c^\dagger_a c^\dagger_b|0\rangle\langle 0|c_{b'}c_{a'}|01\rangle. \qquad (A.12)$$

Making explicit the sum above and using the site representation as before, this matrix element becomes:

$$\langle 01|\rho|01\rangle = 4|\omega_{1,4}|^2|10\rangle\langle 10|. \qquad (A.13)$$

Now, for the third matrix element, that is:

$$\langle 10|\rho|10\rangle = \sum_{a,b=1}^{4}\sum_{a',b'=1}^{4}\omega_{a,b}\omega^*_{a',b'}\langle 10|c^\dagger_a c^\dagger_b|0\rangle\langle 0|c_{b'}c_{a'}|10\rangle, \qquad (A.14)$$

we note that the only vectors that have a non zero contribution in the summatory after the inner product with $\langle 10|$ and $|10\rangle$ are:

$|1010\rangle$: $|n_1\uparrow\rangle \otimes |n_2\uparrow\rangle \rightarrow \omega_{13}$

$|n_2\uparrow\rangle \otimes |n_1\uparrow\rangle \rightarrow \omega_{31}$

$|0110\rangle$: $|n_1\downarrow\rangle \otimes |n_2\uparrow\rangle \rightarrow \omega_{23}$

$|n_2\uparrow\rangle \otimes |n_1\downarrow\rangle \rightarrow \omega_{32}$.

Hence,

$$\langle 10|\rho|10\rangle = 4|\omega_{2,3}|^2|10\rangle\langle 10|. \tag{A.15}$$

Finally, the latest matrix element, is, analogously,

$$\langle 11|\rho|11\rangle = 4|\omega_{3,4}|^2|00\rangle\langle 00|. \tag{A.16}$$

Thus, in the basis $\Big\{|00\rangle;|01\rangle;|10\rangle;|11\rangle\Big\}$, ρ_{n_1} reads

$$\rho_{n_1} = \begin{pmatrix} 4|\omega_{3,4}|^2 & 0 & 0 & 0 \\ 0 & 4|\omega_{2,3}|^2 & 0 & 0 \\ 0 & 0 & 4|\omega_{1,4}|^2 & 0 \\ 0 & 0 & 0 & 4|\omega_{1,2}|^2 \end{pmatrix}. \tag{A.17}$$

Equation (A.17) represents the density operator for the level n_1 and it is important to spend some words on the entryes of the matrix: $\omega_{3,4}$ represents the excitations on the second level so, in the two level system that we consider, $\omega_{3,4}$ is associated with the probability that n_1 is empty; $\omega_{1,2}$ is associated with the possibility that the two electrons are in n_1, the coefficients $\omega_{2,3}$ and $\omega_{1,4}$ are associated with the probability that n_1 can be occupied by one eletron. This fact allows us to introduce the following notation:

$$\rho_{n_1,0} \equiv 4|\omega_{3,4}|^2; \quad \rho_{n_1,2} \equiv 4|\omega_{1,2}|^2; \quad \rho_{n_1,1} \equiv \begin{pmatrix} 4|\omega_{2,3}|^2 & 0 \\ 0 & 4|\omega_{1,4}|^2 \end{pmatrix}, \tag{A.18}$$

where $\rho_{n_1,0}$ denotes an empty orbital, $\rho_{n_1,2}$ denotes two accupied orbitals and $\rho_{n_1,1}$ denotes one electron occupied orbital. In order to obtain some informations about one of the two electrons, we have to make the partial trace of ρ_{n_1} respect one of the sites of the level n_1 ($n_1\uparrow, n_1\downarrow$):

$$\rho_1 = Tr_{n_1\uparrow}\rho_{n_1} = \sum_{n_1\uparrow=0,1} \rho_{n_1}$$

$$= \begin{pmatrix} 4\Big(|\omega_{3,4}|^2 + |\omega_{2,3}|^2\Big) & 0 \\ 0 & 4\Big(|\omega_{1,4}|^2 + |\omega_{1,2}|^2\Big) \end{pmatrix}. \tag{A.19}$$

In terms of CISD expansion coefficients, the transition amplitude $\omega_{i,j}$ can be written as

$$|\omega_{1,2}|^2 = \frac{c_0^2}{4}, \qquad |\omega_{1,4}|^2 = \frac{c_2^2}{4}, \qquad |\omega_{3,4}|^2 = \frac{c_{1,2}^2}{4} \qquad |\omega_{2,3}|^2 = \frac{c_1^2}{4}, \tag{A.20}$$

hence ρ_1 becames:

$$\rho_1^{CISD} = \begin{pmatrix} |c_1|^2 + |c_{1,2}|^2 & 0 \\ 0 & |c_0|^2 + |c_2|^2 \end{pmatrix}. \tag{A.21}$$

Eq (4.9) is obtained as a generalization of this model to a m–level system.

Appendix B

Coincidence counts parameter for the quons

As we described in Chapter 5, the quon algebra is characterized by the following relations:

- the commutation relations for quons are

$$a_j(k)a^\dagger_{j'}(k') - qa^\dagger_{j'}(k')a_j(k) = \delta_{jj'}\ \delta_{kk'}, \tag{B.1}$$

  with $q \in [-1, 1]$;

- with a Fock–like representation, we can describe the action of the annihilator operator on the vacuum state:

$$a_j(k)|\emptyset\rangle = 0, \tag{B.2}$$

  for all j and k;

- the possibility of defining a proper Fock-like structure for the quon algebra (B.1) implies the existence of number operators $n_j(k)$ which satisfy the standard commutation relations

$$\left[n_j(k), a_{j'}(k')\right] = -\delta_{jj'}\ \delta_{kk'}\ a_j(k) \tag{B.3}$$

  and which reduce to $a^\dagger_j(k)a_j(k)$ in the Bosonic and Fermionic limits.

In this Appendix we make explicitly the calculations that bring us to Eq. (5.26) for the coincidence counts of the q–algebra. In other words, startint from Eq. (5.25) we compute the right hand side by inverting the transformation (5.3) and expressing the input state $|\Psi\rangle$ of Eq.(5.2) in terms

of the operators $b_j(k)$. With the help of the relations (B.1), (B.2) and (B.3) one can then verify that the quon "coincidence counts" of the q-algebra are,

$$\mathcal{C}_{12} \equiv \langle\Psi|\frac{N_1N_2+N_2N_1}{2}|\Psi\rangle = \Re e\,\langle\Psi|N_1N_2|\Psi\rangle = \frac{1-q\,w}{2} \qquad \text{(B.4)}$$

In detail, we have

$$\mathcal{C}_{12} = \frac{1}{2}\frac{1}{4}\sum_{\substack{k_1',k_2'\\k_1,k_2\\k,k'}}\phi^\star(k_1',k_2')e^{-i(\varphi_{k_1'}-\varphi_{k_2'})}\phi(k_1,k_2)e^{i(\varphi_{k_1}-\varphi_{k_2})}$$

$$\langle 0|\Big[-b_2(k_2')b_2(k_1')+b_1(k_2')b_2(k_1')-b_2(k_2')b_1(k_1')+b_1(k_2')b_1(k_1')\Big]\Big(n_1(k)n_2(k')+$$
$$+n_2(k')n_1(k)\Big)\Big[b_1^\dagger(k_1)b_1^\dagger(k_2)-b_1^\dagger(k_1)b_2^\dagger(k_2)+b_2^\dagger(k_1)b_1^\dagger(k_2)-b_2^\dagger(k_1)b_2^\dagger(k_2)\Big]|0\rangle. \qquad \text{(B.5)}$$

Let us calculate the left part (or the action of the operator on the bra $\langle 0|$ or, in other words, the upper line) of Eq. (B.5) using the relation and properties in (B.1), (B.2) and (B.3).

- $$\langle 0|-b_2(k_2')b_2(k_1')n_1(k)n_2(k') = \langle 0|-b_2(k_2')n_1(k)b_2(k_1')n_2(k') =$$
$$= \langle 0|-)n_1(k)b_2(k_2')b_2(k_1')n_2(k') =$$
$$= -\langle 0|n_1(k)b_2(k_2')\Big(n_2(k')b_2(k_1')+\delta_{k_1'k'}b_2(k_1')\Big) = 0.$$

- $$\langle 0|b_1(k_2')b_2(k_1')n_1(k)n_2(k') = \langle 0|b_1(k_2')n_1(k)b_2(k_1')n_2(k') =$$
$$= \langle 0|\Big(n_1(k)b_1(k_2')+\delta_{kk_2'}b_1(k)\Big)b_2(k_1')n_2(k') = \langle 0|\delta_{kk_2'}b_1(k)b_2(k_1')n_2(k') =$$
$$= \langle 0|\delta_{kk_2'}b_1(k)\Big(n_2(k')b_2(k_1')+\delta_{k'k_1'}b_2(k')\Big) = \langle 0|\delta_{kk_2'}\delta_{k'k_1'}b_1(k)b_2(k').$$

- $$\langle 0|-b_2(k_2')b_1(k_1')n_1(k)n_2(k') = -\langle 0|b_2(k_2')\Big(n_1(k)b_1(k_1')+\delta_{kk_1'}b_1(k_1')\Big)n_2(k') =$$
$$= -\langle 0|b_2(k_2')b_1(k_1')n_2(k')\delta_{kk_1'} = -\langle 0|b_2(k_2')n_2(k')b_1(k_1')\delta_{kk_1'} =$$
$$= -\langle 0|\Big(n_2(k')b_2(k_2')+\delta_{k_2'k'}b_2(k_2')\Big)b_1(k_1')\delta_{kk_1'} = -\langle 0|b_2(k_2')b_1(k_1')\delta_{k_2'k'}\delta_{kk_1'}.$$

- $$\langle 0|b_1(k_2')b_1(k_1')n_1(k)n_2(k') =$$
$$= \langle 0|b_1(k_2')\Big(n_1(k)b_1(k_1') + \delta_{kk_1'}b_1(k_1')\Big)n_2(k') =$$
$$= \langle 0|b_1(k_2')n_1(k)b_1(k_1')n_2(k') + \langle 0|b_1(k_2')b_1(k_1')n_2(k')\delta_{kk_1'} =$$
$$= \langle 0|\Big(n_1(k)b_1(k_2') + \delta_{kk_2'}b_1(k_2')\Big)b_1(k_1')n_2(k') = 0.$$

- $$\langle 0|b_1(k_2')b_2(k_1')n_2(k')n_1(k) =$$
$$= \langle 0|b_1(k_2')\Big(n_2(k')b_2(k_1') + \delta_{k'k_1'}b_2(k_1')\Big)n_1(k) =$$
$$= \langle 0|b_1(k_2')b_2(k_1')n_1(k)\delta_{k'k_1'} = \langle 0|b_1(k_2')n_1(k)b_2(k_1') + \delta_{k'k_1'} =$$
$$= \langle 0|\Big(n_1(k)b_1(k_2') + \delta_{k'k_2'}b_1(k_2')\Big)b_2(k_1') + \delta_{k'k_1'} = \langle 0|b_1(k_2')b_2(k_1')\delta_{kk_2'}\delta_{k'k_1'}.$$

- $$-\langle 0|b_2(k_2')b_1(k_1')n_2(k')n_1(k) = -\langle 0|b_2(k_2')n_2(k')b_1(k_1')n_1(k) =$$
$$-\langle 0|\Big(n_2(k')b_2(k_2') + \delta_{k'k_2'}b_2(k_2')\Big)b_1(k_1')n_1(k) =$$
$$= -\langle 0|b_2(k_2')b_1(k_1')n_1(k)\delta_{k'k_2'} =$$
$$= -\langle 0|b_2(k_2')\Big(n_1(k)b_1(k_1') + \delta_{kk_1'}b_1(k_1')\Big)n_1(k)\delta_{k'k_2'} =$$
$$= -\langle 0|b_2(k_2')b_1(k_1')n_1(k)\delta_{kk_1'}\delta_{k'k_2'} = -\langle 0|b_2(k_2')b_1(k_1')\delta_{kk_1'}\delta_{kk_1'}\delta_{k'k_2'}.$$

Hence, the matrix elements in Eq. (B.5) can be expressed, by the outcoming fields, as the following:

$$\langle 0|\Big(\underbrace{\delta_{kk_2'}\delta_{k'k_1'}b_1(k)b_2(k')}_{(1)} - \underbrace{b_2(k_2')b_1(k_1')\delta_{k_2'k'}\delta_{kk_1'}}_{(2)} + \underbrace{b_1(k_2')b_2(k_1')\delta_{kk_2'}\delta_{k'k_1'}}_{(3)}$$
$$- \underbrace{b_2(k_2')b_1(k_1')\delta_{kk_1'}\delta_{k'k_2'}}_{(4)}\Big)\Big(\underbrace{b_1^\dagger(k_1)b_1^\dagger(k_2)}_{(5)} - \underbrace{b_1^\dagger(k_1)b_2^\dagger(k_2)}_{(6)} + \underbrace{b_2^\dagger(k_1)b_1^\dagger(k_2)}_{(7)} -$$
$$\underbrace{b_2^\dagger(k_1)b_2^\dagger(k_2)}_{(8)}\Big)|0\rangle$$

Let us calculate the scalar product of the terms each others.

(1)-(5):

$$\langle 0|b_1(k)b_2(k')b_1^\dagger(k_1)b_1^\dagger(k_2)|0\rangle = \langle 0|b_1(k)\Big(qb_1^\dagger(k_1)b_2(k')\Big)b_1^\dagger(k_2)|0\rangle =$$

$$= \langle 0|qb_1(k)b_1^\dagger(k_1)b_2(k')b_1^\dagger(k_2)|0\rangle = 0;$$

(1)-(6):

$$-\langle 0|b_1(k)b_2(k')b_1^\dagger(k_1)b_2^\dagger(k_2)|0\rangle = -\langle 0|b_1(k)\Big(qb_1^\dagger(k_1)b_2(k')\Big)b_2^\dagger(k_2)|0\rangle =$$

$$-\langle 0|b_1(k)qb_1^\dagger(k_1)\Big(\delta_{k'k_2}+qb_2^\dagger(k_2)b_2(k')\Big)|0\rangle = -\langle 0|b_1(k)qb_1^\dagger(k_1)|0\rangle\delta_{k'k_2} =$$

$$= -\langle 0|qb_1(k)b_1^\dagger(k_1)|0\rangle\delta_{k'k_2} = -\langle 0|q\Big(b_1^\dagger(k_1)b_1(k)+\delta_{kk_1}\Big)|0\rangle\delta_{k'k_2} =$$

$$-\langle 0|0\rangle q\delta_{kk_1}\delta_{k'k_2};$$

(1)-(7):

$$\langle 0|b_1(k)b_2(k')b_2^\dagger(k_1)b_1^\dagger(k_2)|0\rangle =$$

$$= \langle 0|b_1(k)\Big(\delta_{k'k_1}+qb_2^\dagger(k_1)b_2(k')\Big)b_1^\dagger(k_2)|0\rangle =$$

$$= \langle 0|b_1(k)b_1^\dagger(k_2)\delta_{k'k_1}|0\rangle + \langle 0|b_1(k)qb_2^\dagger(k_1)b_2(k')b_1^\dagger(k_2)|0\rangle =$$

$$= \langle 0|\delta_{kk_2}\delta_{k'k_1}qb_1^\dagger(k_2)b_1(k)|0\rangle;$$

(1)-(8):

$$-\langle 0|b_1(k)b_2(k')b_2^\dagger(k_1)b_2^\dagger(k_2)|0\rangle =$$

$$= -\langle 0|b_1(k)\Big(\delta_{k'k_1}+qb_2^\dagger(k_1)b_2(k')\Big)b_2^\dagger(k_2)|0\rangle =$$

$$= -\langle 0|\delta_{k'k_1}b_1(k)b_2^\dagger(k_2)|0\rangle - \langle 0|qb_1(k)b_2^\dagger(k_1)b_2(k')b_2^\dagger(k_2)|0\rangle =$$

$$-\langle 0|qb_1(k)b_2^\dagger(k_1)\Big(\delta_{k_2k'}+qb_2^\dagger(k_2)b_2(k')\Big)|0\rangle;$$

(2)-(5):

$$-\langle 0|b_2(k_2')b_1(k_1')b_1^\dagger(k_1)b_1^\dagger(k_2)|0\rangle =$$

$$= -\langle 0|b_2(k')\Big(\delta_{k_1k_1'}+qb_1^\dagger(k_1)b_1(k_1')\Big)b_1^\dagger(k_2)|0\rangle =$$

$$= -\langle 0|b_2(k_2')\delta_{k_1k_1'}b_1^\dagger(k_2)|0\rangle - \langle 0|b_2(k_2')qb_1^\dagger(k_1)b_1(k_1')b_1^\dagger(k_2)|0\rangle =$$

$$= -\langle 0|b_2(k_2')qb_1^\dagger(k_1)\Big(\delta_{k_2k_1'}+qb_1^\dagger(k_2)b_1(k_1')\Big)|0\rangle =$$

$$= -\langle 0|b_2(k_2')qb_1^\dagger(k_1)\delta_{k_2k_1'}|0\rangle = 0;$$

(2)-(6):

$$\langle 0|b_2(k_2')b_1(k_1')b_1^\dagger(k_1)b_2^\dagger(k_2)|0\rangle =$$

$$= \langle 0|b_2(k_2')\Big(\delta_{k_1k_1'} + qb_1^\dagger(k_1)b_1(k_1')\Big)b_2^\dagger(k_2)|0\rangle =$$

$$= \langle 0|b_2(k_2')\delta_{k_1k_1'}b_2^\dagger(k_2)|0\rangle = \langle 0|\delta_{k_1k_1'}\Big(\delta_{k_2k_2'} + qb_2^\dagger(k_2)b_2(k_2')\Big)|0\rangle =$$

$$= \langle 0|0\rangle\delta_{k_1k_1'}\delta_{k_2k_2'};$$

(2)-(7):

$$\langle 0|b_2(k_2')b_1(k_1')b_2^\dagger(k_1)b_1^\dagger(k_2)|0\rangle = \langle 0|b_2(k_2')qb_2^\dagger(k_1)b_1(k_1')b_1^\dagger(k_2)|0\rangle =$$

$$= \langle 0|qb_2(k_2')b_2^\dagger(k_1)\Big(\delta_{k_2k_1'} + qb_1^\dagger(k_2)b_1(k_1')\Big)|0\rangle =$$

$$= \langle 0|b_2(k_2')b_2^\dagger(k_1)\delta_{k_2k_1'}q|0\rangle =$$

$$= -\langle 0|0\rangle q\delta_{k_2k_1'}\delta_{k_1k_2'};$$

(2)-(8):

$$-\langle 0|b_2(k_2')b_1(k_1')b_2^\dagger(k_1)b_2^\dagger(k_2)|0\rangle = -\langle 0|b_2(k_2')b_2^\dagger(k_1)b_1(k_1')\delta_{k_1k_1'}b_2^\dagger(k_2)|0\rangle;$$

(3)-(5):

$$\langle 0|b_1(k_2')b_2(k_1')b_1^\dagger(k_1)b_1^\dagger(k_2)|0\rangle = \langle 0|b_1(k_2')qb_1^\dagger(k_1)b_2(k_1')b_1^\dagger(k_2)|0\rangle =$$

$$= \langle 0|qb_1(k_2')b_1^\dagger(k_1)\Big(qb_1^\dagger(k_2)b_2(k_1')\Big)|0\rangle = 0;$$

(3)-(6):

$$\langle 0|b_1(k_2')b_2(k_1')b_1^\dagger(k_1)b_2^\dagger(k_2)|0\rangle = \langle 0|b_1(k_2')qb_1^\dagger(k_1)b_2(k_1')b_2^\dagger(k_2)|0\rangle =$$

$$= \langle 0|b_1(k_2')qb_1^\dagger(k_1)\Big(\delta_{k_2k_1'} + qb_2^\dagger b_2\Big)|0\rangle = \langle 0|q\delta_{k_2k_1'}b_1(k_2')b_1^\dagger(k_1)|0\rangle =$$

$$-\langle 0|q\delta_{k_2k_1'}\Big(\delta_{k_1k_2'} + qb_1^\dagger b_1\Big)|0\rangle = -\langle 0|0\rangle q\delta_{k_2k_1'}\delta_{k_1k_2'};$$

(3)-(7):

$$\langle 0|b_1(k_2')b_2(k_1')b_2^\dagger(k_1)b_1^\dagger(k_2)|0\rangle =$$

$$= \langle 0|b_1(k_2')\Big(\delta_{k_1k_1'} + qb_2^\dagger(k_1)b_2(k_1')\Big)b_1^\dagger(k_2)|0\rangle =$$

$$\langle 0|b_1(k_2')b_1^\dagger(k_2)\delta_{k_1k_1'} + qb_1(k_2')b_2^\dagger(k_1))b_2(k_1')b_1^\dagger(k_2)|0\rangle =$$

$$\langle 0|\delta_{k_1k_1'}\delta_{k_2k_2'} + qb_1^\dagger(k_2)b_1(k_2') + qb_1(k_2')b_2^\dagger(k_1)qb_1^\dagger(k_2)b_2(k_1')|0\rangle =$$

$$\langle 0|0\rangle\delta_{k_1k_1'}\delta_{k_2k_2'}$$

(3)-(8):

$$-\langle 0|b_1(k_2')b_2(k_1')b_2^\dagger(k_1)b_2^\dagger(k_2)|0\rangle =$$

$$= -\langle 0|b_1(k_2')\Big(\delta_{k_1k_1'} + qb_2^\dagger(k_1)b_2(k_1')\Big)b_1^\dagger(k_2)|0\rangle =$$

$$-\langle 0|\delta_{k_1k_1'}b_1(k_2')b_1^\dagger(k_2)+qb_1(k_2')b_2^\dagger(k_1)b_2(k_1')b_1^\dagger(k_2)|0\rangle = -\langle 0|0\rangle\delta_{k_1k_1'}\delta_{k_2k_2'};$$

(4)-(5):

$$-\langle 0|b_2(k_2')b_1(k_1')b_1^\dagger(k_1)b_1^\dagger(k_2)|0\rangle =$$

$$= -\langle 0|b_2(k_2')\Big(\delta_{k_1k_1'} + qb_1^\dagger(k_1)b_1(k_1')\Big)b_1^\dagger(k_2)|0\rangle =$$

$$-\langle 0|b_2(k_2')qb_1^\dagger(k_1)b_1(k_1')b_1^\dagger(k_2)|0\rangle = -\langle 0|qb_2(k_2')b_1^\dagger(k_1)\Big(\delta_{k_2k_1'}+qb_1^\dagger b_1\Big)|0\rangle =$$

$$= -\langle 0|qb_2(k_2')b_1^\dagger(k_1)\delta_{k_2k_1'}|0\rangle = 0;$$

(4)-(6):

$$\langle 0|b_2(k_2')b_1(k_1')b_1^\dagger(k_1)b_2^\dagger(k_2)|0\rangle =$$

$$= \langle 0|b_2(k_2')\Big(\delta_{k_1k_1'} + qb_1^\dagger(k_1)b_1(k_1')\Big))b_2^\dagger(k_2)|0\rangle =$$

$$\langle 0|\delta_{k_1k_1'}b_2(k_2')b_2^\dagger(k_2)|0\rangle = \langle 0|\delta_{k_1k_1'}\Big(\delta_{k_2k_2'} + qb_2^\dagger b_2\Big)|0\rangle = \langle 0|0\rangle\delta_{k_1k_1'}\delta_{k_2k_2'};$$

(4)-(7):

$$-\langle 0|b_2(k_2')b_1(k_1')b_2^\dagger(k_1)b_1^\dagger(k_2)|0\rangle = -\langle 0|b_2(k_2')qb_2^\dagger(k_1)b_1(k_1')b_1^\dagger(k_2)|0\rangle =$$

$$= -\langle 0|qb_2(k_2')b_2^\dagger(k_1)\Big(\delta_{k_2k_1'} + qb_1^{dag}b_1\Big)|0\rangle = -\langle 0|qb_2(k_2')b_2^\dagger(k_1)\delta_{k_2k_1'}|0\rangle =$$

$$= -\langle 0|q\delta_{k_2k_1'}\Big(\delta_{k_1k_2'} + qb_2^\dagger b_2\Big)|0\rangle = -\langle 0|0\rangle q\delta_{k_2k_1'}\delta_{k_1k_2'};$$

(4)-(8):

$$\langle 0|b_2(k_2')b_1(k_1')b_2^\dagger(k_1)b_2^\dagger(k_2)|0\rangle = 0.$$

Finally, summing all the contributions we have obtained, the coincidence counts parameter of the q–algebra becomes:

$$\mathcal{C}_{12} = \frac{1}{2}\sum_{\substack{k_1,\,k_2\\ k_1',\,k_2'}} \phi^\star(k_1',k_2')e^{-i(\varphi_{k_1'}-\varphi_{k_2'})}\phi(k_1,k_2)e^{i(\varphi_{k_1}-\varphi_{k_2})}$$

$$\Big(\sum_{\substack{k_1,\,k_2\\ k_1',\,k_2'}}\langle 0|0\rangle - q\sum_{\substack{k_1,\,k_2\\ k_1',\,k_2'}}\langle 0|0\rangle\Big) = \frac{1-q\omega}{2} \qquad \text{(B.6)}$$

Appendix C

List of used acronyms

ALDA	Adiabatic Local Density Approximation
AO	Atomic Orbital
ATZVP	Atomic Triple Zeta Valence Polarization
B	Becke
B3LYP	Becke three parameters Lee–Yang–Parr
BH–LYP	Becke88 exchange, Lee–Yang–Parr
BLYP	Becke–Lee–Yang–Parr
BS	Beam Splitter
CC	Coupled Cluster
CC2	Doubles Coupled Cluster
CCSD	Coupled Cluster Single Double
CISD	Configuration Interaction Single Double
CS	Colle–Salvetti
DFT	Density Functional Theory
DSCF	Dynamic Self Consistent Field
DTP	Di Phenyl Thiophene
EPR	Einstein Podolsky Rosen
ESCF	Energy Self Consistent Field
FCI	Full Configuration Interaction
FTP	File Transfer Protocol
GGA	Generalized Gradient Approximation
HF	Hartree–Fock
HOM	Hong–Ou–Mandel
HOMO	Highest Occupied Molecular Orbital
HK	Hohenberg–Kohn

KS	Kohn–Sham
LDA	Local Density Approximation
LUMO	Lowest Unoccupied Molecular Orbital
Me	Methyl
MRCI	Multi Reference Configuration Interaction
ox	oxygeneted
Phe	Phenyl
PD	Photodetector
QM	Quantum Mechanics
QI	Quantum Information
RHF	Restricted Hartree–Fock
RICC2	Resolution of the Identity Second order Coupled Cluster
RPA	Random Phase Approximation
ST	Theoretical Study
T3	Ter–Thiophene
TDDFT	Time–Dependent Density Functional Theory
THF	Tetrahydrofuran
TZVP	Triple Zeta Valence Polarization
TZVPP	Valence triple–zeta plus polarization
URH	Unrestricted Hartree–Fock
XC	Exchange–Correlation

Bibliography

[1] Slater, J. C. Phys. Rev. **35**, 210 (1930).

[2] Phyllips, J. C. Phys. Rev. **123**, 420 (1961).

[3] Thomas, T. H. Proc. Camb. Phil. Soc **23**, 542 (1927).

[4] Lieb, E. H. Rev. Mod. Phys. **53**, 603 (1981).

[5] Szabo, A. and Ostlund, N. S. "Modern Quantum Chemistry:Introduction to Advanced Electronic Structure Theory ",Mc Graw–Hill 1982.

[6] Barnett, G. P. and Shull, H. Phys. Rev. **153**, 61 (1967).

[7] McWeeny, R. Rev. Mod. Phys **32**, 335 (1960).

[8] Parr, R. G. and Yang, W. "Density Functional Theory of Atoms and Molecules", Oxford University Press, Oxford 1989.

[9] Fermi, E. Rend. Accad. Lincei **6**, 602 (1927).

[10] Fermi, E. Z. Phys **48**, 73 (1928).

[11] Fermi, E. Rend. Accad. Lincei **7**, 342 (1928).

[12] von Barth, U. and Hedin, L. J. Phys. C **5**, 1629 (1972).

[13] Gunnaarsson, O. and Lundqvist, B., Phys. Rev. B **13**, 4274 (1976).

[14] Ceperley, D. M. and Alder, B. J. Phys. Rev. Lett **45**, 566 (1980).

[15] Vosko, S. H.; Wilk, L. and Nusair M. Can J. Phys. **58**, 1200 (1980).

[16] Perdew, J. P. and Zunger, A. Phys Rev B **23**, 5048 (1981).

[17] Perdew, J. P. and Wang, Y. Phys Rev B **45**, 13244 (1992).

[18] Becke, A. D. Phys. Rev. A **38**, 3098 (1988).

[19] Perdew, J. P.; Burke, K. and Ernzerhof. M. Phys. Rev. Lett **77**, 3865 (1996).

[20] Lee, C.; Yang, W. and Parr, R. G. Phys. Rev. B **37**, 785 (1988).

[21] Colle, R. and Salvetti, O. Theor. Chim. Acta **37**, 329 (1975).

[22] Becke, A. D. J. Chem. Phys. **98**, 1372 (1993).

[23] Perdew, J. P.;Ernzerhof. M. and Burke, K. J. Chem. Phys. **105**, 9982 (1996).

[24] Colle, R. and Salvetti, O. J. Chem. Phys **93**, 534 (1990).

[25] van Leeuwen, R. Phys. rev. Lett. **80**, 1280 (1998).

[26] Bauernshmitt, R. and Ahlrichs, R. Chem. Phys. Lett. **256**, 454 (1996).

[27] Piacenza, M.; Della Sala, F.; Fabiano, E.; Maiolo, T.; Gigli, G. J. Comp. Chem. July **18**,17639501 (2007).

[28] Fichou, D. Ed. Handbook of Oligo and Polythiophenes; Wiley-VCH: Weinheim, Germany, 1999.

[29] Barbarella, G.; Pudova, O.; Arbizzani, C.; Mastragostino, M.; Bongini, A. J Org Chem **63**, 5497 (1998).

[30] Barbarella, G.; Melucci, M.; Sotgiu, G. Adv Mater **17**, 1581 (2005).

[31] Wu, C.; Decker, E. R.; Blok, N.; Bui, H.;You, T. J.;Wang, J.; Bourgoyne, A. R.; Knowles, V.; Berens, K. L.; Holland, G.W.; Brock, T. A.; Dixon, R. A. F. J Med Chem **47**, 1969 (2004).

[32] Dore, K.; Dubus, S.; Ho, H. A.; Levesque, I.; Brunette, M.; Corbeil, G.; Boissinot, M.; Boivin, G.; Bergeron, M. G.; Boudreau, D.; Leclerc, M. J Am Chem Soc **126**, 4240 (2004).

[33] Garnier, F.; Horowitz, G.; Fichou, D.; Peng, X. Adv Mater **2**, 592 (1990).

[34] Geiger, F.; Stoldt, M.; Schweizer, H.; Bauerle, P.; Umbach, E. Adv Mater **5**, 922 (1993).

[35] Dodabalapur, A.; Katz, H. E.; Torsi, L.; Haddon, R. C. Science **269**, 1560 (1995).

[36] Horowitz, G.; Delannoy, P.; Bouchriha, H.; Deloffre, F.; Fave, J.; Garnier, F.; Hajlaoui, H.; Heyman, M.; Kouki, F.; Valat, P.; Wintgens, V.; Yassar, A.; Adv Mater **6**, 752 (1994).

[37] Uchiyama, K.; Akimichi, H.; Hotta, S.; Noge, H.; Sakai, H. Synth Met **63**, 57 (1994).

[38] Noda, T.; Ogawa, H.; Noma, N.; Shirota, Y. Adv Mater **9**, 720 (1997).

[39] Noda, T.; Ogawa, H.; Noma, N.; Shirota, Y. Appl Phys Lett **70**, 699 (1997).

[40] Gigli, G.; Barbarella, G.; Favaretto, L.; Cacialli, F.; Cingolani, R. Appl Phys Lett **75**, 439 (1999).

[41] Barbarella, G.; Favaretto, L.; Sotgiu, G.; Zambianchi, M.; Fattori, V.; Cocchi, M.; Cacialli, F.; Gigli, G.; Cingolani, R. Adv Mater **11**, 1375 (1999).

[42] Shirota,Y.; Kinoshita, M.; Noda, T.; Okumoto, K.; Ohara, T. JAm-Chem Soc **122**, 11021 (2000).

[43] Doi, H.; Kinoshita, M.; Okumoto, K.; Shirota, Y. Chem Mater **15**, 1080 (2003).

[44] Ackermann, J.; Videlot, C.; El Kassmi, A. Thin Solid Films **404**, 157 (2002).

[45] Telesca, R.; Bolink, H.; Yunoki, S.; Hadziioannou, G.; Th. Van Duijnen, P.; Snijders, J. G.; Jonkman, H. T.; Sawatzky, G. A. Phys Rev B **63**, 155112 (2001).

[46] Rubio, M.; Merchan, M.; Pou-Amerigo, R.; Orti, E. Chem Phys Chem **4**, 1308 (2003).

[47] Casado, J.; Pappenfus,T. M.; Miller,L. L.; Mann, K. R.; Ort, E.;Viruela, P. M.; Pou-Amerigo, R.; Hernandez, V.; Lopez Navarrete, J. T. J Am Chem Soc **125**, 2524 (2003).

[48] Ruiz Delgado, M. C.; Hernandez, V.; Casado, J.; Lopez Navarrete, J. T.; Raimundo, J.-M.; Blanchard, P.; Roncali, J. J Mol Struct (Theochem) **709**, 187 (2004).

[49] Fabiano, E.; Della Sala, F.; Cingolani, R.; Weimer, M.; Görling, A. J Phys Chem A **109**, 3078 (2005).

[50] Rubio, M.; Merchan, M.; Ort, E. Chem Phys Chem **6**, 1357 (2005).

[51] Clarke, T. M.; Gordon, K. C.; Officer, D. L.; Grant, D. K. J Phys Chem A **109**, 1961 (2005).

[52] Sancho-Garcia, J. C. J Chem Phys **124**, 124112 (2006).

[53] Della Sala, F.; Heinze, H. H.; Görling, A. Chem Phys Lett **339**, 343 (2001).

[54] Della Sala, F.; Raganato, M. F.; Anni, M.; Cingolani, R.; Weimer, M.; Görling, A.; Favaretto, L.; Barbarella, G.; Gigli, G. Synth Met**139**, 895 (2003).

[55] Raganato, M. F.;Vitale,V.; Della Sala, F.; Anni, M.; Cingolani, R.; Gigli, G.; Favaretto, L.; Barbarella, G.;Weimer, M.; Görling, A. J Chem Phys **121**, 3784 (2004).

[56] Anni, M.; Della Sala, F.; Raganato, M. F.; Fabiano, E.; Lattante, S.; Cingolani, R.; Gigli, G.; Görling, A. J Phys Chem B **109**, 6004 (2005).

[57] Casado, J.; Zgierski, M. J.; Ewbank, P. C.; Burand, M. W.; e. Janzen abd, D.; Mann, K. R.; Pappenfus, T.; Berlin, A.; Perez-Inestrosa, E.; Ortiz, R. P.; Lopez Navarette, J. T. J Am Chem Soc **128**, 10134 (2006).

[58] Gigli, G.; Della Sala, F.; Lomascolo, M.; Anni, M.; Barbarella, G.; Lugli, P.; Di Carlo, A.; Cingolani, R. Phys Rev Lett **86**, 167 2001.

[59] Aleman, C.; Julia, L. J Phys Chem **100**, 1524 (1996).

[60] DiCesare, N.; Belletete, M.; Durocher, G.; Leclerc, M. Chem Phys Lett **275**, 533 (1997).

[61] DiCesare, N.; Belletete, M.; Marrano, C.; Leclerc, M.; Durocher, G. J Phys Chem A **102**, 5142 (1998).

[62] DiCesare, N.; Belletete, M.; Marrano, C.; Leclerc, M.; Durocher, G. J Phys Chem A **103**, 795 (1999).

[63] Daminelli, G.; Widany, J.; Di Carlo, A.; Lugli, P. J Chem Phys**115**, 4919 (2001).

[64] Gross, E.; U. K.; Dobson, J. F.; Petersilka, M. Density Functional Theory (Topics in Current Chemistry); Springer: Heidelberg, Germany, 1996.

[65] Casida, M. E. Recent Advances in Density Functional Methods; Vol. 1; World Scientific: Singapore, 1995.

[66] Bauernschmitt, R.; Ahlrichs, R. Chem Phys Lett **256**, 454 (1996).

[67] Furche, F. J Chem Phys **114**, 5982 (2001).

[68] Koch,W.; Holthausen, M. C. A Chemists Guide to Density Functional Theory; Wiley-VCH: New York, 2001.

[69] Grimme, S.; Parac, M. Chem Phys Chem **3**, 292 (2003).

[70] Christiansen, O.; Koch, H.; Jørgensen, P. Chem Phys Lett **243**, 409 (1995).

[71] Hättig, C.; Hald, K. Phys Chem Chem Phys **4**, 2111 (2002).

[72] Hättig, C.; Weigend, F. J Chem Phys **113**, 5154 (2000).

[73] Köhn, A.; Hättig, C. J Chem Phys **119**, 5021 (2003).

[74] Jansen, C. L.; Nielsen, I. M. B. Chem Phys Lett **290**, 423 (1998).

[75] Grimme, S.; Waletzke, M. J Chem Phys **111**, 5645 (1999).

[76] Roos, B. O.; Fülscher,M. P.; Malmqvist, P.-A. In Quantum Mechanical Electronic Structure Calculations with Chemical Accuracy; Langhoff, S. R. Ed., Kluwer Academic: Dordrecht, The Netherlands, 1995; p. 357.

[77] Roos, B. O.; Andersson, K.; Fülscher,M. P.; Malmqvist, P.-A.; Serrano-Andres, L.; Pierloot, K.; Merchan, M. In Advances in Chemical Physics: New methods in Computational Quantum Mechanics, Vol. XCIII; Prigogine, I.; Rice, S. A.; Eds.; Wiley: New York, 1996.

[78] Ahlrichs, R.; Bär, M.; Baron, H.-P.; Bauernschmitt, R.; Böcker, S.; Ehrig, M.; Eichkorn, K.; Elliott, S.; Furche, F.; Haase, F.; Häser, M.; Horn, H.; Huber, C.; Huniar, U.; Kattannek, M.; Kölmel, C.; Kollwitz, M.; May, K.; Ochsenfeld, C.; Öhm, H.; Schäfer, A.; Schneider, U.; Treutler, O.; von Arnim, M. Weigend, F.; Weis, P.; Weiss, H. TURBOMOLE (Vers. 5.7) Universität Karlsruhe 2004. Available at http://www.turbomole.com.

[79] Treutler, O.; Ahlrichs, R. J Chem Phys **102**, 346 (1995).

[80] Becke, A. D. J Chem Phys **98**, 5648 (1993).

[81] Becke, A. D. J Chem Phys **98**, 1372 (1993).

[82] http://www.turbomole.com

[83] Weigend, F.; Häser, M.; Patzelt, H.; Ahlrichs, R. Chem Phys Letters **294**, 143 (1998).

[84] Eichkorn, K.; Weigend, F.; Treutler, O.; Ahlrichs, R. Theor Chem Acc **97**, 119 (1997).

[85] Schäfer, A.; Huber, C.; Ahlrichs, R. J Chem Phys **100**, 5829 (1994).

[86] Raganato, M. F. Laurea Thesis in Physics, Lecce University, Italy, 2002.

[87] Görling, A. Phys Rev A **54**, 3912 (1996).

[88] Schödinger,E. Naturwissenschaften **23**, 807 (1935).

[89] Nielsen, M. A. and Chuang, I. L. *Quantum computation and quantum information*, Cambridge Univ. Press, Crambridge, 2000.

[90] Schmidt, E. Math. Annalen., 63:433, (1906).

[91] Einstein, A.; Podolsky, B. and Rosen, N. Phys. Rev **47**, 777 (1935).

[92] Bell, J. S. Phys. **1**, 195 (1964).

[93] Plenio, M. and Virmani, S. E-print arXiv quant–ph/0504163.

[94] Maiolo, T.A.C.; Della Sala, F.; Martina, L.; Soliani, G. Theor. and Math. Phys. **152**(2), 1146 (2007).

[95] Maiolo, T.A.C.; Della Sala, F.; Martina, L.; Soliani, G. Quantum Computers and Computing **6**(1), 43 (2006).

[96] J. S. Bell, Rev. Mod. Phys. **38** 447 (1966).

[97] C. H. Bennet, *et al.*, Phys. Rev. Lett. **70** 1895 (1993).

[98] A. K. Ekert, Phys. Rev. Lett **67** 661 (1991).

[99] C. A. Fuchs, Phys. Rev. Lett. **79** 1162 (1997).

[100] C. Machiavello *et al.* Phys. Rev. **A 69**, 010303 (2004).

[101] Banaszek *et al.* Phys. Rev. Lett **92**, 257901 (2004).

[102] J. Schliemann *et al.* Phys. Rev .**A 64**, 022303 (2001).

[103] G. C. Ghirardi and L. Marinatto, Phys. Rev. **A 70**, 012109 (2004).

[104] Z. Huang, S. Kais Chem. Phys. Lett. **413** 1-5 (2005).

[105] D. M. Collin, Z. Naturforsch. **A 48**, 68 (1993).

[106] J. C. Ramirez. *et al.* Phys. Rev. **A 56** 4477 (1997).

[107] A. Szabo, N. S. Ostlund *Modern Quantum Chemistry: Introduction to Advanced Electronic Structure Theory* McGraw Hill (1989).

[108] E. Schrödinger, Naturwissenschaften **23** (1935)807 .

[109] A. C. Doherty, *et al.*, Phys. Rev. Lett. **88** (2002) 187904.

[110] J. R. Gittings, and A. J. Fisher Phys. Rev. **A 66**, 032305 (2002).

[111] J. Paldus, *et al.*, J. Chem. Phys. **76**, 2458–2470 (1982).

[112] G. E. Scuseria, A. C. Scheiner, T. J. Lee, J. E. Rice, H. F. Schaefer J. Chem. Phys. **86** 2881 (1987).

[113] P. Zanardi, Phys. Rev. **A 65** 042101 (2002).

[114] C. H. Bennett, H. Bernstein, S. Popescu, and B. Schumacher, Phys. Rev **A 53**, 2046 (1996).

[115] A. D. Gottlieb and N. J. Mauser, Phys. Rev. Lett. **95** 123003 (2005).

[116] R. Grobe, K. Rzazewski, and J. H. Eberly, J. Phys. **B 27**, L503 (1994).

[117] P. Gersdorf, *et al.*, Int. J. Quantum Chem. **61**, 935 (1997).

[118] M. J. Frish et al., GAUSSIAN 98, Revision A. 11.3, Gaussian, Inc., Pittsburg PA, 1998.

[119] J. Cizek, J. Chem. Phys. **45**, 4256 (1966).

[120] G. E. Scuseria, *et al.*, J. Chem. Phys. **89**,7382 (1988).

[121] V. Giovannetti, laser Physics, **16**, 1406 (2006).

[122] V. Giovannetti, *et al.* con–mat/0606413.

[123] Greenberg, O. W., Phys. Rev. Lett. **64**, 705 (1990).